

For Reference

NOT TO BE TAKEN FROM THIS ROOM

For Reference

NOT TO BE TAKEN FROM THIS ROOM

Ex LIBRIS
UNIVERSITATIS
ALBERTAEISIS





Digitized by the Internet Archive
in 2018 with funding from
University of Alberta Libraries

<https://archive.org/details/Burns1964>

Thesis
1964
11

UNIVERSITY OF ALBERTA

AN INVESTIGATION INTO THE BUCKLING
OF LIGHT CLAMPED ARCHES

by

DAVID ASHWORTH BURNS, B.Sc. Tech. (Manchester)

A THESIS
SUBMITTED TO THE FACULTY OF GRADUATE STUDIES
IN PARTIAL FULFILMENT OF THE REQUIREMENTS FOR
THE DEGREE OF MASTER OF SCIENCE

DEPARTMENT OF MECHANICAL ENGINEERING

EDMONTON, ALBERTA


1964

ABSTRACT

An experimental and theoretical study has been undertaken which considers large deflections of a light arch under the action of a radial centrally applied load. The arch has a circular span and the ends of the arch are built in. Symmetrical and asymmetrical buckling is considered.

Experiments are described in which a variety of arch dimensions are considered, and the results are compared with those given by two recent theories. These theories are also compared to each other.

Discrepancies arise between the experimental considerations and the theoretical predictions. It is suggested that the weight of the arches is responsible for such discrepancies.

ACKNOWLEDGEMENTS

The author wishes to extend his gratitude to Dr. J. S. Kennedy for supervising this thesis, and to the Mechanical Engineering Department for its kind assistance throughout his graduate studies.

NOTATION

- a Non-dimensional amplitude of symmetrical deflection
where $a = \frac{A}{R\beta^2}$
- a_U Non-dimensional deflection corresponding to upper buckling load
- a_L Non-dimensional deflection corresponding to lower buckling load
- a_T Non-dimensional deflection corresponding to transitional buckling load
- \bar{a} Function, where $\bar{a} = d - 4$
- b Width of arch cross-section, inches
- d Function, where $d = \pi^2 a$
- e Strain
- h_1 Function, where $h_1 = \frac{\pi^2 a}{48u}$
- h_2 Function, where $h_2 = \frac{1}{u} \left(\frac{d}{16} - \frac{1}{3} \right)$
- k Change of curvature of arch
- m Number of terms in a series
- n Number of terms in a series
- p Function, where $p = 48uP^* - 4$
- r Refers to the rth term in a series
- t Thickness of arch, inches

NOTATION

u	Function, where $u = \frac{x}{\pi^2}$
v	Tangential displacement at middle surface of arch
w	Radial displacement at middle surface of arch
x	Function, where $x = \frac{\alpha}{\beta}$
A	Amplitude of deflection, inches
B	Amplitude of deflection, inches
C	Constant of integration
C_{1n}	Definite integral, where $C_{1n} = \int_{-1}^1 w_n dx$
C_{2n}	Definite integral, where $C_{2n} = \int_{-1}^1 \left(\frac{dw_n}{dx}\right)^2 dx$
C_{3n}	Definite integral, where $C_{3n} = \int_{-1}^1 \left(\frac{d^2w_n}{dx^2}\right)^2 dx$
C_{4n}	Function, where $C_{4n} = (w_n)_x = 0$
D_1	Summation, where $D_1 = \sum_1^r \left[\frac{C_{2n} C_{4n}^2}{(C_{3n} - KC_{2n})^2} \right]$
D_2	Summation, where $D_2 = \sum_1^r \left[\frac{C_{1n} C_{3n} C_{4n}}{(C_{3n} - KC_{2n})^2} \right]$
D_3	Summation, where $D_3 = \sum_1^r \left[\frac{C_{1n}^2 (2C_{3n} - KC_{2n})}{(C_{3n} - KC_{2n})^2} \right]$
E	Young's Modulus (Appendix A)
H	Total energy of system
H^*	Function, where $H^* = \frac{HX}{\beta^5}$
I	Second moment of area of arch cross-section

NOTATION

K	Constant, where $K = 2.0246\pi^2$
K_o	Function, where $K_o = \bar{a}^3 [36 + 3u^2 (9 \bar{a}^2 - 116)]$
K_1	" " $K_1 = \bar{a}^2 [-12 + 3u^2 (6 \bar{a}^2 - 120)]$
K_2	" " $K_2 = \bar{a} [-20 + 3u^2 (\bar{a}^2 - 20)]$
P	Applied load, lbs.
P_E	Intermediate buckling load, or energy load
P_L	Lower buckling load
P_T	Transitional buckling load
P_U	Upper buckling load
P^*	Non-dimensional load, $P^* = \frac{PR}{Et^2 b \beta}$
\bar{P}	Non-dimensional load, $\bar{P} = \frac{PR^2}{EI}$
R	Radius of curvature of arch centre line
U_b	Non-dimensional strain energy, due to bending
U_m	Non-dimensional strain energy, due to axial deformation.
U_p	Non-dimensional potential energy
X	Non-dimensional parameter, where $X = \frac{\beta^2 R}{t}$
∞	Angular coordinate of arch (measured from centre line)
β	Half-angle subtended by arch
δ	Non-dimensional central deflection, where $\delta = \frac{A}{R}$
'	Initial state prior to buckling
"	Change in quantities during transition of arch from unbuckled to buckled state.

TABLE OF CONTENTS

CHAPTER	PAGE
1. INTRODUCTION	1
2. THEORY	5
(A) General Formulation	5
(B) Determination of Buckling Loads by the Classical Eigenvalue Theory.	9
(C) Series Solution of the Non-Linear Deformations of the Clamped Arch.	17
(D) Application of a General Displacement Function to the Series Solution.	23
3. APPARATUS AND EXPERIMENTAL PROCEDURE	29
(A) Apparatus	29
(B) Test Specimens	39
(C) Experimental Procedure	41
4. RESULTS AND DISCUSSION	43
(A) Symmetrical Buckling	43
(B) Asymmetrical Buckling	49
5. CONCLUSIONS	73
BIBLIOGRAPHY	76
APPENDIX A	77
APPENDIX B	79

LIST OF FIGURES

FIGURE	PAGE
1. Clamped Circular Arch Under Concentrated Load	6
2. Variation of Buckling Modes	16
3. Sketch of Function (43) for Initial n Values	23
4. General View of Apparatus	30
5. Plan View of Arch Bed	31
6. Close-up of Arch Clamp	33
7. Symmetric Head - No Load	34
8. Symmetric Head - Arch Buckled Symmetrically	35
9. Arch Prior to Buckling, Retaining Symmetrical Mode	36
10. Arch in Unstable Region, Exhibiting Pronounced Asymmetry	37
11. Arch Deflected to Second Stable Region, and Shows Return to Symmetry	38
12. Theoretical Load Deflection Curves by Gjelsvik and Bodner's Theory for Pieces S1 - S4	54
13. Theoretical and Experimental Load Deflection Curves, Piece S1	55
14. Theoretical and Experimental Load Deflection Curves, Piece S2	56
15. Theoretical and Experimental Load Deflection Curves, Piece S3	57
16. Theoretical and Experimental Load Deflection Curves, Piece S4	58

FIGURE	PAGE
17. Theoretical Upper Buckling Loads	59
18. Experimental Load Deflection Curves Compared With van Wijngaarden Theory, $\frac{b}{t}$ Constant	60
19. Experimental Load Deflection Curves Compared With van Wijngaarden Theory, $\frac{R}{t}$ Constant	61
20. Experimental Load Deflection Curves, Piece S5	62
21. Experimental Load Deflection Curves, Piece S6	63
22. Theoretical Results for Varying X Compared to Curve Obtained by van Wijngaarden Theory	64
23. Theoretical Buckling Loads Expressed as \bar{P}	65
24. Piece S7 Buckled Under Own Weight	66
25. Theoretical and Experimental Load Deflection Curves, Piece S7	67
26. Comparison with Gjelsvik and Bodner's Theoretical Buckling Load Calculations	68
27. Comparison with Gjelsvik and Bodner's Results, $X = 11.62$	69
28. Load Deflection Curve Predicted by Gjelsvik and Bodner for Large X Values	70
29. Theoretical Upper and Transitional Buckling Loads	71
30. Theoretical Buckling Displacements	72
31. Load-Strain Curve to Determine Young's Modulus	78

LIST OF TABLES

TABLE	PAGE
1. List of Test Specimens	40
2. Arch Weight-Buckling Load Ratios	46
3. Buckling Loads by Gjelsvik-Bodner Theory Transformed to van Wijngaarden Coordinates	48

CHAPTER 1

INTRODUCTION

Little work considering the phenomenon of clamped arch buckling was published until the completion of the Second World War, when A. van Wijngaarden¹ presented a theoretical treatise upon large distortions of circular rings under the action of a concentrated radial load. In his paper, by introducing boundary conditions to adapt to the case of a clamped circular arch, he derived a non-linear differential equation which satisfied the geometrical conditions and the equilibrium state of the arch. This was subsequently solved by algebraic transformation and the introduction of elliptic integral theory. Symmetrical deflections only were discussed.

Experimental investigation was also undertaken, some results of which were presented, although no description of this work was offered.

J. S. Kennedy² reviewed van Wijngaarden's paper much later in 1955 and conducted a series of experiments with light thin arches whereby he induced the arches to buckle symmetrically by clamping the centre of the arch. The arch centre, therefore, was allowed to move only in a

vertical direction, and the tangent at the midpoint was always horizontal. The application of van Wijngaarden's theory gave only one load deflection curve for non-dimensional plotting, whereas Kennedy obtained several different, although similar, curves experimentally by employing varying arch geometrics. He suggested that this discrepancy was due to poor arch clamping. The experiments were conducted on arches fashioned from banding steel, from 0.012 inches to 0.025 inches in depth, with a radius variation of 12 inches to 30 inches, and upon arches of circular section, made from piano wire.

In a recent text on flexible bars, R. Frisch-Fay³ summarized the van Wijngaarden treatment, together with similar theoretical work on the buckling of a semi-circular ring by Biezono and Koch, completed at about the same time in 1946.

The only other approach to this problem was that employed by Gjelsvik and Bodner⁴, who presented an energy methods solution as late as 1962, which is discussed at length in a later section of this thesis. Their theory covered asymmetrical as well as symmetrical buckling modes and related the relative occurrence of both to a dimensionless parameter of the arch.

3

In the same paper experimental evidence was also presented which compared favourably with the theoretical solution. Load deflection curves were included for some of the specimens they used, but the results from the experimental work do not seem to have been adequately evaluated. The arch specimens were manufactured from aluminum alloy one inch wide and $\frac{3}{16}$ inch thick, and the desired circular profile was achieved by rolling.

With no confirmatory experimental consideration on Gjelsvik and Bodner's work to date, the author at the instigation of Dr. J. S. Kennedy, felt it worthwhile to examine thoroughly and re-appraise this subject. Gjelsvik and Bodner's approach was adopted for the theoretical analysis, as it had the advantage of encompassing transitional mode buckling.

The van Wijngaarden method, evolved before digital computers were in common use, has its solution in elliptic integral form. This is most difficult to incorporate in computer programmes, because of the necessity to store in the machine's memory sections many tabulated values from integral tables.

The Mathematics Department, at the University of Alberta, advised that a direct trial and error method of substituting numerical values should be employed in

the attempt to satisfy van Wijngaarden's equations.

Such a procedure had been adopted previously by Kennedy, and the curve he obtained is reproduced in Chapter 4 for comparison with Gjelsvik and Bodner's theory.

Further modification of this method, to include the possibility of an asymmetrical buckling mode resulted in non-linear equations, the solution of which, thus far, it has been found impossible to determine.

CHAPTER 2

THEORY

Since some of the conclusions Gjelsvik and Bodner presented in their treatise on snap buckling are questioned by this author, in the light of their own theory, their theoretical considerations are given in this chapter.

(A) General Formulation

Consider a circular arch with built-in ends as shown in Figure 1. For a thin curved beam the axial strain is given by

$$e = \frac{1}{R} \frac{dv}{d\alpha} - w + \frac{1}{2R} \left(\frac{dw}{d\alpha} \right)^2 \quad (1)$$

where v and w are the tangential and radial displacements respectively.

k , the change in curvature, is given by

$$k = \frac{1}{R^2} \frac{d^2w}{d\alpha^2} \quad (2)$$

The strain energy due to axial deformation is

$$U_m = \frac{1}{2} \int_{-\beta}^{\beta} e^2 d\alpha \quad (3)$$

where U_m has been put in non-dimensional form by dividing by the factor $EtbR$.

In a similar non-dimensional form the strain energy due to bending is

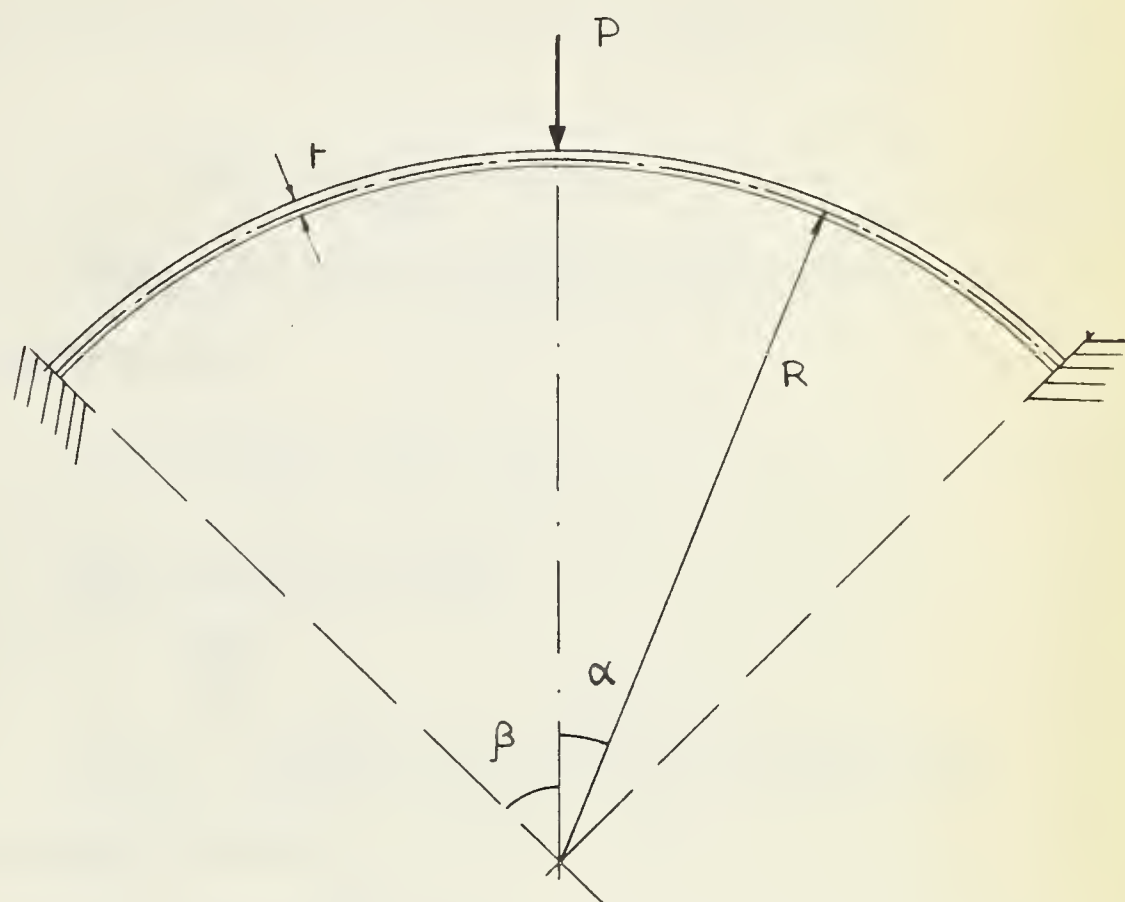


FIG. I CLAMPED CIRCULAR ARCH UNDER CONCENTRATED LOAD

$$U_b = \frac{\pi^2}{24} \int_{-\beta}^{\beta} k^2 d\alpha \quad (4)$$

The change in potential energy of the load which has undergone a vertical displacement is

$$U_p = - \frac{P}{EtbR} (w)_{\alpha=0} \quad (5)$$

Hence the total energy of the system may be expressed as

$$H = U_m + U_p + U_b \quad (6)$$

Now for equilibrium

$$\frac{dH}{dv} = 0$$

Since v appears only in U_m , the membrane strain energy, we have

$$\begin{aligned} U_m &= \frac{1}{2} \int_{-\beta}^{\beta} e^2 d\alpha \\ \frac{dH}{dv} &= \frac{dU_m}{dv} = \frac{dU_m}{de} \frac{de}{dv} = \frac{dU_m}{de} \frac{de}{d\alpha} \frac{d\alpha}{dv} \\ &= \frac{dU_m}{de} \frac{de}{d\alpha} \left(\frac{1}{dv/d\alpha} \right) \\ &= \left[\int_{-\beta}^{\beta} e d\alpha \right] \left[\frac{de}{d\alpha} \right] \left[\frac{1}{eR} \right] \end{aligned}$$

Since e will be a symmetrical function, the first

bracket is not zero. The strain cannot be infinite, so that the third bracket cannot be zero. Thus for the equilibrium condition to be fulfilled we must have

$$\frac{de}{d\alpha} = 0$$

so that

$$e = C \quad (7)$$

where C is a constant term.

Thus re-arranging equation (1)

$$\frac{dv}{d\alpha} = w - \frac{1}{2R} \left(\frac{dw}{d\alpha} \right)^2 + CR$$

Integrating between the limits $\alpha = \pm \beta$, and employing the boundary conditions ($v = 0$ at the ends of the arch) yields

$$e = C = -\frac{1}{2R\beta} \int_{-\beta}^{\beta} \left(w - \frac{1}{2R} \left(\frac{dw}{d\alpha} \right)^2 \right) d\alpha \quad (8)$$

Equation (6) becomes

$$H = \frac{1}{2} \int_{-\beta}^{\beta} e^2 d\alpha + \frac{t^2}{24} \int_{-\beta}^{\beta} k^2 d\alpha - \frac{P}{EtR} (w)_{\alpha} = 0 \quad (9)$$

so that substituting for e from (8) and for k from (2), H can now be expressed in the form

$$H = \frac{1}{4R^2\beta} \left\{ \int_{-\beta}^{\beta} \left[w - \frac{1}{2R} \left(\frac{dw}{d\alpha} \right)^2 \right] d\alpha \right\}^2 + \frac{t^2}{24R^4} \int_{-\beta}^{\beta} \left(\frac{dw}{d\alpha} \right)^2 d\alpha - \frac{P}{EtR} (w)_{\alpha} = 0 \quad (10)$$

(B) Determination of Buckling Loads by the Classical Eigenvalue Theory

The buckling load is taken as the load for which geometrically adjacent equilibrium states can exist in addition to the original state at the same load.

Consider small displacements about an equilibrium position at the centre of the arch, such that with the application of a further small deflection, the arch will change from the unbuckled to the buckled state.

Denoting the initial state prior to buckling of the arch by a single superscript, and pursuing a similar line of thought to that outlined in the previous section, we have

$$\begin{aligned} U_m' &= \frac{1}{2} \int_{-\beta}^{\beta} (e')^2 d\alpha \\ U_b' &= \frac{t^2}{24} \int_{-\beta}^{\beta} (k')^2 d\alpha \\ U_p' &= \frac{-P}{EtbR} (w')_{\alpha=0} \end{aligned} \quad (11)$$

Similar expressions to those obtained in the previous section can also be obtained for H' , e' and k' .

Now applying the double superscript to denote the change in these quantities during the transition from the unbuckled to the buckled state,

then,

$$\begin{aligned} U_m'' &= \frac{1}{2} \int_{-\beta}^{\beta} \left[(e'')^2 + 2e''e' \right] d\alpha \\ U_b'' &= \frac{t^2}{24} \int_{-\beta}^{\beta} \left[(k'')^2 + 2k'k'' \right] d\alpha \\ U_p'' &= \frac{-P}{EtR} (w'')_{\alpha=0} = 0 \end{aligned} \quad (12)$$

so that the change in total energy is

$$H'' = U_m'' + U_p'' + U_b''$$

For equilibrium in the buckled state

$$\frac{de''}{d\alpha} = 0$$

so that upon integration

$$e'' = C'' \quad (13)$$

Further, adapting equation (1), the change in axial strain during buckling is

$$e'' = \frac{1}{R} \left[\frac{dv''}{d\alpha} - w'' \right] + \frac{1}{2R^2} \left[\left(\frac{dw''}{d\alpha} \right)^2 + 2 \frac{dw'}{d\alpha} \frac{dw''}{d\alpha} \right] \quad (14)$$

Hence solving for $\frac{dv''}{d\alpha}$

$$\frac{dv''}{d\alpha} = w'' - \frac{1}{2R} \left[\left(\frac{dw''}{d\alpha} \right)^2 + 2 \frac{dw'}{d\alpha} \frac{dw''}{d\alpha} \right] + C''R \quad (15)$$

Integration of the above expression, and a consideration of the boundary conditions yields

$$C'' = - \frac{1}{2R\beta} \int_{-\beta}^{\beta} \left\{ w'' - \frac{1}{2R} \left[\left(\frac{dw''}{d\alpha} \right)^2 + 2 \frac{dw'}{d\alpha} \frac{dw''}{d\alpha} \right] \right\} d\alpha \quad (16)$$

The difference in the curvature change is

$$k'' = \frac{1}{R^2} \frac{d^2 w''}{d\alpha^2} \quad (17)$$

Thus substituting (16) and (17) into equation (12)

the total energy change is

$$H'' = \frac{1}{4R^2\beta} \left\{ \int_{-\beta}^{\beta} \left(w'' - \frac{1}{2R} \left[\left(\frac{dw''}{d\alpha} \right)^2 + 2 \frac{dw'}{d\alpha} \frac{dw''}{d\alpha} \right] \right) d\alpha \right\}^2 \quad (18)$$

$$\begin{aligned} & - \int_{-\beta}^{\beta} \left\{ \frac{e'}{2R\beta} \int_{-\beta}^{\beta} \left(w'' - \frac{1}{2R} \left[\left(\frac{dw''}{d\alpha} \right)^2 + 2 \frac{dw'}{d\alpha} \frac{dw''}{d\alpha} \right] \right) d\alpha \right\} d\alpha \\ & + \frac{t^2}{24R^4} \int_{-\beta}^{\beta} \left(\frac{d^2 w''}{d\alpha^2} \right)^2 d\alpha + \frac{t^2}{12R^2} \int_{-\beta}^{\beta} k' \frac{d^2 w''}{d\alpha^2} d\alpha - \frac{P}{EtR} (w'')_{\alpha} = 0 \end{aligned}$$

Neglecting terms in w which are of greater order than second and noting since the initial state is an equilibrium state all linear terms in w must cancel, equation (18) reduces to

$$\begin{aligned} H'' = & \frac{1}{4R^2\beta} \left\{ \int_{-\beta}^{\beta} \left(w'' - \frac{1}{R} \frac{dw'}{d\alpha} \frac{dw''}{d\alpha} \right) d\alpha \right\}^2 \\ & + \frac{e'}{2R^2} \int_{-\beta}^{\beta} \left(\frac{dw''}{d\alpha} \right)^2 d\alpha + \frac{t^2}{24R^4} \int_{-\beta}^{\beta} \left(\frac{d^2 w''}{d\alpha^2} \right)^2 d\alpha \quad (19) \end{aligned}$$

A general deformed shape may be composed of a symmetrical function of α , w_1 , and an asymmetrical

function of α , w_2 . So we may write

$$w'' = A'' w_1 + B'' w_2$$

The functions are thus orthogonal in the range

$$-\beta \leq \alpha \leq \beta$$

Hence (19) becomes

$$\begin{aligned} H'' &= \frac{1}{4R^2\beta} \left\{ \int_{-\beta}^{\beta} \left[A'' w_1 + B'' w_2 - \frac{1}{R} \frac{dw'}{d\alpha} \left(A'' \frac{dw_1}{d\alpha} + B'' \frac{dw_2}{d\alpha} \right) \right] d\alpha \right\}^2 \\ &+ \frac{e'}{2R^2} \int_{-\beta}^{\beta} \left(A'' \frac{dw_1}{d\alpha} + B'' \frac{dw_2}{d\alpha} \right)^2 d\alpha \\ &+ \frac{t^2}{24R^4} \int_{-\beta}^{\beta} \left(A'' \frac{d^2 w_1}{d\alpha^2} + B'' \frac{d^2 w_2}{d\alpha^2} \right)^2 d\alpha \end{aligned} \quad (20)$$

Because of the orthogonality properties H'' can again be reduced to

$$\begin{aligned} H'' &= A''^2 \left\{ \frac{1}{4R^2\beta} \left[\int_{-\beta}^{\beta} \left(w_1 - \frac{1}{R} \frac{dw'}{d\alpha} \frac{dw_1}{d\alpha} \right) d\alpha \right]^2 \right. \\ &+ \frac{e'}{2R^2} \int_{-\beta}^{\beta} \left(\frac{dw_1}{d\alpha} \right)^2 d\alpha + \frac{t^2}{24R^4} \int_{-\beta}^{\beta} \left(\frac{d^2 w_1}{d\alpha^2} \right)^2 d\alpha \Big\} \\ &+ B''^2 \left\{ \frac{e'}{2R^2} \int_{-\beta}^{\beta} \left(\frac{dw_2}{d\alpha} \right)^2 d\alpha + \frac{t^2}{24R^4} \int_{-\beta}^{\beta} \left(\frac{d^2 w_2}{d\alpha^2} \right)^2 d\alpha \right\} \end{aligned} \quad (21)$$

For equilibrium in the buckled state

$$\frac{\partial H''}{\partial A''} = 0 \quad \frac{\partial H''}{\partial B''} = 0$$

Hence each of the two expressions in parenthesis in (21) must be zero.

From the second equilibrium expression

$$e' = -\frac{t^2}{12R^2} \frac{\int_{-\beta}^{\beta} \left(\frac{dw_2}{d\alpha}\right)^2 d\alpha}{\int_{-\beta}^{\beta} \left(\frac{dw_2}{d\alpha}\right)^2 d\alpha} \quad (22)$$

or, if written in terms of $x = \frac{\alpha}{\beta}$

$$e' = -\frac{t^2}{12R^2\beta^2} \frac{\int_{-1}^1 \left(\frac{dw_2}{dx}\right)^2 dx}{\int_{-1}^1 \left(\frac{dw_2}{dx}\right)^2 dx} \quad (23)$$

Examining the form of (23) above, it is seen that the force is equal to the second mode Euler load of a clamped column of the same length as the arch.⁵

Substituting from (8) for e' , the deflection at buckling, which will be when the transitional or asymmetrical buckling load is reached, is obtained from

$$\frac{1}{2R\beta} \int_{-\beta}^{\beta} \left[w' - \frac{1}{2R} \left(\frac{dw'}{d\alpha} \right)^2 \right] d\alpha = \frac{t^2}{12R^2\beta^2} \frac{\int_{-1}^1 \left(\frac{dw_2}{dx}\right)^2 dx}{\int_{-1}^1 \left(\frac{dw_2}{dx}\right)^2 dx} \quad (24)$$

Introducing non-dimensional amplitude

$a = \frac{A}{R\beta^2}$ and the parameter $X = \frac{R\beta^2}{t}$, the above expression becomes

$$a^2 \int_{-1}^1 \left(\frac{dw_1}{dx} \right)^2 dx - 2a \int_{-1}^1 w_1 dx + \frac{1}{3x^2} \int_{-1}^1 \left(\frac{dw_2}{dx} \right)^2 dx = 0 \quad (25)$$

from which a can be evaluated provided the displacements w_1 and w_2 can be determined. This value of a is actually a_T , the displacement at which transitional buckling occurs.

The first equilibrium equation, obtained from (20) by setting $\frac{\partial H''}{\partial A''} = 0$

gives the following relationship

$$\frac{1}{2\beta} \left\{ \int_{-\beta}^{\beta} \left[w_1 - \frac{1}{R} \frac{dw'}{d\alpha} \frac{dw_1}{d\alpha} \right] d\alpha \right\}^2 + \frac{t^2}{12R^2} \int_{-\beta}^{\beta} \left(\frac{dw_1}{d\alpha} \right)^2 d\alpha - \frac{1}{2\beta R} \left\{ \int_{-\beta}^{\beta} \left[w' - \frac{1}{2R} \left(\frac{dw'}{d\alpha} \right)^2 \right] d\alpha \right\} \left\{ \int_{-\beta}^{\beta} \left(\frac{dw_1}{d\alpha} \right)^2 d\alpha \right\} = 0 \quad (26)$$

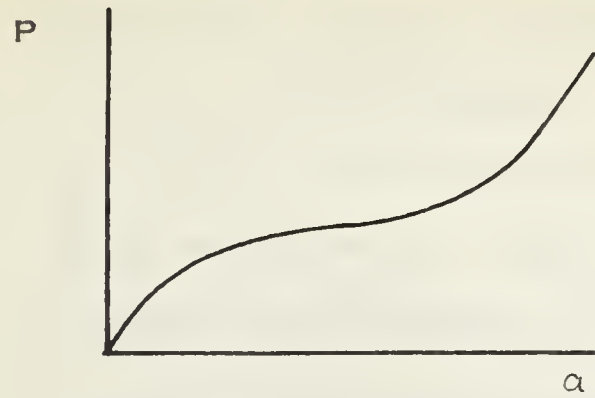
which gives an expression eventually for the deflection of the arch a_U at the upper, or symmetrical, buckling load.

This line of thought was elaborated further by Gjelsvik and Bodner and the theoretical results they obtained were compared with the results of another approximate method (which is contained in the same paper).

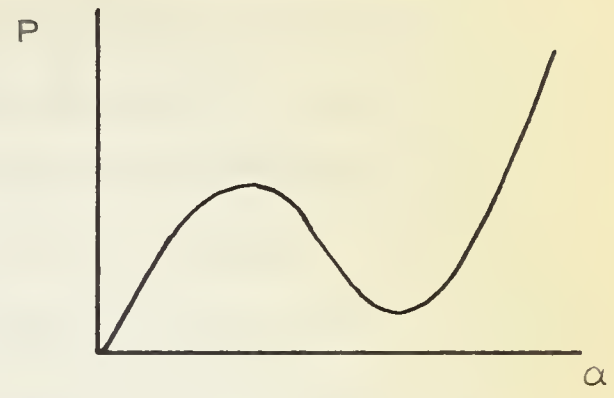
The algebraic expression for the various loads

and deflections agreed exactly. Using these results they derived a series of relationships which for varying X would enable one to predict whether transitional buckling would occur at all, and if it did whether the transitional mode would occur before or after the occurrence of symmetrical buckling. The various possibilities for arch buckling are described diagrammatically in Figure 2. Gjelsvik and Bodner's contention was that for sufficiently low values of X , no buckling as such would occur at all for increasing central deflection, and the resulting load deflection curve would have no unstable portion. As the value of X was increased, symmetrical buckling only would occur. Further increases in X would initially cause a transitional mode of asymmetry to occur after symmetrical buckling as such had occurred, and eventually conditions would be attained whereby the transitional buckling mode would occur first. In this case of course P_U would never be reached for the arch would have buckled, and the subsequent values of P would decrease.

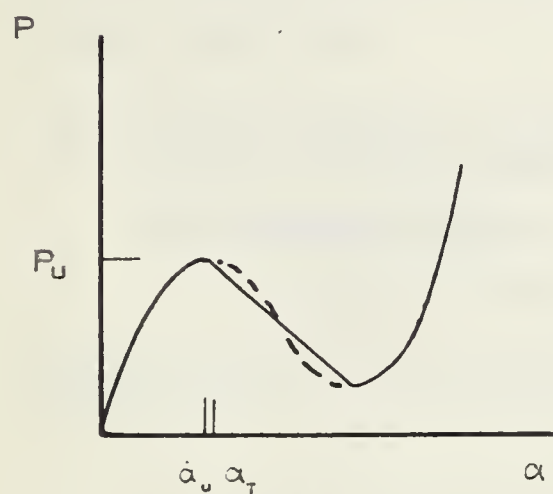
By the nature of the equation for the transitional mode, it was shown by Gjelsvik and Bodner that a straight line would always indicate such a mode. For exceptionally large values of X transitional mode buckling could happen shortly after the load had risen to the intermediate buckling load value; the intermediate



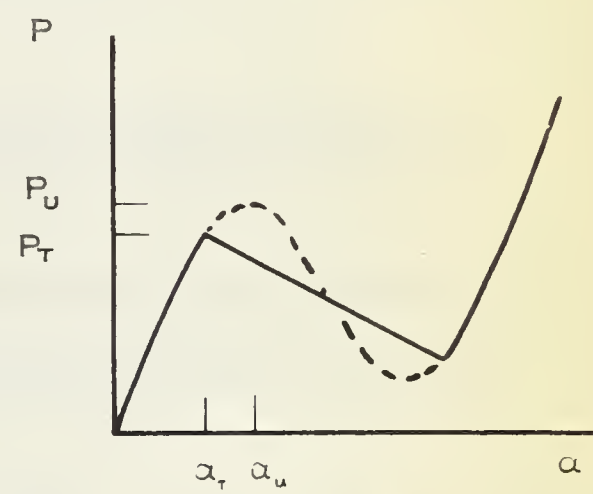
NO BUCKLING



SYMMETRICAL BUCKLING



SYMMETRICAL BUCKLING
WITH TRANSITIONAL MODE
PRESENT IN UNSTABLE REGION



TRANSITIONAL ASYMMETRICAL BUCKLING

FIG. 2 VARIATION OF BUCKLING MODES

buckling load was shown to be a lower bound for snap buckling, which is buckling involving a large deformation before another equilibrium position is attained.

Unfortunately these methods and the resulting criteria for the form of buckling are difficult to check numerically. The author could not find an asymmetrical function, w_2 , which would satisfy the boundary conditions required for the built-in ends, and no such function was suggested by Gjelsvik and Bodner.

Therefore only sufficient of the above theory has been developed that is necessary for the following series approach.

(C) Series Solution of the Non-Linear Deformations of the Clamped Arch.

Consider initially a symmetrically deflected shape, and let this shape be described by the function

$$w = \sum_{n=1}^r A_n w_n(x) \quad (27)$$

where w_n is a symmetrical function, and A_n is the amplitude of this function.

Substituting the deflected shape into equation (10) the total energy may be expressed as

$$\begin{aligned}
 H^* &= \frac{X}{4} \left\{ \int_{-1}^1 \left[\sum_1^r a_n w_n \right] dx - \frac{1}{2} \int_{-1}^1 \left[\sum_1^r a_n \frac{dw_n}{dx} \right]^2 dx \right\}^2 \\
 &+ \frac{1}{24X} \int_{-1}^1 \left[\sum_1^r a_n \frac{d^2 w_n}{dx^2} \right]^2 dx - P^* \left[\sum_1^r a_n w_n \right] x = 0
 \end{aligned} \tag{28}$$

$$\text{where } a_n = \frac{A_n}{R\beta^2} \quad \text{and } H^* = \frac{HX}{\beta^5} \tag{29}$$

w_n should be selected so that $\frac{dw_n}{dx}$ and $\frac{d^2 w_n}{dx^2}$ form

orthogonal sets such that

$$\int_{-1}^1 \frac{dw_n}{dx} \frac{dw_m}{dx} dx = 0 \quad n \neq m \tag{30}$$

$$\int_{-1}^1 \frac{d^2 w_n}{dx^2} \frac{d^2 w_m}{dx^2} dx = 0 \quad n \neq m$$

Then H^* can be reduced to

$$\begin{aligned}
 H^* &= \frac{X}{4} \left\{ \sum_1^r \left[a_n \int_{-1}^1 w_n dx - \frac{1}{2} \sum_1^r \left[a_n^2 \int_{-1}^1 \left(\frac{dw_n}{dx} \right)^2 dx \right] \right]^2 \right\} \\
 &+ \frac{1}{24X} \sum_1^r \left[a_n^2 \int_{-1}^1 \left(\frac{d^2 w_n}{dx^2} \right)^2 dx - P^* \sum \left[a_n (w_n)_x = 0 \right] \right]
 \end{aligned} \tag{31}$$

The equilibrium condition is

$$\frac{\partial H}{\partial a_n} = 0$$

which then renders r equations of the form

$$\begin{aligned}
 & \frac{x}{2} \left\{ \sum_1^r \left[a_n \int_{-1}^1 w_n dx \right] - \frac{1}{2} \sum_1^r \left[a_n^2 \int_{-1}^1 \left(\frac{dw_n}{dx} \right)^2 dx \right] \right\} \\
 & \cdot \left\{ \int_{-1}^1 w_n dx - a_n \int_{-1}^1 \left(\frac{dw_n}{dx} \right)^2 dx \right\} \\
 & + \frac{1}{12x} a_n \int_{-1}^1 \left(\frac{d^2 w_n}{dx^2} \right)^2 dx - P^* (w_n)_x = 0 = 0
 \end{aligned} \tag{32}$$

After Gjelsvik and Bodner the following notation is introduced

$$\begin{aligned}
 c_{1n} &= \int_{-1}^1 w_n dx & c_{2n} &= \int_{-1}^1 \left(\frac{dw_n}{dx} \right)^2 dx \\
 c_{3n} &= \int_{-1}^1 \left(\frac{d^2 w_n}{dx^2} \right)^2 dx & c_{4n} &= (w_n)_x = 0
 \end{aligned} \tag{33}$$

Thus modifying equation (32)

$$\begin{aligned}
 & \frac{x}{2} \left[\sum_1^r a_n c_{1n} - \frac{1}{2} \sum_1^r a_n^2 c_{2n} \right] \left[c_{1n} - a_n c_{2n} \right] \\
 & + \frac{1}{12x} a_n c_{3n} - P^* c_{4n} = 0
 \end{aligned} \tag{34}$$

The set of equations (34) are the equilibrium equations for symmetrical deflections of the arch. These equations are later transformed in order that P^* can be plotted against a .

Now applying the condition obtained by the classical eigenvalue considerations for asymmetrical buckling to occur, that is, expression (24), but keeping

$$w = \sum_{n=1}^r A_n w_n(x)$$

then

$$\sum_{n=1}^r (a_n \int_{-1}^1 w_n dx) - \frac{1}{2} \sum_{n=1}^r (a_n^2 \int_{-1}^1 \left(\frac{dw_n}{dx}\right)^2 dx) = \frac{K}{6X^2} \quad (35)$$

where

$$K = \frac{\int_{-1}^1 \left(\frac{dw_a}{dx}\right)^2 dx}{\int_{-1}^1 \left(\frac{dw_a}{dx}\right)^2 dx} \quad (36)$$

The constant K is the coefficient in the second mode buckling equation for a clamped column⁵,

so that

$$K = 2.0426\pi^2$$

Here w_a is the asymmetrical buckled shape.

Now substituting the conditions defined in (33) the criterion for asymmetrical buckling becomes

$$\sum_{n=1}^r a_n c_{1n} - \frac{1}{2} \sum_{n=1}^r a_n^2 c_{2n} = \frac{K}{6X^2} \quad (37)$$

Hence to obtain the asymmetrical buckling load P_T^* the right hand side of equation (37) is

inserted into (34) yielding

$$\frac{K}{12X} \left[C_{1n} - a_n C_{2n} \right] + \frac{1}{12X} a_n C_{3n} - P_T^* C_{4n} = 0 \quad (38)$$

And so a_{nT} , the non-dimensional deflection at P_T^* , is

$$a_{nT} = \frac{12 X P_T^* C_{4n} - K C_{1n}}{C_{3n} - K C_{2n}} \quad (39)$$

If P_T^* is known, then this expression may be applied directly to evaluate a_{nT} .

Reworking (37), by replacing a_n with expression (39) above, the criterion for asymmetrical buckling becomes

$$(12 X P_T^*)^2 \sum_1^r \left[\frac{C_{2n} C_{4n}^2}{(C_{3n} - K C_{2n})^2} \right] - 24 X P_T^* \sum_1^r \left[\frac{C_{1n} C_{3n} C_{4n}}{(C_{3n} - K C_{2n})^2} \right] + \frac{K}{3X^2} + K \sum_1^r \left[\frac{C_{1n}^2 (2C_{3n} - K C_{2n})}{(C_{3n} - K C_{2n})^2} \right] = 0 \quad (40)$$

Introducing the following notation

$$D_1 = \sum_1^r \left[\frac{C_{2n} C_{4n}^2}{(C_{3n} - K C_{2n})^2} \right] \quad (41)$$

$$D_2 = \sum_1^r \left[\frac{C_{1n} C_{3n} C_{4n}}{(C_{3n} - KC_{2n})^2} \right] \quad (41)$$

$$D_3 = \sum_1^r \left[\frac{C_{1n}^2 (2C_{3n} - KC_{2n})}{(C_{3n} - KC_{2n})^2} \right]$$

the asymmetrical buckling load is given in the following equation

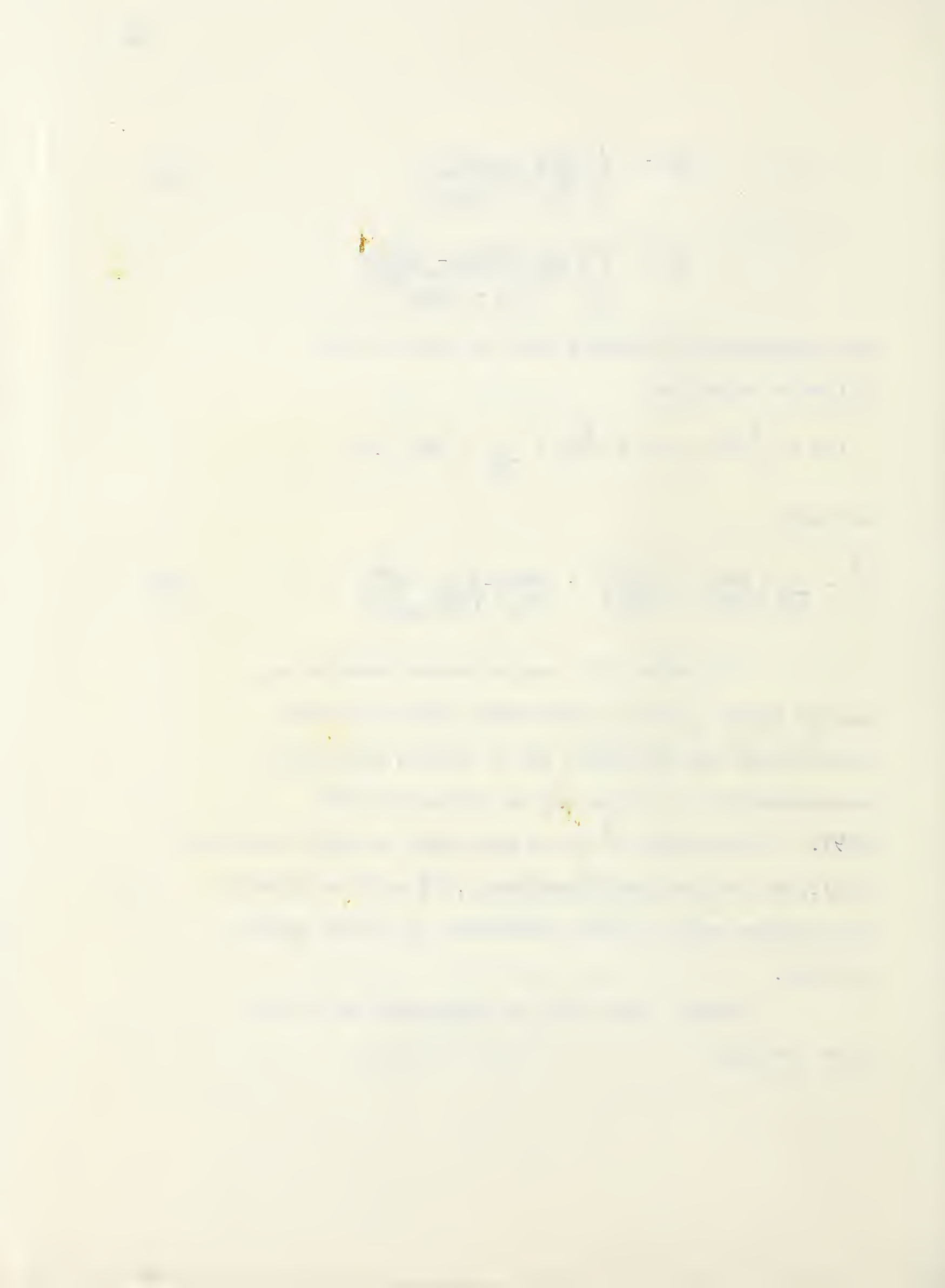
$$(12 \times P_T^*)^2 D_1 - 24 \times P_T^* D_2 + \frac{K}{3X^2} + KD_3 = 0$$

so that

$$P_T^* = \frac{1}{12X} \left\{ \left(\frac{D_2}{D_1} \right) \pm \left[\left(\frac{D_2}{D_1} \right)^2 - \left(\frac{KD_3}{D_1} \right) - \left(\frac{K}{3X^2 D_1} \right) \right]^{\frac{1}{2}} \right\} \quad (42)$$

Therefore if a satisfactory function w_n can be found P_T^* may be calculated after initially determining the various C and D values, and its corresponding a_{nT} value may be evaluated from (39). To determine P_U^* it is necessary to apply equations (34), and by plotting P^* against a , P_U^* will be given at the maximum value, which terminates the first stable section.

These steps will be elaborated on in the next section.



(D) Application of a General Displacement Function to the Series Solution.

Consider the following function

$$w_n = \frac{1}{2} (1 + \cos n\pi x), \quad n \text{ odd}$$

$$w_n = \frac{1}{2} (1 - \cos n\pi x), \quad n \text{ even}$$

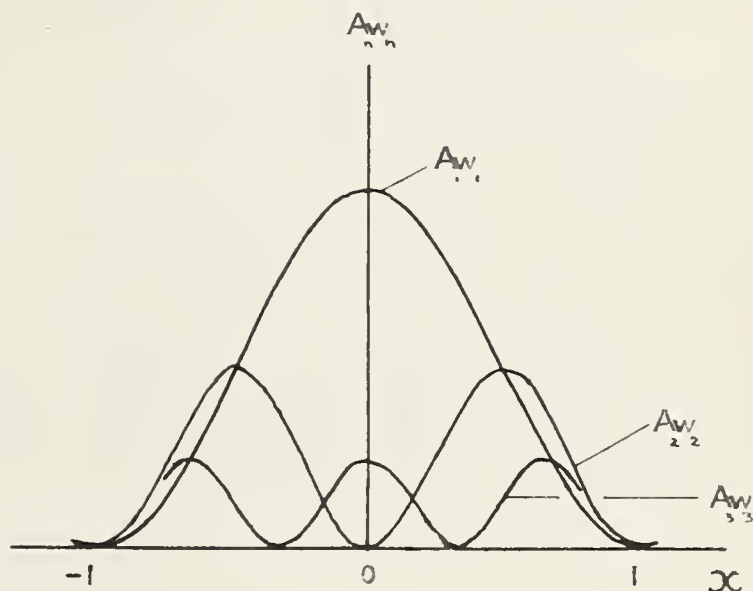


FIG. 3 SKETCH OF FUNCTION [43] FOR INITIAL VALUES

This function satisfies the boundary conditions imposed by clamping the arch at its ends and also it meets the conditions of orthogonality required by equation (30).

Determining now the various C and D values,

- all n, $C_{1n} = 1$
-
- $C_{2n} = n^2\pi^2/4$
-
- $C_{3n} = n^4\pi^4/4$ (44)
- odd n, $C_{4n} = 1$
- even n, $C_{4n} = 0$

The ensuing D terms are thus

$$D_1 = \sum_1^r \left[n^2 \pi^6 \frac{4}{(n^2 - 2.0426)^2} \right], \text{ odd } n$$

$D_1 = 0 \quad , \text{ even } n$

$$D_2 = \sum_1^r \left[\pi^4 \frac{4}{(n^2 - 2.0426)^2} \right] \quad , \text{ odd } n \quad (45)$$

$$D_2 = 0 \quad , \text{ even } n$$

$$D_3 = \sum_1^r \left[\frac{4(2n^2 - 2.0426)}{n^2 \pi^4 (n^2 - 2.0426)^2} \right] \quad , \text{ all } n$$

Hence P_T^* may be calculated for solutions containing a varying number of terms. In their paper Gjelsvik and Bodner stated that although a substantial

difference is obtained between the one and the two term solution, very little deviation is recorded between the latter and a six term solution.

However the application of a series with more than two terms to evaluate the upper buckling load is an extremely arduous undertaking and subsequently the two term solution will be derived. This is later shown to be of sufficient adequacy.

Taking $r = 2$, from equation (42)

$$P_T^* = \frac{\pi^2}{12X} \left[1 + (0.2245 - 0.1847 \frac{\pi^4}{X^2})^{\frac{1}{2}} \right] \quad (46)$$

To obtain the load deflection curve and the upper buckling load, equations (34) are now developed. For any number of terms, the expression below follows immediately

$$\frac{P^* c_{4n} - \left(\frac{a_n c_{3n}}{12X} \right)}{c_{1n} - a_n c_{2n}} = \frac{P^* c_{4m} - \left(\frac{a_m c_{3m}}{12X} \right)}{c_{1m} - a_m c_{2m}}$$

Solving for a_n

$$a_n = \frac{P^* (c_{4n}c_{1m} - c_{1n}c_{4m} - a_m c_{4n}c_{2m}) + a_m \left(\frac{c_{1n}c_{3m}}{12X} \right)}{- P^* c_{2n}c_{4m} + \frac{a_m}{12X} (c_{2n}c_{3m} - c_{3n}c_{2m}) + \left(\frac{c_{1m}c_{3n}}{12X} \right)} \quad (47)$$

For $r = 2$, equation (47) reduces to

$$a_2 = \frac{1}{\pi^2} \left[\frac{P^* - \left(\frac{d}{48u} \right)}{\frac{1}{u} \left(\frac{d}{16} - \frac{1}{3} \right) + P^*} \right] \quad (48)$$

where $d = \pi^2 a_1$ and $u = \frac{X}{\pi^2}$

Thus in the first of the equilibrium equations (34), a_2 can be replaced by (48), which results in an expression relating P^* and a . In a two term series solution, it should be noted that a , the non-dimensional central deflection of the arch, is equal to a_1 . This is adequately clarified by Figure 3.

Developing the first equilibrium equation

$$\left[\pi^2 a_1 + \pi^2 a_2 - \frac{a_1^2 \pi^4}{8} - \frac{a_2^2 \pi^4}{2} \right] \left[1 - \frac{a_1 \pi^2}{4} \right] + \frac{a_1 \pi^6}{24X^2} - \frac{2\pi^2 P^*}{X} = 0 \quad (49)$$

Substituting for a_2 from (48)

$$\left[\left(d - \frac{d^2}{8} \right) (h_2 + P^*)^2 - (h_1 - P^*) (h_2 + P^*) - \frac{1}{2} (h_1 - P^*)^2 \right] \cdot \left(1 - \frac{d}{4} \right) + \left(\frac{d}{24u^2} - \frac{2P^*}{u} \right) (h_2 + P^*)^2 = 0 \quad (50)$$

where

$$h_1 = \frac{d}{48u}$$

$$h_2 = \frac{1}{u} \left(\frac{d}{16} - \frac{1}{3} \right)$$

The load deflection relation is thus determined, although in a particularly awkward fashion, by (50) above. For simplification consider the new variables

$$\bar{a} = d - 4 \quad p = 48uP^* - 4 \quad (51)$$

Rewriting (50), we have

$$K_0 + K_1 p + K_2 p^2 - 4p^3 = 0 \quad (52)$$

where

$$K_0 = \bar{a}^3 \left[36 + 3u^2 (9\bar{a}^2 - 116) \right]$$

$$K_1 = \bar{a}^2 \left[-12 + 3u^2 (6\bar{a}^2 - 120) \right] \quad (53)$$

$$K_2 = \bar{a} \left[-20 + 3u^2 (\bar{a}^2 - 20) \right]$$

With the aid of (52) values of p , and thus P^* from (51), may be obtained for varying d values for any given X .

Gjelsvik and Bodner did not state how they obtained successive values from (52), which is a lengthy

process by manual calculation.

A computer programme was devised (Appendix B) which rendered the successive values of P^* against a_1 for a wide range of X values. The X values selected included those in the range which Gjelsvik and Bodner examined experimentally and theoretically, through to quite large values.

The load deflection curves from the results furnished by the University of Alberta IBM 1620 computer are presented in Chapter 4, where they may be simultaneously compared with the experimental plots.

Also depicted in the same section is the theoretical curve of load against deflection by applying van Wijngaarden's theory, which was evaluated by J. S. Kennedy at an earlier date.

CHAPTER 3

APPARATUS AND EXPERIMENTAL PROCEDURE

(A) Aparatus

The experimental equipment used is shown in Figure 4.

The arch bed was a length of 65S-T6 6" x 2 $\frac{3}{4}$ " aluminum channel, weighing 4.07 pounds per foot; the top face and the tips of the channel side walls were milled in the Department workshop to ensure that these surfaces would be smooth and parallel to each other.

The top face of the channel was then machined as in Figure 5. The centre slot would thus enable sufficiently large deformations to be applied to the arch, should it prove necessary during a test for the arch centre to be deflected to a very low position. The parallel rows of holes were drilled so that the arch clamp base would slot in via guide pegs, and would thus be aligned correctly with no further effort. The holes tapped at regular intervals along the channel centre-line were so placed to mate with the fixing bolt of each clamp base.

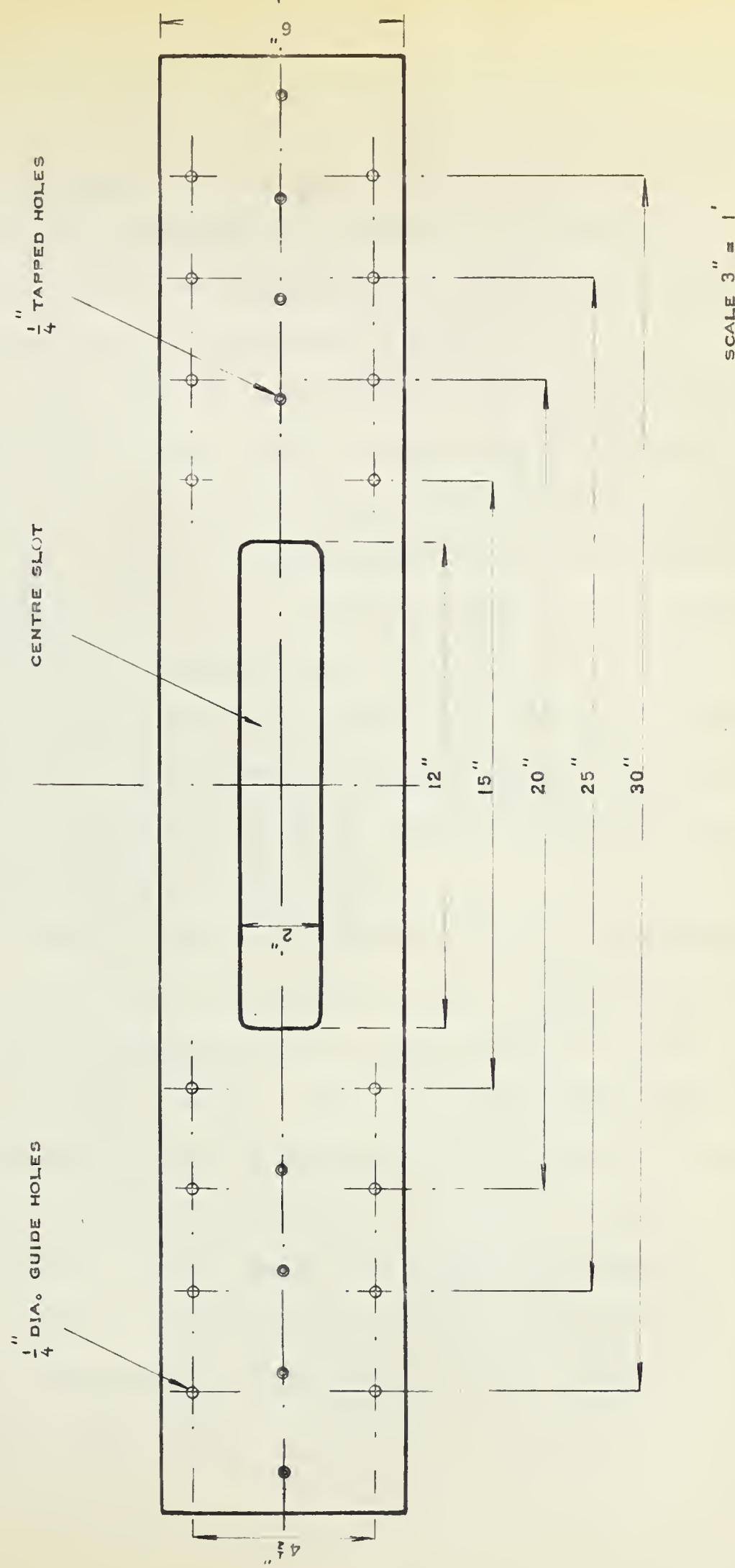
The arch clamp surfaces were milled so that



FIG. 4 GENERAL VIEW OF APPARATUS



FIG. 5 PLAN VIEW OF ARCH BED



when the clamps were set in position on the arch bed, the angle of inclination of the arch built-in end would be at 30° to the horizontal. Details of the arch clamp structure are depicted in Figure 6.

The arch bed was fixed to the scale pan of a Troemner field scale, which in turn had been securely located on a firm timber bench. The scale pan had been skimmed on a lathe to ensure that the arch bed would rest squarely upon it. Careful adjustment of the bed scale system now followed and it was checked with a sensitive spirit level to ensure that the upper surface of the channel lay in the horizontal plane. The eventual degree of horizontal register compared favourably with the Department milling machine bed.

Subsequent arch deflections were procured by a hook gauge, which was supported by a tubular steel frame. The vertical alignment of the gauge measure was set with the aid of a field transit. Two interchangeable loading heads were constructed to fit squarely on the bottom of the gauge measure; a loading head which would permit any of the ensuing test arches to deform only in a symmetrical mode, as in Figures 7 and 8, and an asymmetrical loading head which would not restrict the manner of the deformations. Figures 9 to 11 illustrate the latter.

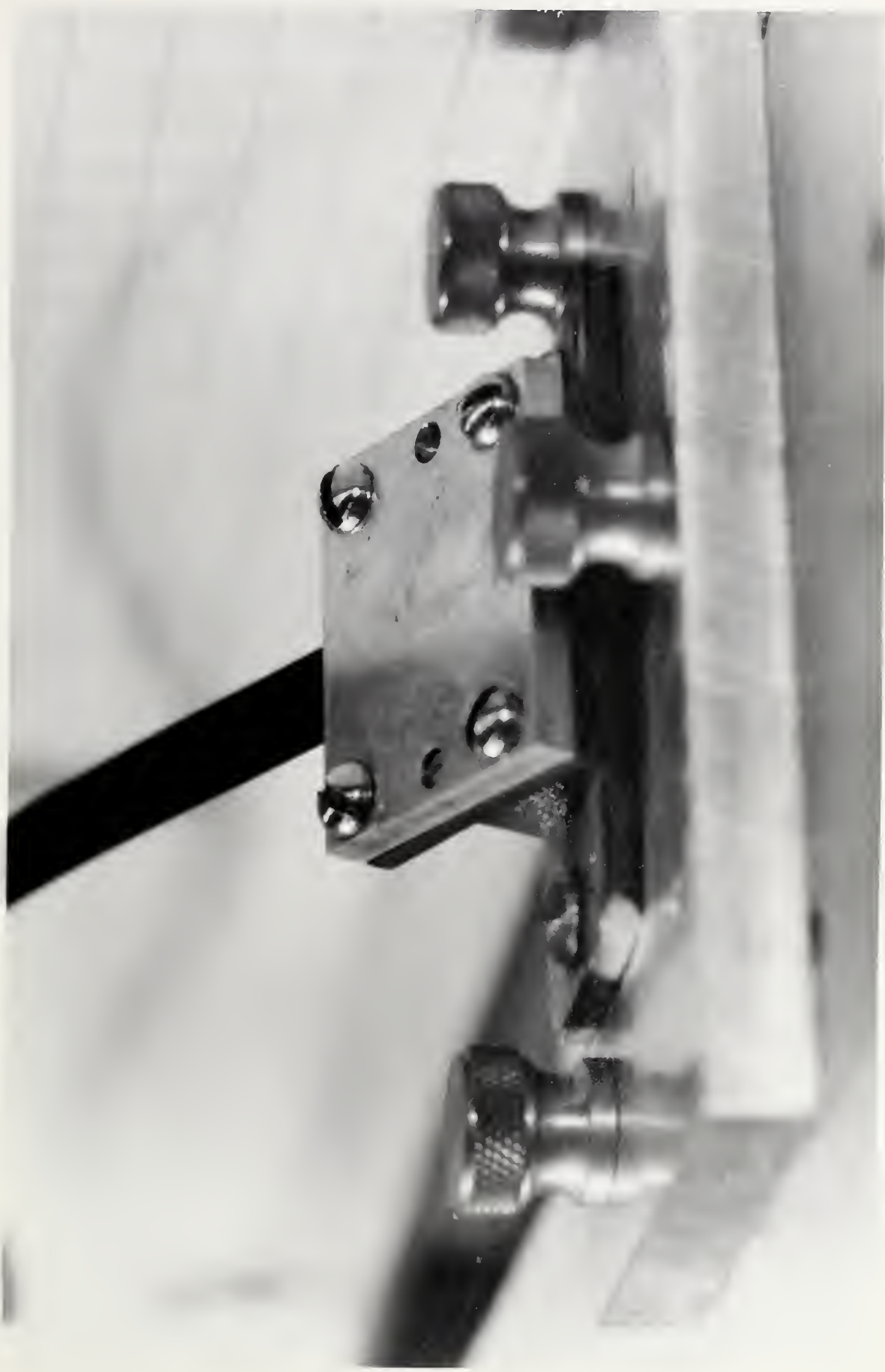


FIG. 6 CLOSE-UP OF ARCH CLAMP

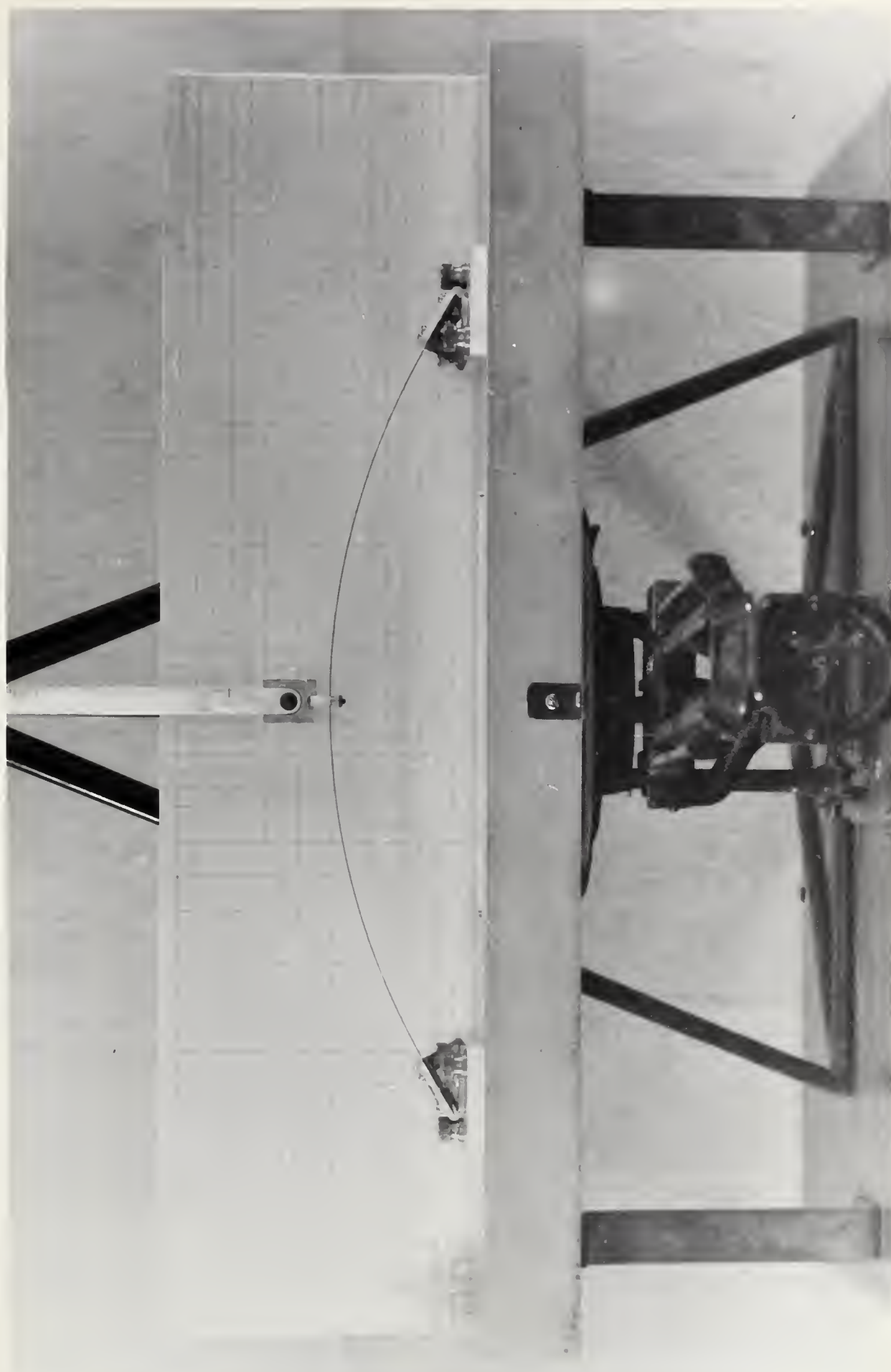


FIG. 7 SYMMETRIC HEAD, NO LOAD

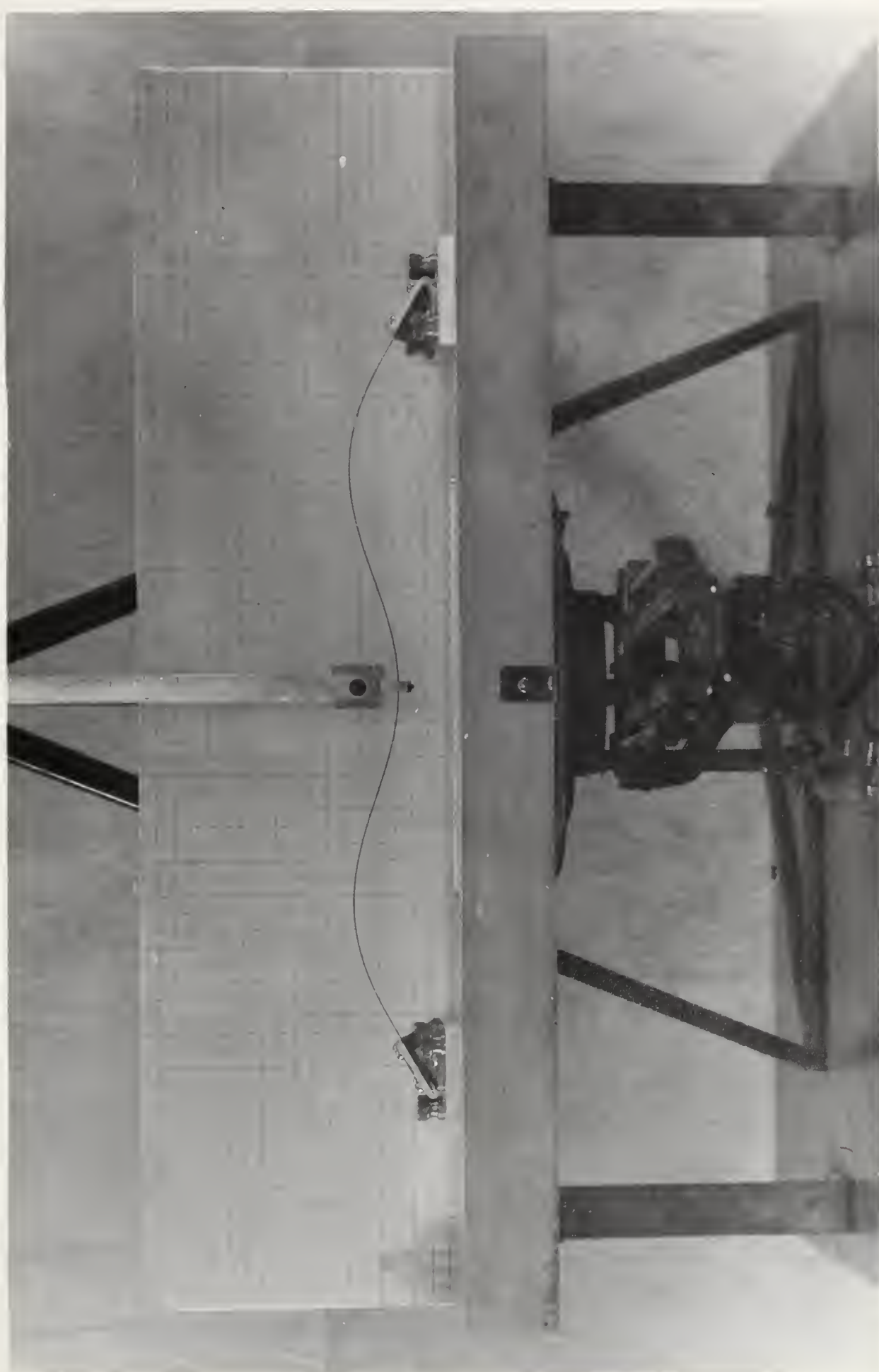


FIG. 8 SYMMETRIC HEAD, ARCH BUCKLED SYMMETRICALLY

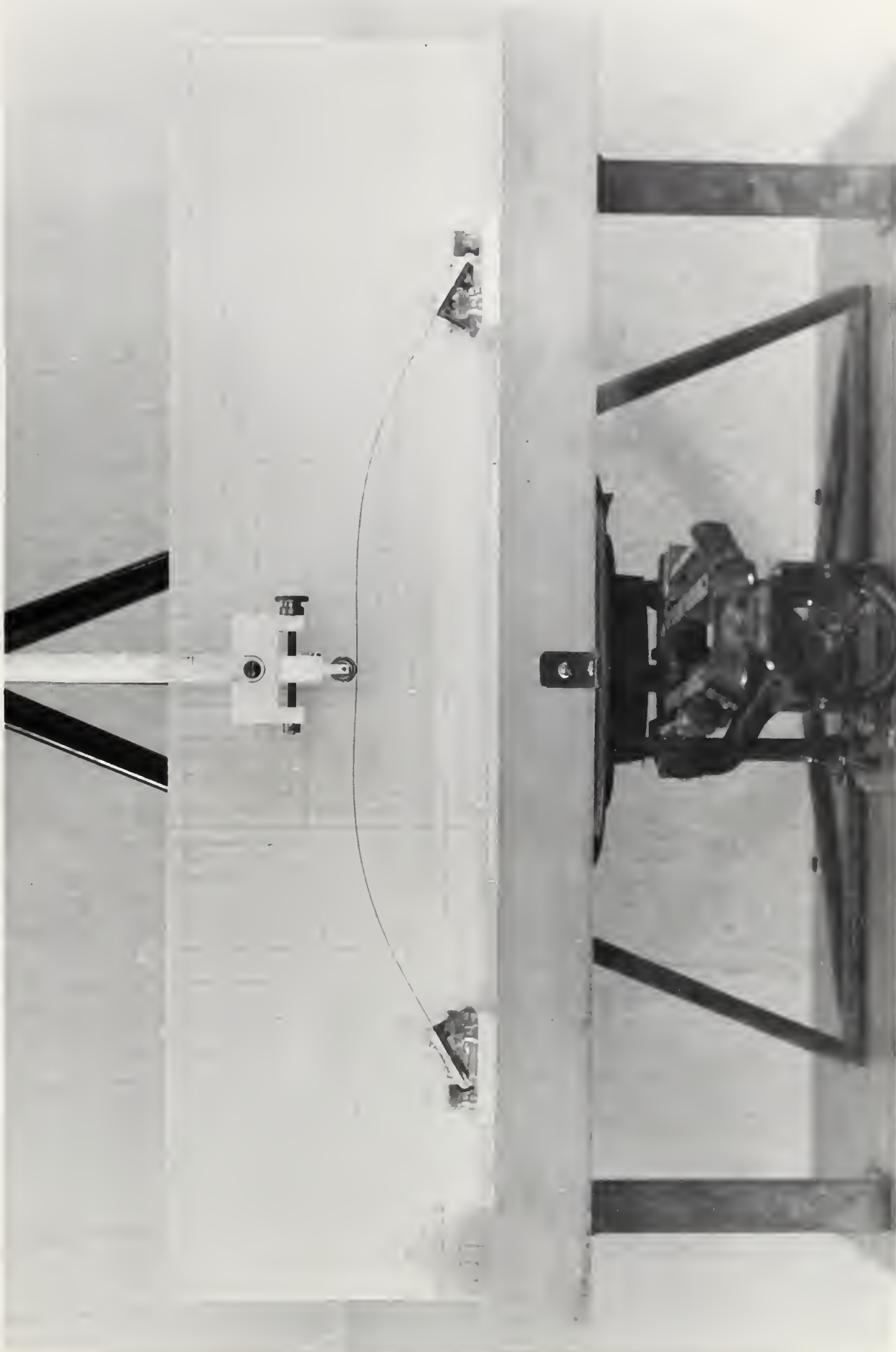


FIG. 9 ARCH PRIOR TO BUCKLING RETAINING SYMMETRICAL MODE

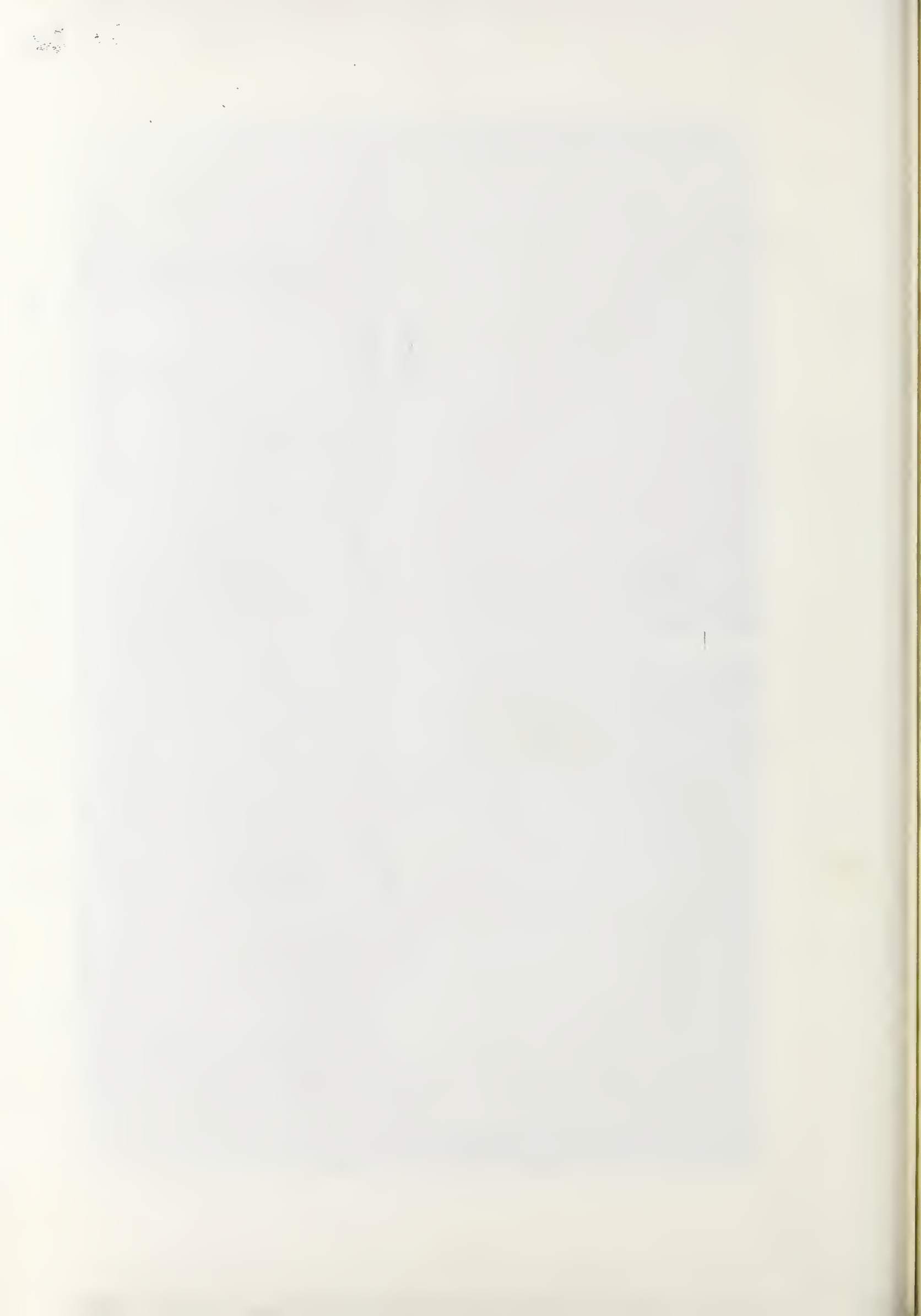
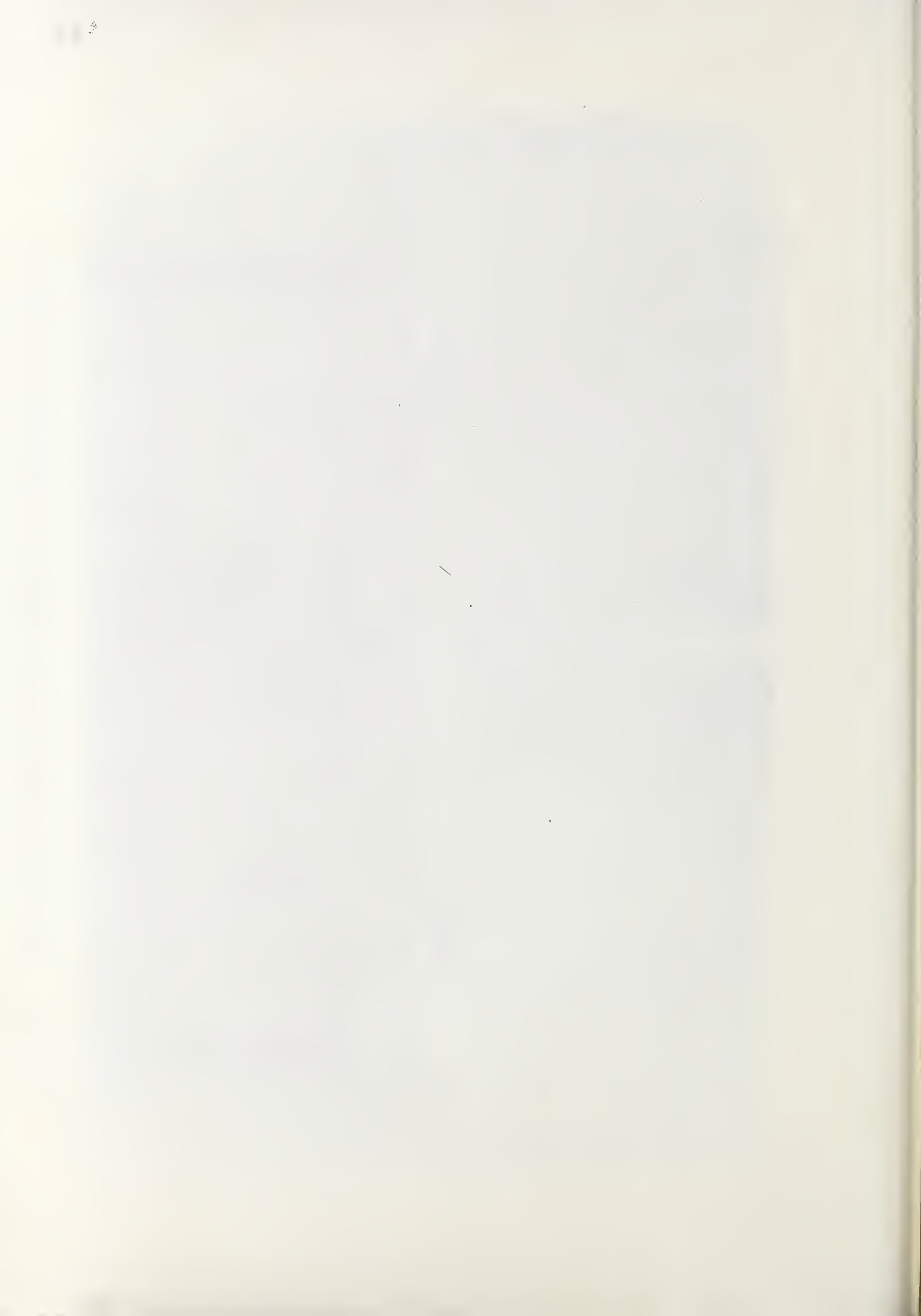




FIG. 10 ARCH IN UNSTABLE REGION, EXHIBITING PRONOUNCED ASYMMETRY



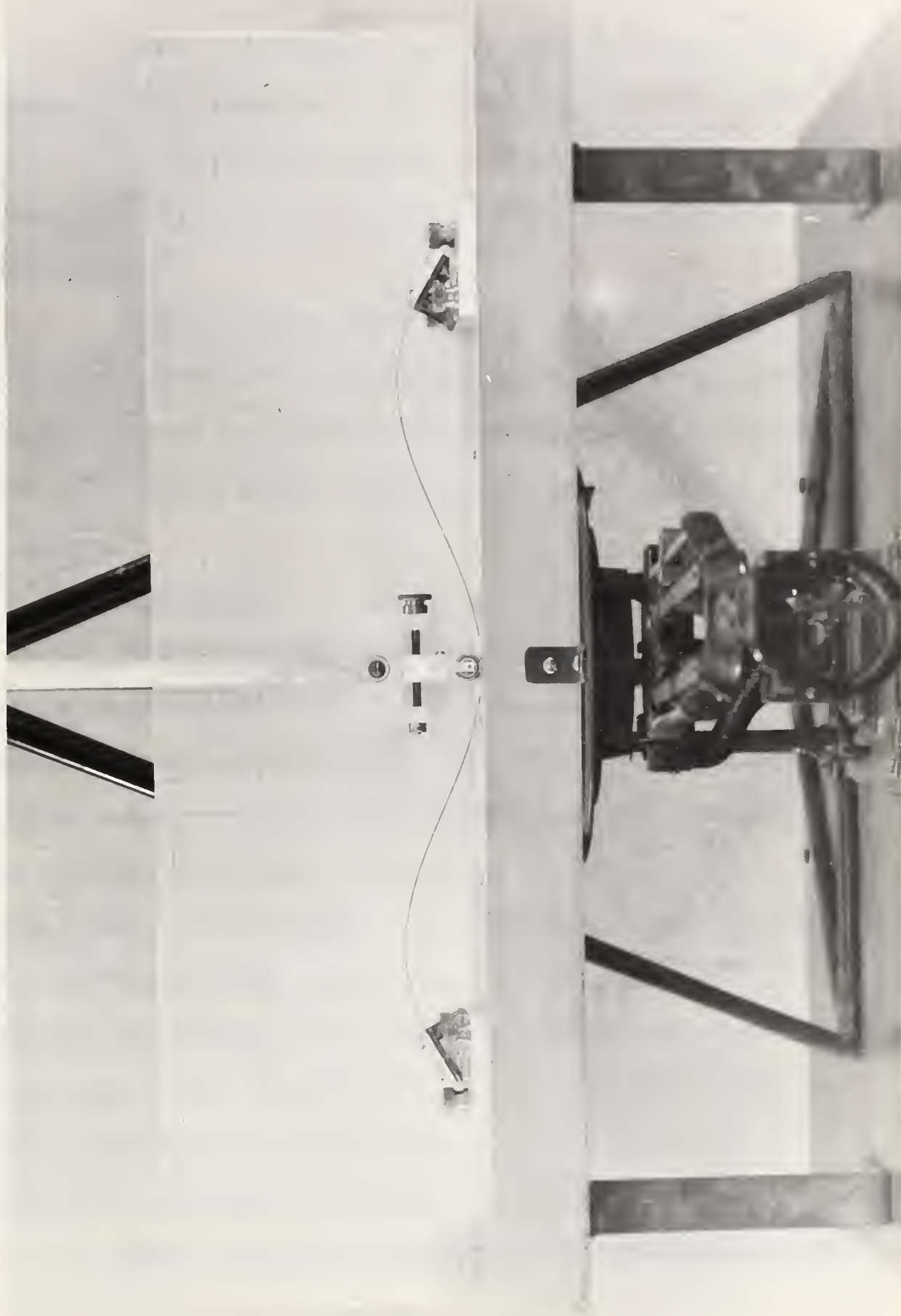


FIG. II ARCH DEFLECTED TO SECOND STABLE REGION, SHOWING RETURN TO SYMMETRY

Care was taken to place the scale-arch bed system and the gauge support frame relative to each other, so that final adjustment would leave the loading head accurately lined up with the arch bed centre-lines.

Prior to its installation, the Troemner field scale had been investigated for accuracy, using weights checked on a Mettler comparater scale. The scale cumulative error was found to be a maximum of ± 5 grams.

(B) Test Specimens

All the arch test-pieces were cut from banding steel kindly supplied by Acme Steel. The circumferential arch lengths for the varying clamp settings were scribed by a milling machine, in each case leaving sufficient overlap to be accomodated comfortably in the clamps. In addition centre-lines were scribed on each piece to correspond to similar marks on the clamps and thereby assisted in alignment. The painted black finish of the banding steel lent itself readily to this process. Each length was diligently inspected for imperfections and kinks.

Seven arches were considered experimentally;

dimensions are given in Table 1 and, for the sake of convenience, each specimen has been given an identity number.

TABLE 1. TEST SPECIMENS

IDENTITY NO.	SPAN	DEPTH	WIDTH	$X = \beta^2 R/t$
S1	15"	0.0152"	0.75"	270.5
S2	20"	0.0149"	0.75"	369.0
S3	25"	0.0144"	0.75"	475.9
S4	30"	0.0155"	0.75"	530.6
S5	20"	0.0197"	0.625"	278.3
S6	20"	0.0210"	0.5 "	261.1
S7	30"	0.0127"	0.5 "	647.6

The X values of these arches were all quite large, compared to the range Gjelsvik and Bodner investigated, which varied from $X = 3.69$ to $X = 16.25$. Although it was felt desirable to include specimens which did have smaller X values, the correspondingly higher buckling loads which would result were outside the scope of the Troemner scale. But had a large scale been employed initially, then a considerable loss of accuracy would have been sustained in the low load readings.

(C) Experimental Procedure

With a test piece firmly located by the clamps the jockey weight of the scale was adjusted so that the scale reading was zero under the action of the undeformed arch and the arch bed. The hook gauge measure was now lowered until the loading head just touched the arch. In the case of the symmetrical head, the head was securely fixed to the arch centre.

The measure was then deflected incrementally, and for each setting the balancing weight registered on the scale arm was noted; hence with the scale adjusted so that the scale pan was again held at the original height, a situation was obtained whereby a known central load induced the given arch to deflect a measured distance.

For each specimen the asymmetrical loading head was set onto the hook gauge measure immediately after a test with the restrictive head, to facilitate direct comparisons. The symmetrical head was replaced afterwards to check the scale zero reading for consistency. With the advent of any such deviation, the recently acquired readings were rejected.

Precautions were taken to load the arch with the free head very gently in the region of the upper buckling

load as sudden deflections would possibly cause the arch to buckle transitionally under the influence of the sudden motion, rather than the static load. Whenever the arch was deformed asymmetrically, the point of application of the load was moved until it was again at the mid-length of the arch. However, lateral movement of the head's roller registered little, if any, difference with the scale and so the roller was kept slightly to the inner side of the centre scribe line. This minor precaution prevented inconvenient snap-throughs of the asymmetry to the opposite side of the arch.

Results recorded in this manner were repeatable to within the scale error. Difficulty was experienced with the shortest arch length, where it was found that repeated discrepancies were caused by yielding at the ends. By avoiding any further deflection just after the lower buckling load was attained, this problem was overcome.

CHAPTER 4

RESULTS AND DISCUSSION

(A) Symmetrical Buckling

Dimensional analysis of the problem revealed a function containing the following possible dimensionless groups, $\frac{PR^{z-2}}{Ebt^{z-1}}$, where z is any number, $\frac{\delta}{R}$, $\frac{b}{t}$, $\frac{R}{t}$, β and Poisson's ratio. By the use of only one material for the test-pieces, Poisson's ratio was kept at a constant value; all the experiments were conducted for a particular angle subtended at the centre of the circular arch, which fixed β . This left the relationship

$$\frac{PR^{z-2}}{Ebt^{z-1}} = F\left(\frac{\delta}{R}, \frac{b}{t}, \frac{R}{t}\right)$$

Neither van Wijngaarden nor Gjelsvik and Bodner indicated that the variation of the breadth to thickness ratio of the arch would have an effect on the resulting load deflection curves. To examine any possible influence of this dimensionless parameter, the load deflection curves for three specimens S1, S5, and S6, which had an approximately common $\frac{R}{t}$ ratio, have been plotted in Figure 19. Van Wijngaarden coordinates were chosen for later convenience, otherwise the effect could have been examined as easily on

a Gjelsvik-Bodner basis whereby $X = \frac{R\beta^2}{t}$ was held constant. From this diagram it may be observed that any variation in the parameter $\frac{b}{t}$, over the range involved in the tests, seems to have no predictable influence upon the relative position, or shape, of the curve.

Theoretical load deflection curves for the four pieces S1 - S4 of varying X values, obtained by application of the Gjelsvik-Bodner theory, have been plotted in Figure 12. On this non-dimensional basis it may be seen that the upper and lower buckling loads occurred at consistent deflections, a values of 0.155 and 0.65 respectively. As the value of X was increased, the buckling loads for each X decreased; this effect is further illustrated in Figure 17.

The experimental results for these X values are depicted in Figures 13 - 16, plotted in Gjelsvik-Bodner coordinates, showing values obtained with the symmetrical and asymmetrical heads. The latter are discussed in Section (B) of this chapter. The theoretical and experimental values for a_U and a_L agreed quite closely for the symmetrical case. However, there was a consistent discrepancy evident whereby each experimental curve was lower than the theoretical counterpart, that is for any given deflection the experimental load value was less than the

theoretical.

Developement of the van Wijngaarden theory yields only one load deflection curve, and by transforming the experimental load displacement values for specimens S1 - S4 to van Wijngaarden coordinates, the curves given in Figure 18 were acquired. From this figure it may be seen that as the radius to thickness ratio of the arch was increased, the curves were correspondingly lowered. In each case the experimental curve was lower than the theoretical van Wijngaarden curve. Thus it appeared that possibly van Wijngaarden, in his solution, unlike Gjelsvik and Bodner, did not make allowance for the parameter $\frac{R}{t}$.

Investigating further this seeming lack of a parameter, the theoretical results obtained for the specimens S1 - S4 were transferred to van Wijngaarden coordinates, and a single load deflection curve was obtained. This is shown in Figure 22, where it may be compared with the curve given by van Wijngaarden's theory. The only deviation at all between these two curves is a difference of 2 in \bar{P} , at the lower buckling load, and otherwise they concur most favourably.

Kennedy calculated the following values:

$$\begin{array}{ll} \bar{P}_U = 28.7 & \bar{P}_L = 10.2 \text{ occurring at} \\ \delta_U = 0.041 & \delta_L = 0.170 \end{array}$$

The transformed Gjelsvik-Bodner values yielded

$$\bar{P}_U = 28.73 \quad \bar{P}_L = 8.96 \text{ occurring at}$$

$$\delta_U = 0.0417 \quad \delta_L = 0.180$$

Following on from this comparative analysis, the discrepancies between the theoretical and experimental results were still unaccounted for satisfactorily. Since the two theories were in agreement it was concluded that the experimental results must be in error and it was suspected that the weight of the arch, neglected in both theories, was the cause of the consistently low results. Subsequent weighing of a length of banding steel, 1' x 0.75" x 0.015", lent support to this line of thought, as its weight was 17 grams. On this basis the arch weight for pieces S1 - S4 have been calculated and are given in Table 2.

TABLE 2. ARCH WEIGHT- BUCKLING LOAD RATIOS

SPECIMEN	X	BUCKLING LOAD (gms.)	ARCH LENGTH	WEIGHT (gms.)	WEIGHT/P _U
S1	270.5	354	15.708"	22.2	.063
S2	368.0	178	20.944"	29.6	.166
S3	475.9	96	26.180"	37.1	.386
S4	530.6	78	31.416"	44.5	.570

The weight to buckling load ratio increased considerably as

the X value increased, which would explain why the discrepancy between theoretical and experimental results became greater for the larger X values.

From Figure 16, it appeared that for test specimens with X greater than 550, a portion of the curve would be below the deflection axis, that is, the lower buckling load would be negative. Test piece S7 was therefore made up, and it was discovered that this specimen would indeed remain freely in the buckled state as surmised; Figure 24 confirms this. This contradicts Gjelsvik and Bodner's general statement "The lower buckling load of the clamped arch is greater than zero and therefore the arch cannot remain in the buckled state when the load is removed." The actual curve obtained is presented in Figure 25, although it should be emphasized that it is of dubious accuracy, due to a combination of the poor sensitivity of the Troemner scale and the small loads being measured (0 to 30 grams).

Nonetheless, the characteristic difference resulting from the use of the two different loading heads is still preserved. Such traits are reviewed in the next section.

Gjelsvik and Bodner declared that for a very low X ratio, no buckling at all would be experienced by the arch, or, that at no time would there be a region of

instability. Accordingly P_U and P_L were calculated for a wide range of X values and are stated in van Wijngaarden non-dimensional terms in Table 3.

TABLE 3. BUCKLING LOADS BY GJELSVIK-BODNER THEORY
TRANSFORMED TO VAN WIJNGAARDEN COORDINATES

X	P_U^*	\bar{P}_U	P_L^*	\bar{P}_L
3.69	0.2318	19.6	.2140	18.1
5.00	.1943	22.2	.1369	15.7
8.01	.1402	25.7	.06516	12.0
11.62	.1024	27.3	.03916	10.4
14.50	.08357	27.8	.02987	9.93
18.00	.06808	28.1	.02330	9.61
25.00	.04954	28.4	.01626	9.32
30.00	.04144	28.5	.01339	9.21
35.00	.03560	28.6	.01140	9.15
40.00	.03120	28.60	.009924	9.10
45.00	.02776	28.63	.008793	9.07
50.00	.02500	28.65	.007896	9.05
100.00	.01253	28.71	.003919	8.98
150.00	.008357	28.73	.002609	8.97
270.50	.004635	28.74	.001445	8.96
320.00	.003918	28.73	.001221	8.96
368.00	.003407	28.73	.001062	8.96
420.00	.002985	28.73	.000930	8.97
475.90	.002634	28.73	.000821	8.95
530.60	.002363	28.74	.000736	8.95

$$\bar{P} = \frac{12X}{\beta} P^* \text{ where } \beta = 0.5236$$

Inspection of this table, and of Figure 23, indicates that one theoretical curve can indeed be forecast for values of X greater than 100. However, for lower

values of X , particularly values less than 20, this is not so and van Wijngaarden's theory is not adequate. Figure 23 infers that buckling is first encountered at an X ratio of approximately 3.5, whence with subsequent increases in this parameter, \bar{P}_U and \bar{P}_L diverge rapidly to approach asymptotically the values 28.73 and 8.96 respectively.

At this stage it should be pointed out that, in their paper, Gjelsvik and Bodner stated emphatically that around $X = 10$, the asymmetrical mode became dominant, and they alluded that P_U^* values became very large after this criterion. The author does not believe this, and this point is discussed in the ensuing section.

(B) Asymmetrical Buckling

The experimental transitional modes recorded are presented in the diagrams which contain the experimental symmetrical plots, discussed previously; namely Figures 13 - 16, 20, 21 and 25. It was found that employing the non-restrictive loading head, the arches initially displayed symmetrical deformations until a deflection a_U had been applied to the arch centre. At this stage the load was slightly less than the upper buckling load. Snap buckling into the transitional mode occurred at about this deflection and the arch profile assumed a noticeable degree of asymmetry. Further vertical deflections gave a load deflection relation

which in each case, fitted approximately to a straight line when plotted. This line passed through a point near to the intersection of the intermediate buckling load line and the symmetrical load deflection curve, as predicted by theoretical considerations. For high loads the points actually lay on a curve which did not merge into a definite straight line until shortly before the aforementioned intersection. Even so, the experimental occurrence of secondary buckling is clearly noticeable on the graphs. With the exception of the S7 plot, which was not constructed for the negative lower buckling load region, each asymmetry plot rejoined the symmetrical curve slightly before the minimum part of the curve; by this time, in actual practice, the arch had regained its symmetrical shape, and further deflections yielded both the arch shape and load deflection values which were the same as those obtained with the restrictive loading head.

The degree of variation experienced at the upper load portion of the curves fell within experimental error allowances. But each arch tested had consistently slightly lower load readings in this region, under the action of the asymmetrical loading head, than those obtained using the restrictive head.

The above experimental trends did not tally with

the conclusion of Gjelsvik and Bodner that "...for large X buckling is governed by the anti-symmetrical modes." The shape acquired by the arch is irrefutably asymmetrical, yet they state this phenomenon could be observed only by careful experimentation as in their own case they witnessed very little. This was due to the very shallow arches they investigated. The author assumes therefore that the above phrase refers to the load values and the shape of the resulting curve.

Presumably they drew such a conclusion from Figure 26, reproduced from their paper. This writer is at a loss to interpret their symmetrical mode curve for it can infer only that at the critical value, P_U^* and P_T^* begin to diverge rapidly. Gjelsvik and Bodner presented only one full set of curves, for $X = 11.62$, and this is also reproduced in Figure 27; this curve, it is claimed, supports the view that after the critical value of $X = 10.6$, the transitional mode occurs before the upper buckling load is reached. Hence it follows that a_T is less than a_U , and supposedly for large values of X , the situation given in Figure 28 would arise.

Such a curve was not found for any of the experimental graphs obtained by the author. Further, for no value of X did the author, in applying the Gjelsvik-Bodner theory

find that a_U was greater than a_T . Although a passing glance at Figure 29 would perhaps indicate that P_T^* occurred before P_U^* , Figure 30 leaves no doubt that the upper buckling load is achieved first at deflection a_U . Thence at deflection at the secondary buckling mode sets in.

The critical value of 10.6 is not derived mathematically in Gjelsvik and Bodner's paper, and its exactitude is puzzling. Taking the two term series for the shape function (27), expression (46) for the transitional buckling load is

$$P_T^* = \frac{\pi^2}{12X} \left\{ 1 + \left[0.2245 - \frac{0.1847\pi^4}{X^2} \right]^{\frac{1}{2}} \right\}$$

Manipulation of the portion under the radical reveals that the lowest value of X for which an arch can experience a transitional mode is $X = 8.96$. Since at this value

$$P_T^* = P_E^* = \frac{\pi^2}{12X}$$

it may be deduced that P_T^* occurs first at the intermediate buckling load, with the mode reverting to symmetry immediately upon further deflection. For subsequent increases in X , the relative position of secondary buckling occurrence rises until the mode occurs consistently at $a = 0.2211$,

and vanishes at a constant deflection value, just before the lower buckling load is reached.

Employing a shape function with six terms, Gjelsvik and Bodner derived that

$$P_T^* = \frac{\pi^2}{12X} \left\{ 1.0219 + \left[0.1685 - \frac{0.1843\pi^4}{X^2} \right]^{\frac{1}{2}} \right\}$$

Since the lowest value of X for which P_T^* is real is now $X = 10.3$, and at this value, secondary buckling deformations are instantaneous, it would seem most unreasonable to surmise that at $X = 10.6$, the transitional mode becomes dominant. The author, therefore, on the basis of Gjelsvik and Bodner's own theory, does not agree with their conclusions.

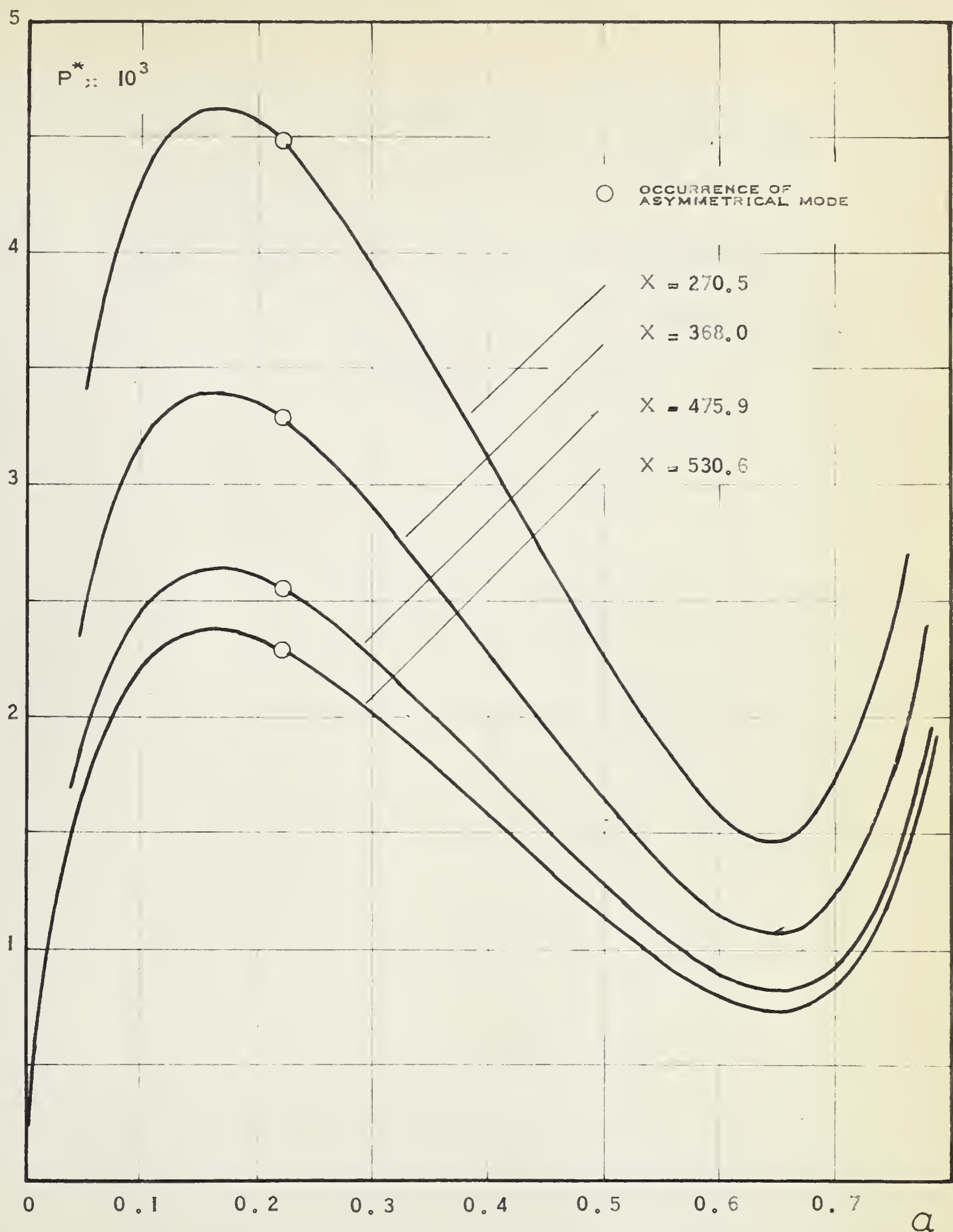


FIG. 12 THEORETICAL LOAD DEFLECTION CURVES BY GJELSVIK AND BODNER'S THEORY, FOR PIECES S1-S4



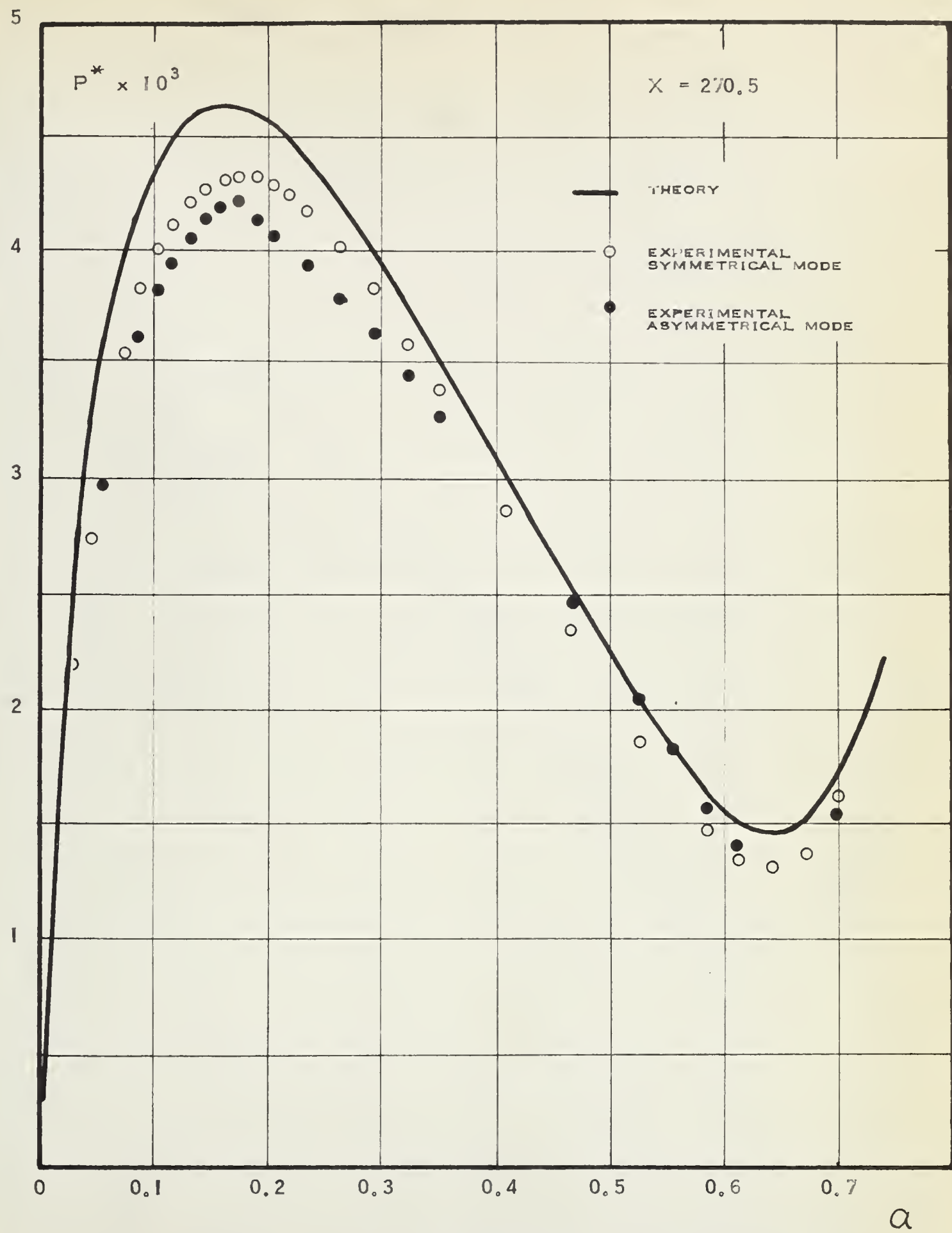


FIG. 13 THEORETICAL AND EXPERIMENTAL LOAD DEFLECTION CURVES, PIECE SI

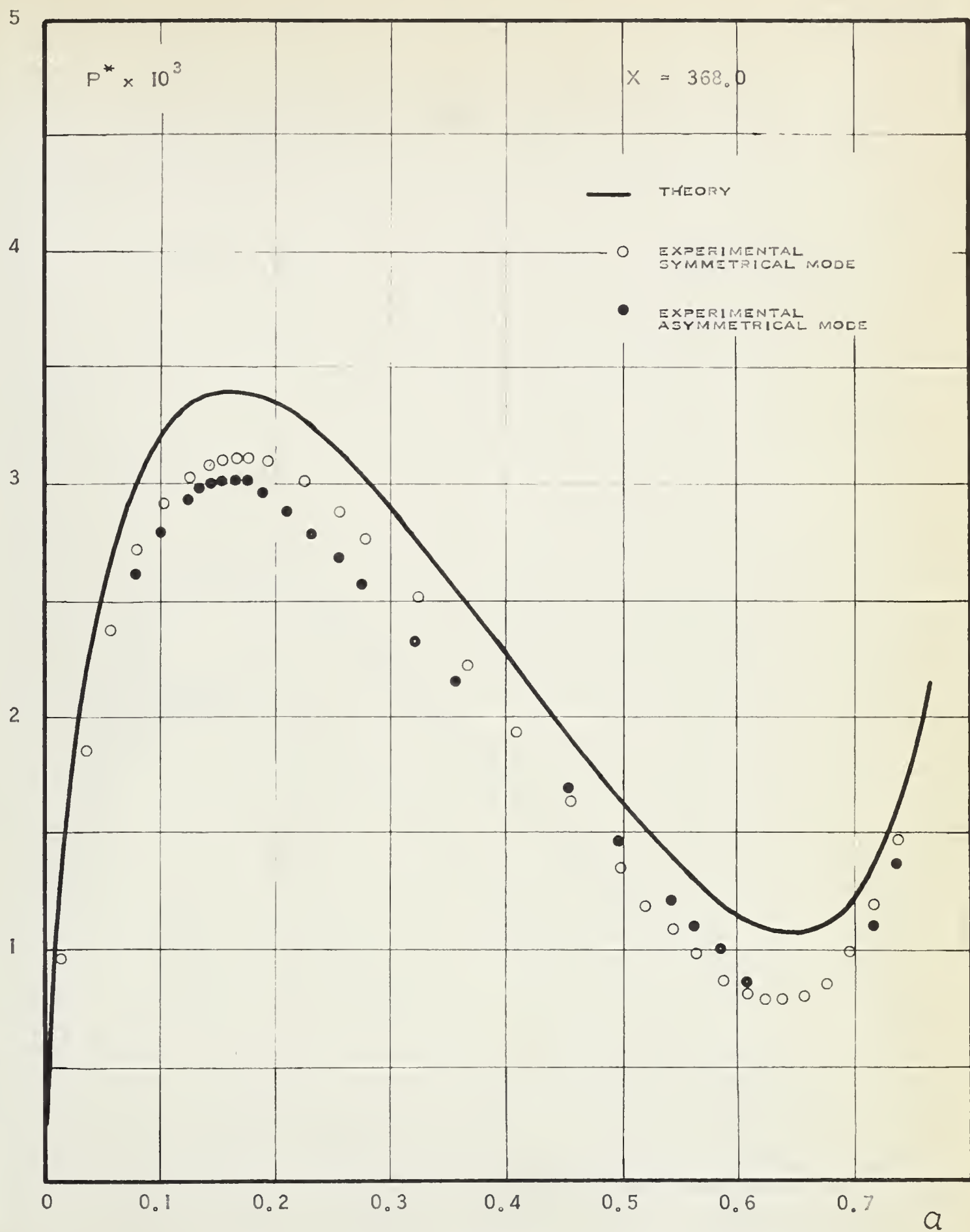


FIG. 14 THEORETICAL AND EXPERIMENTAL LOAD DEFLECTION
CURVES, PIECE S2



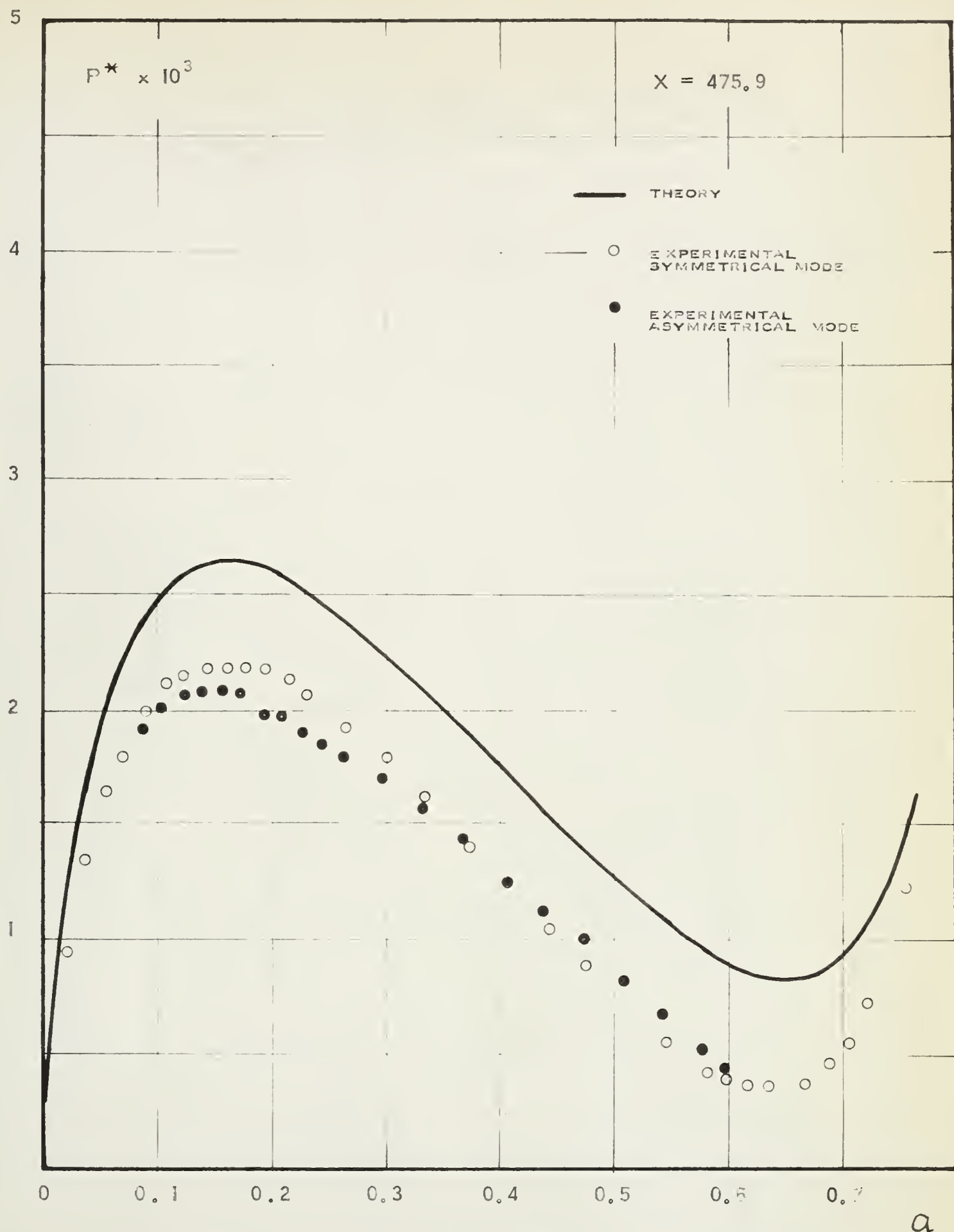


FIG. 15 THEORETICAL AND EXPERIMENTAL LOAD DEFLECTION CURVES, PIECE S3

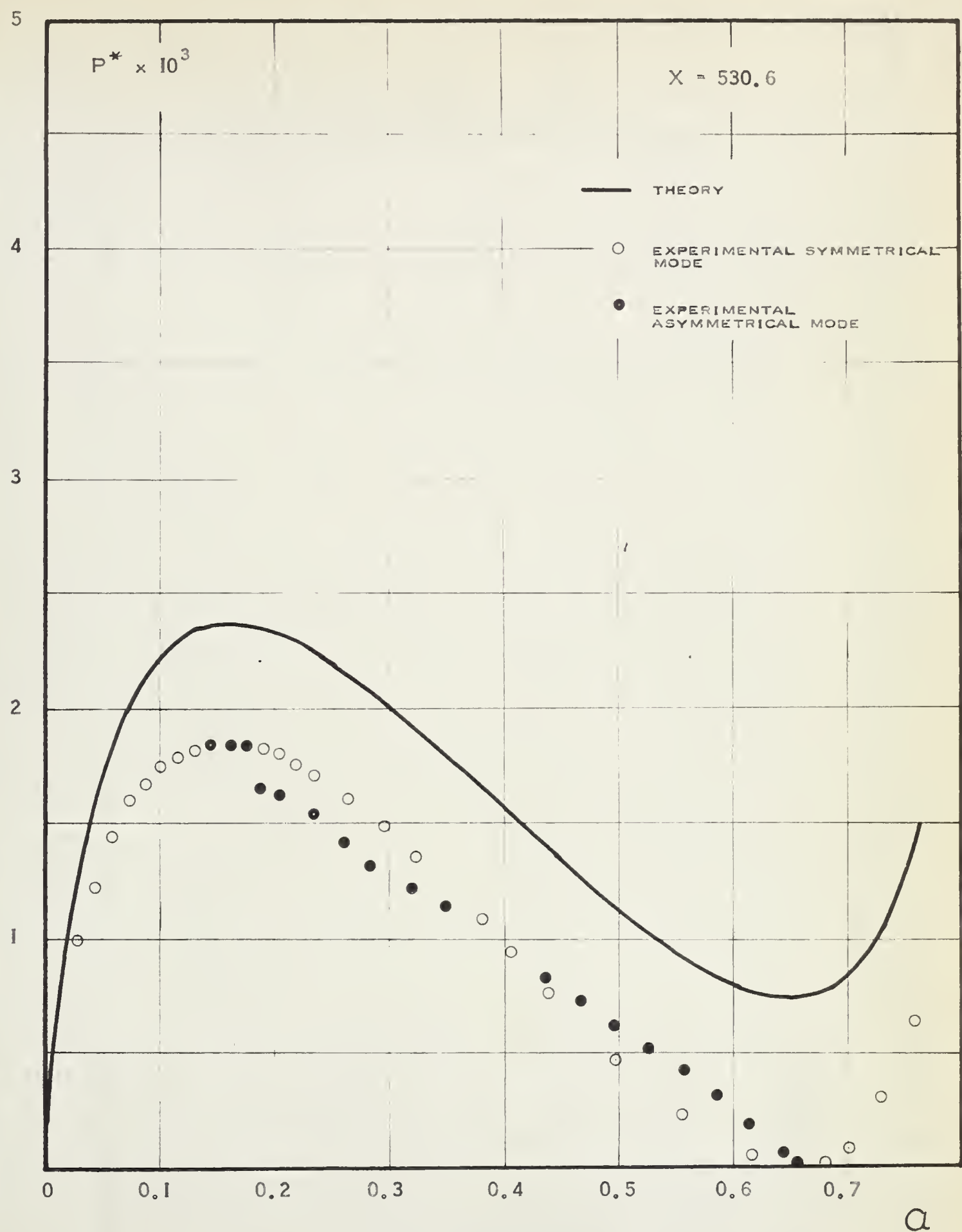


FIG. 16 THEORETICAL AND EXPERIMENTAL LOAD DEFLECTION CURVES, PIECE S4



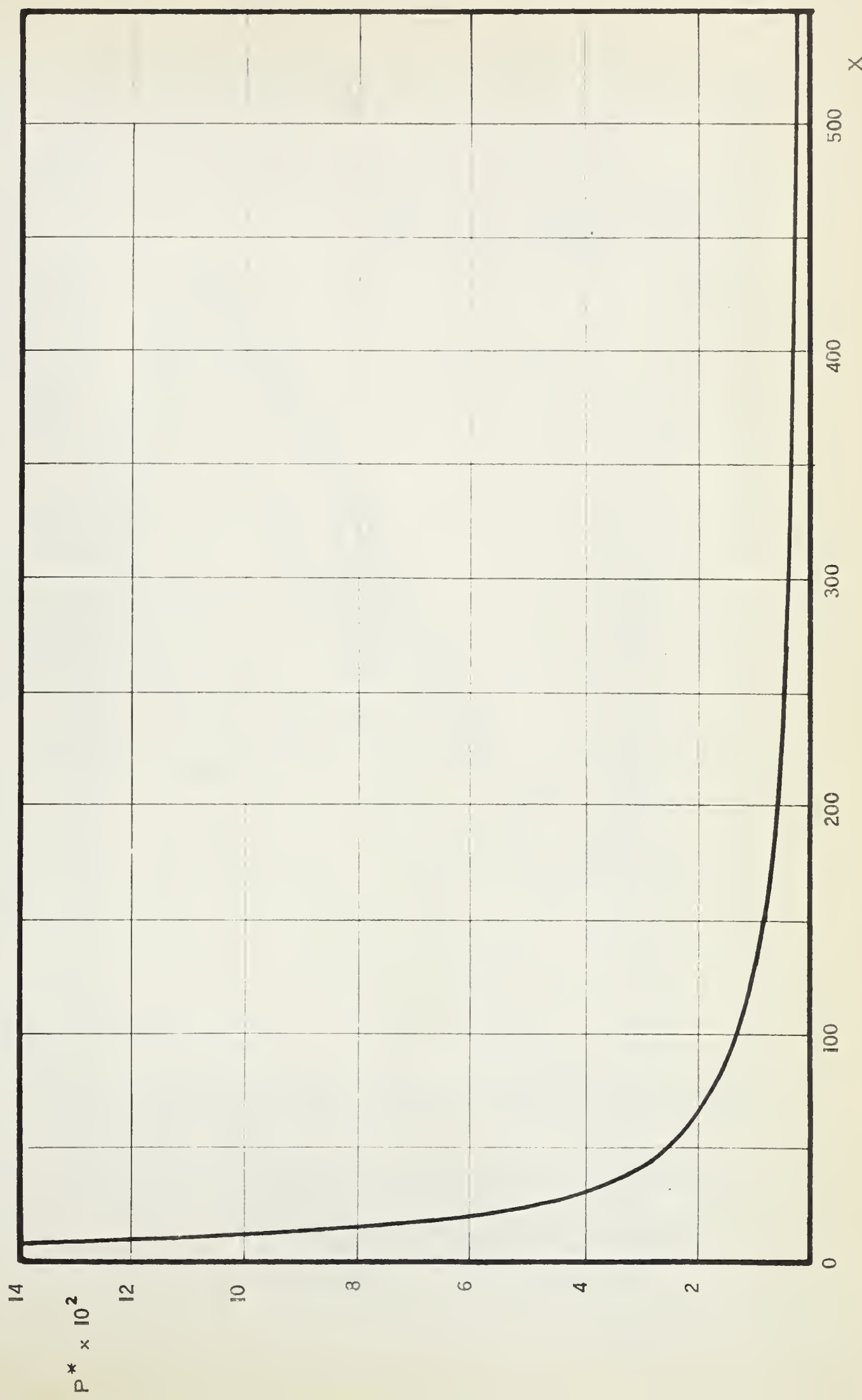
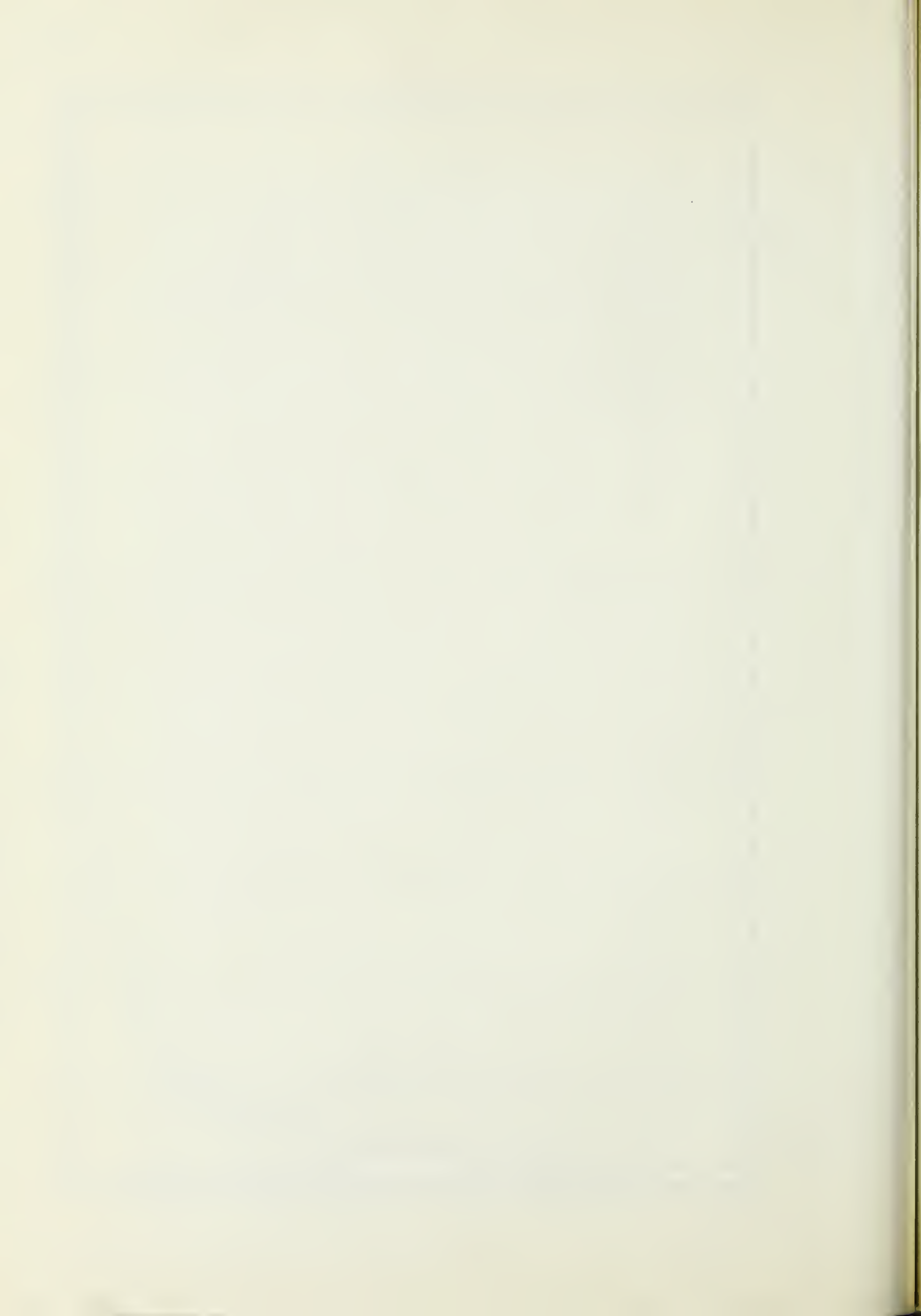


FIG. 17 THEORETICAL UPPER BUCKLING LOADS



P

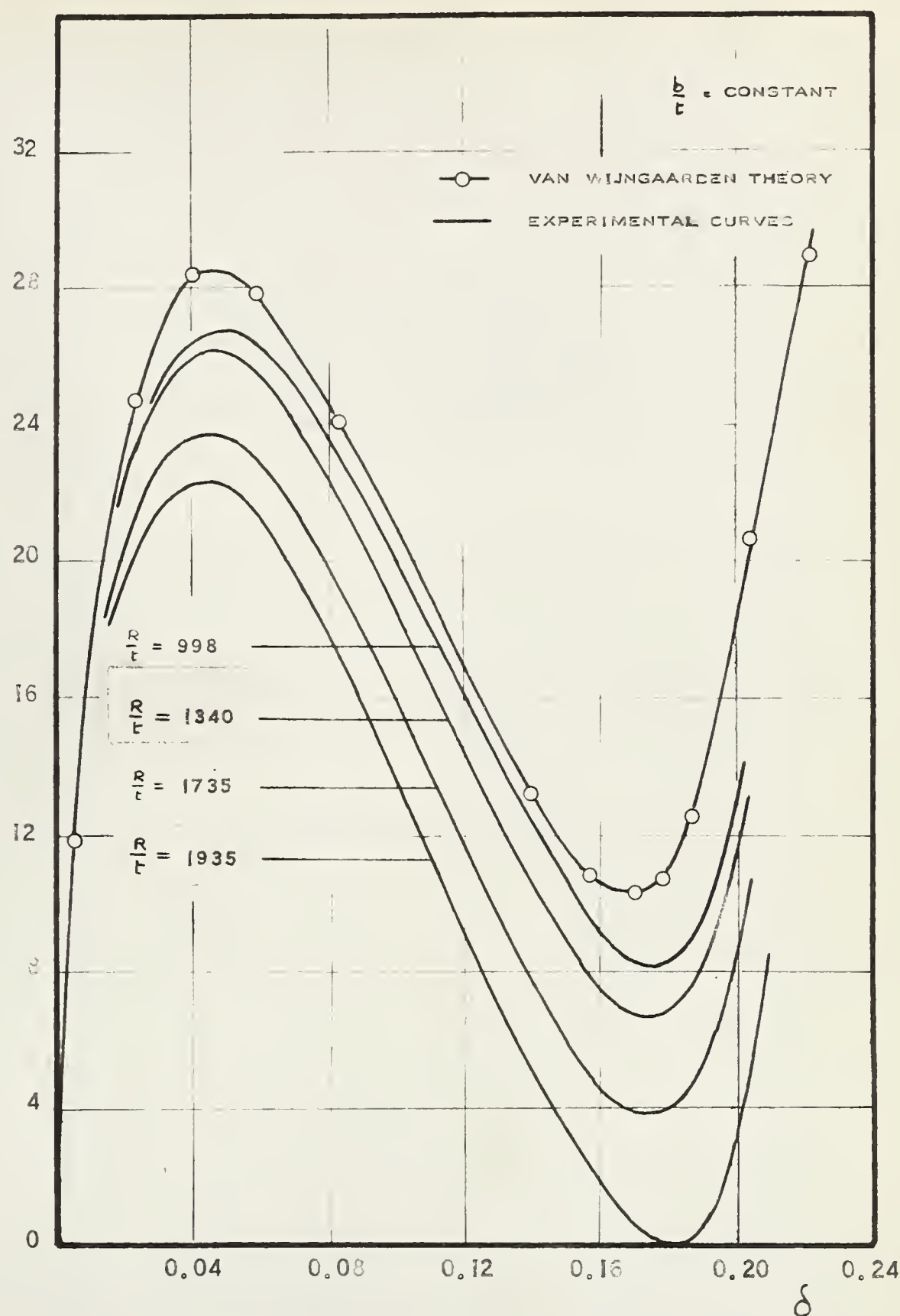
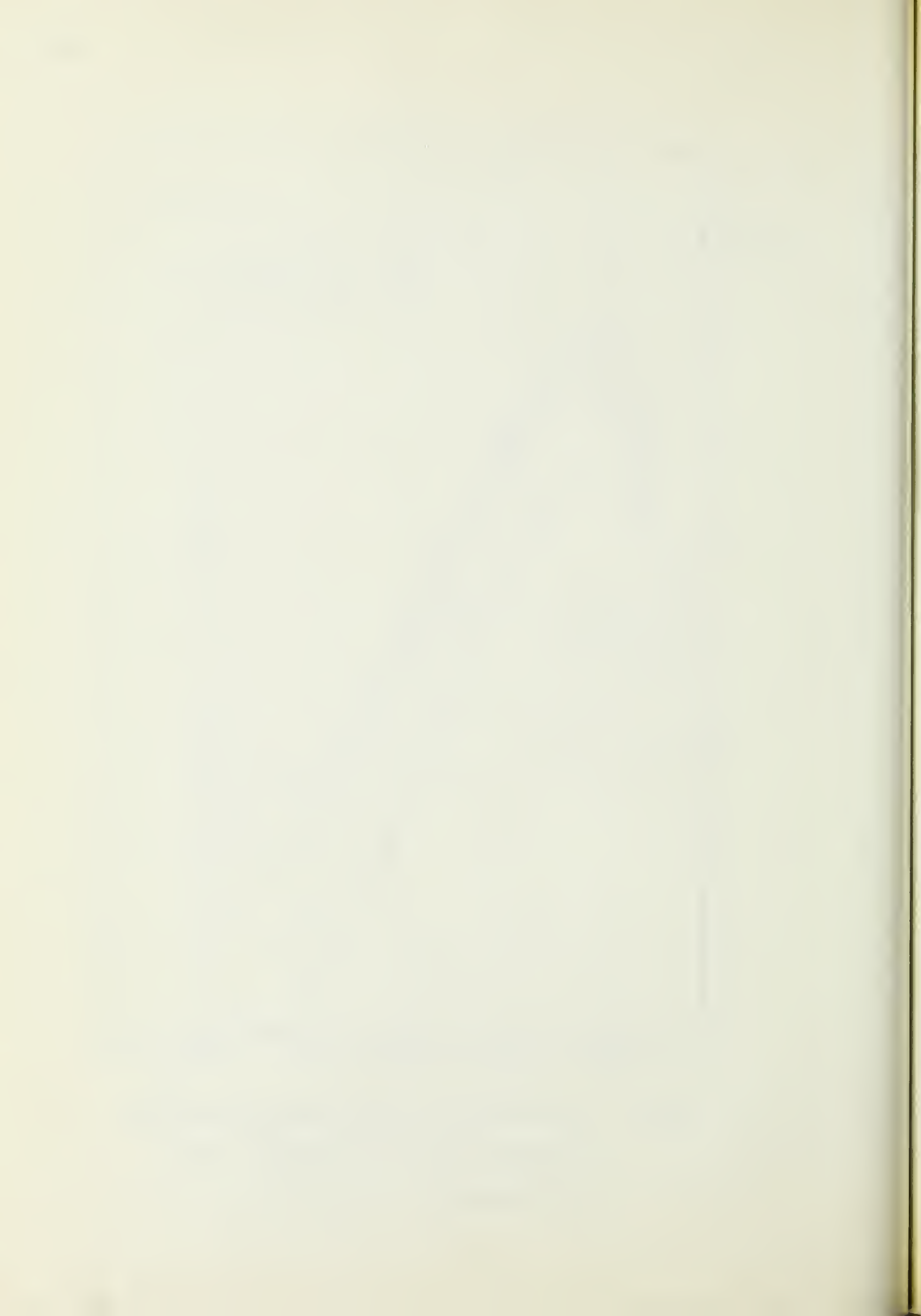


FIG. 18 EXPERIMENTAL LOAD DEFLECTION CURVES

COMPARED WITH WIJNGAARDEN THEORY,

 $\frac{b}{t}$ CONSTANT



P

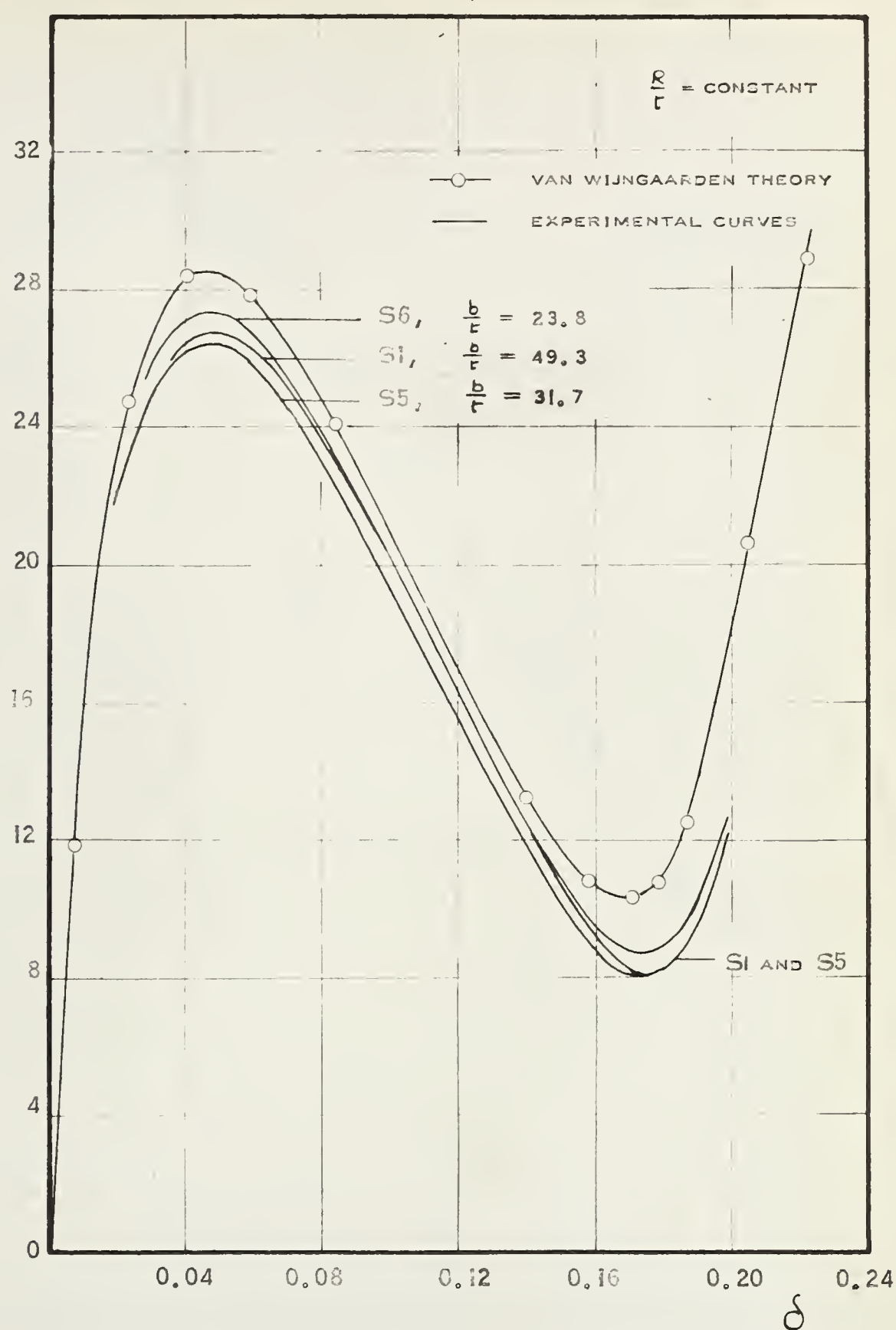


FIG. 19 EXPERIMENTAL LOAD DEFLECTION CURVES
COMPARED WITH WIJNGAARDEN THEORY,
 $\frac{R}{t}$ CONSTANT



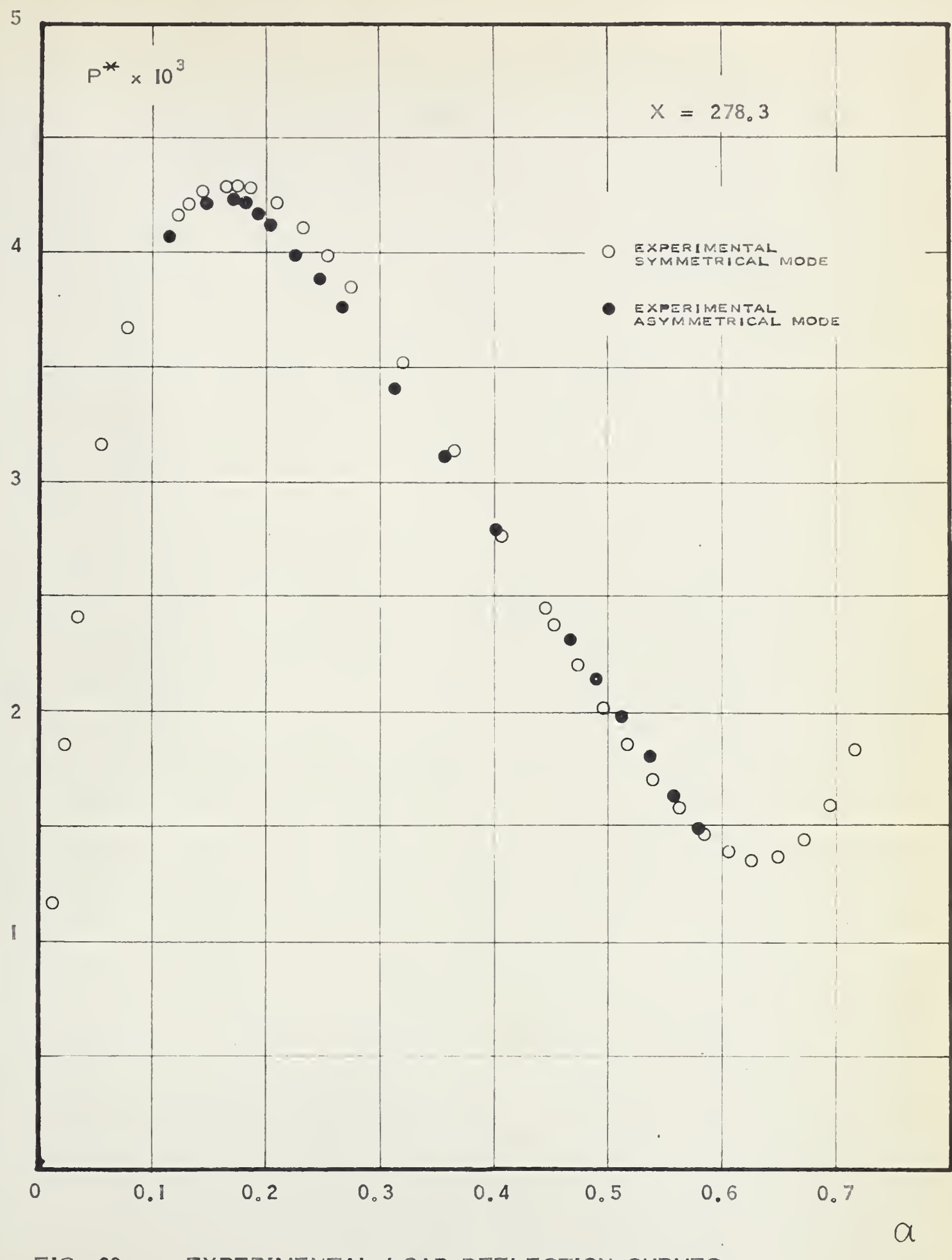
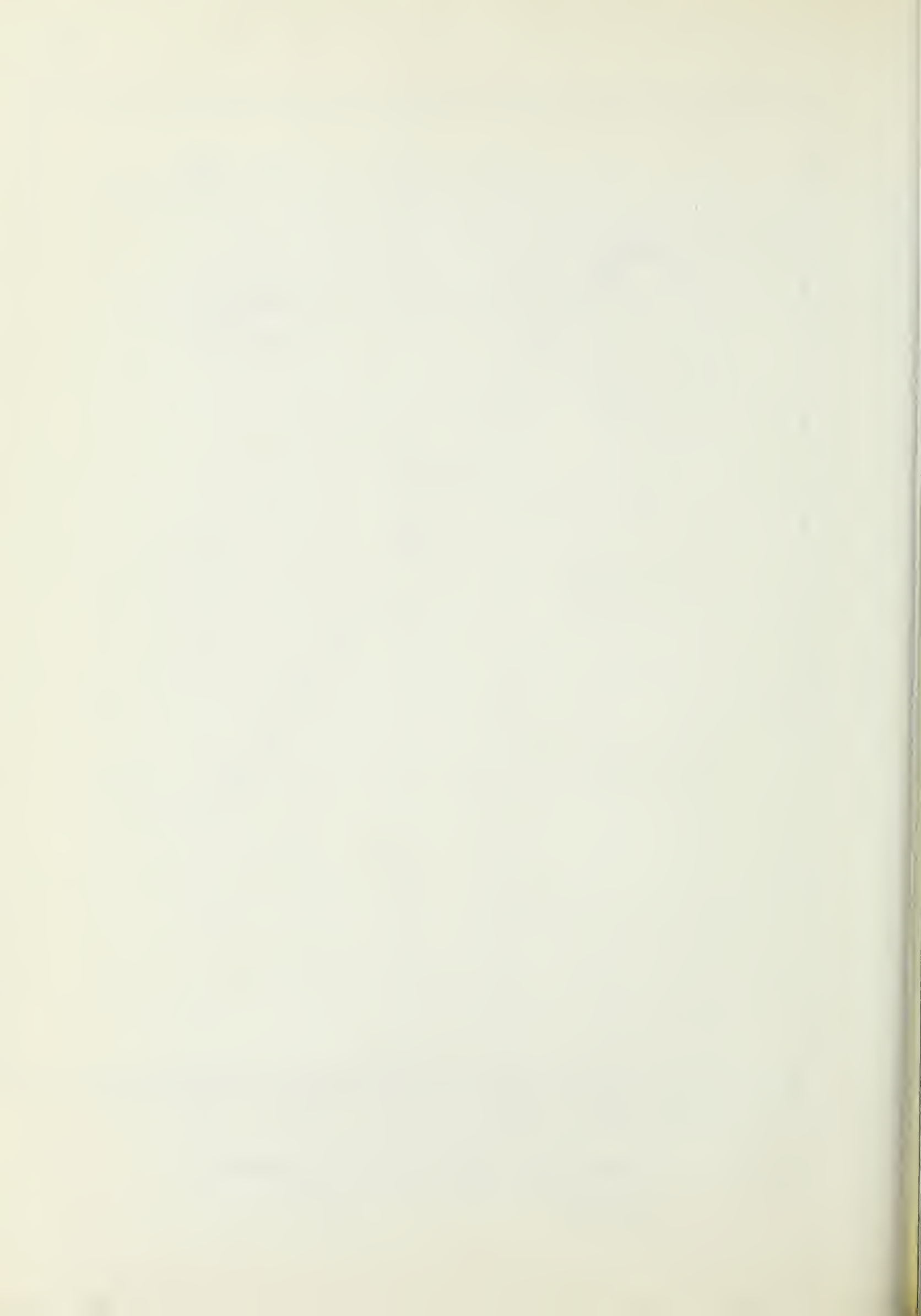


FIG. 20 EXPERIMENTAL LOAD DEFLECTION CURVES,
PIECE S5

α



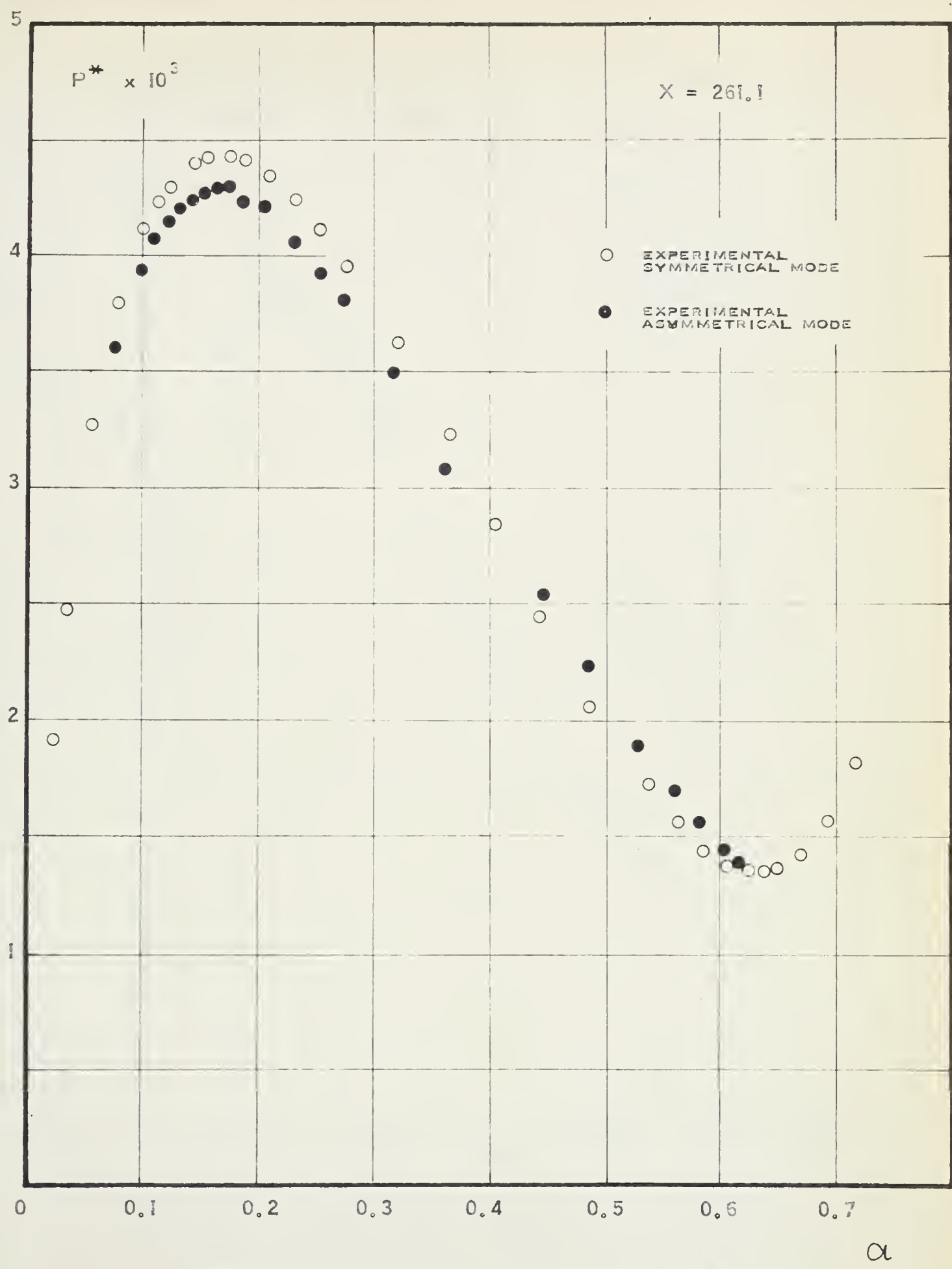
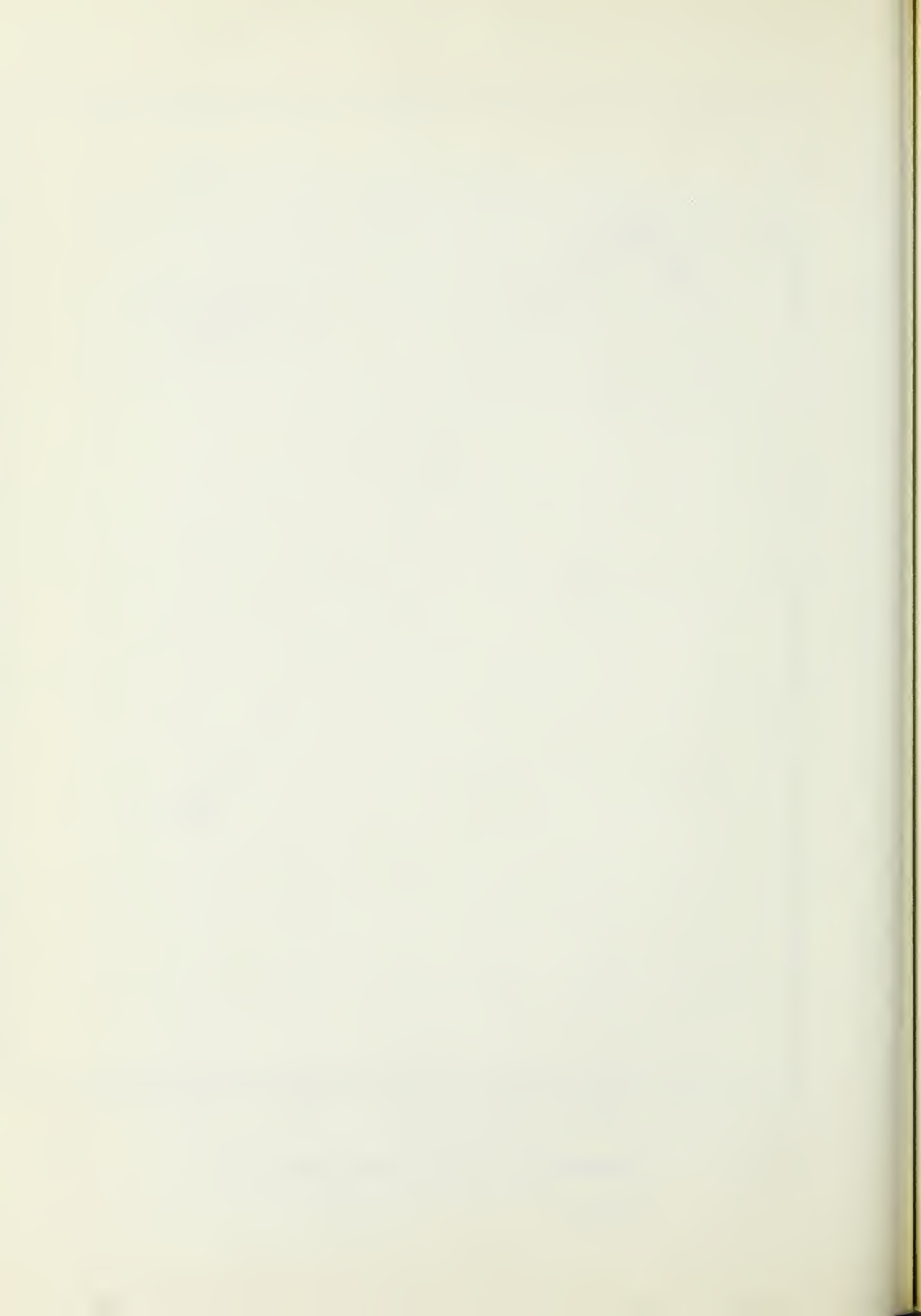


FIG. 21 EXPERIMENTAL LOAD DEFLECTION CURVES,
PIECE S6



P

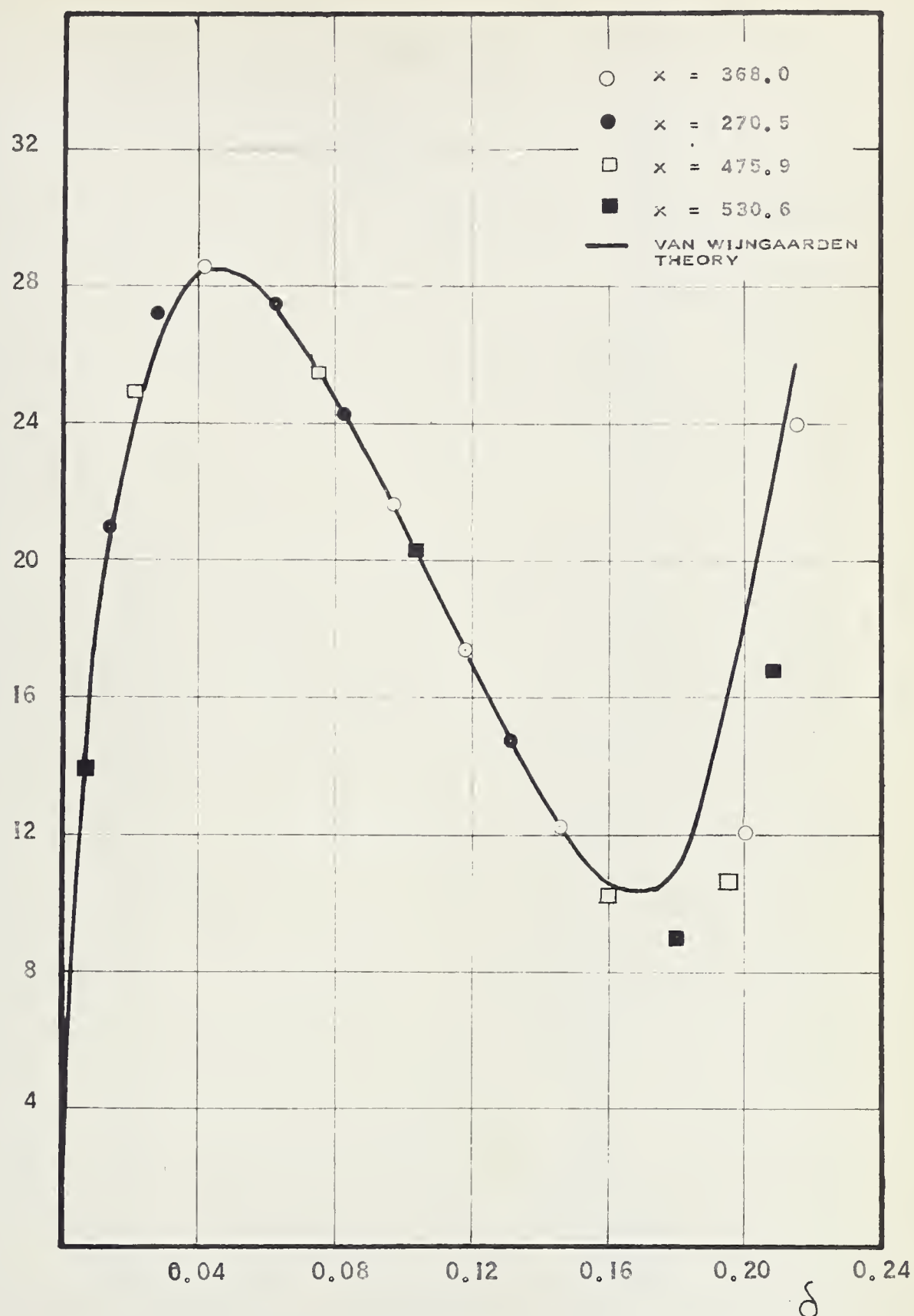


FIG. 22 THEORETICAL RESULTS FOR VARYING x
COMPARED TO CURVE OBTAINED BY
VAN WIJNGAARDEN THEORY

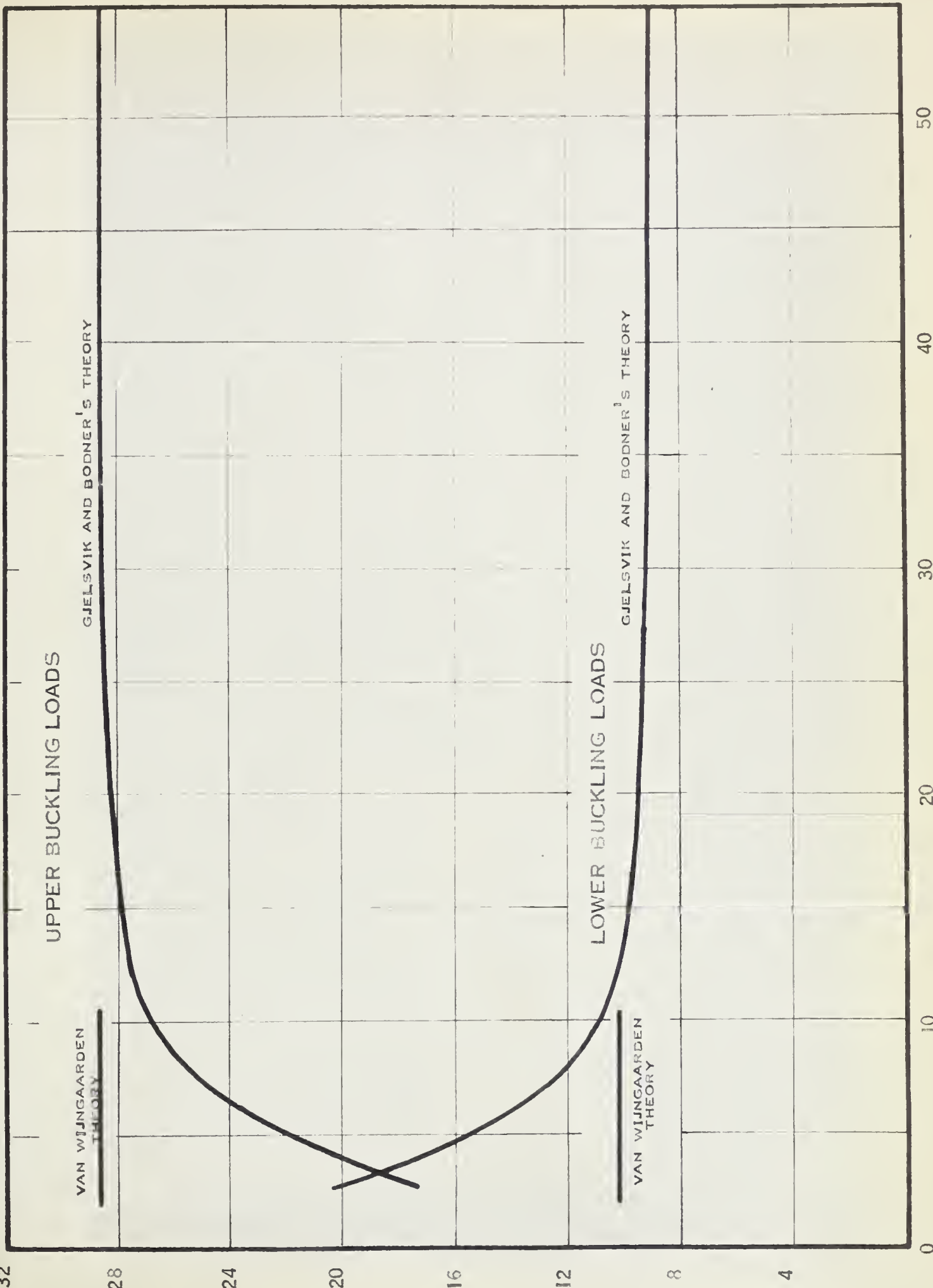


FIG. 23

THEORETICAL BUCKLING LOADS EXPRESSED AS \bar{P}



FIG. 24
PIECE S7 BUCKLED UNDER OWN WEIGHT

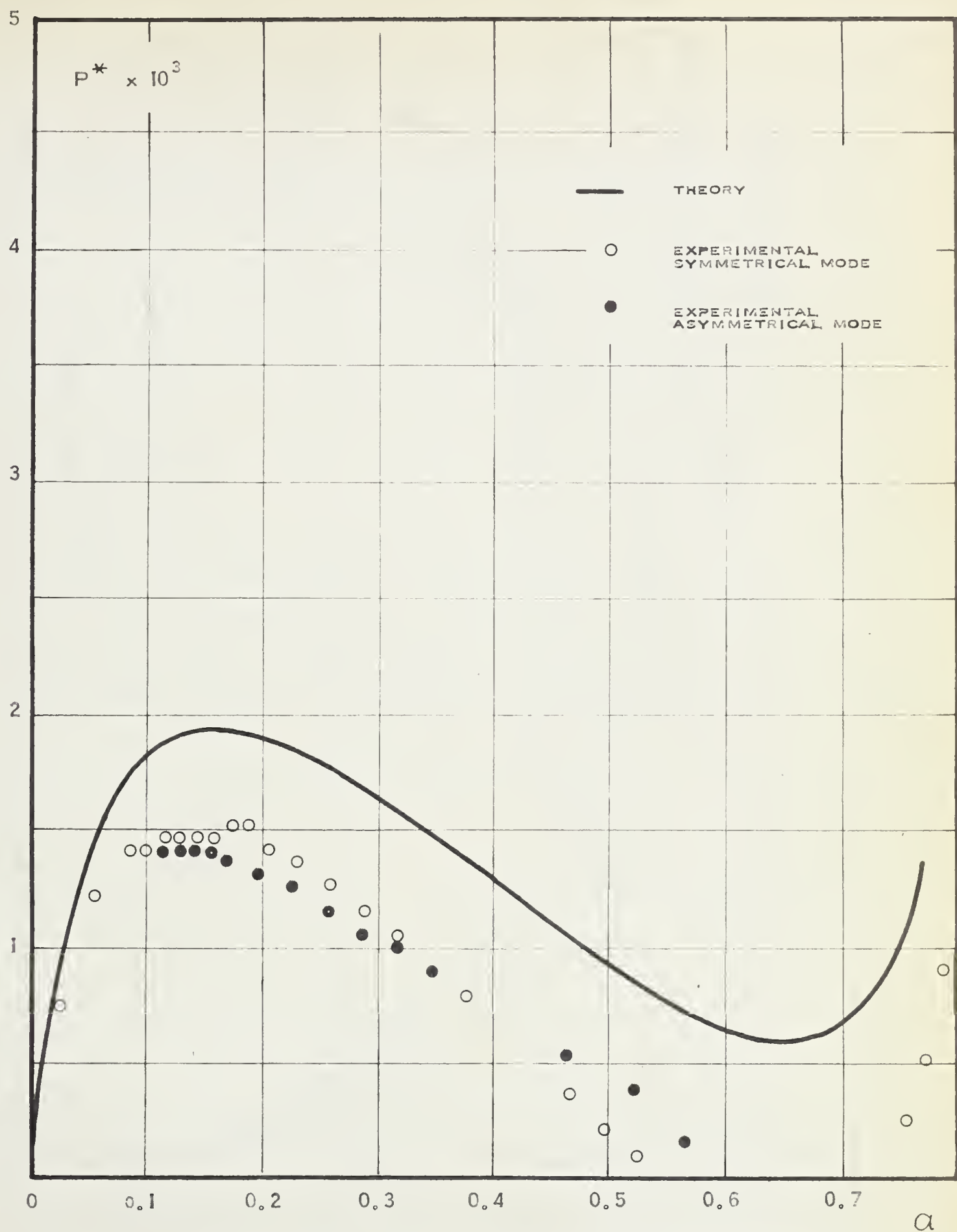


FIG. 25 THEORETICAL AND EXPERIMENTAL LOAD DEFLECTION
CURVE, PIECE S7

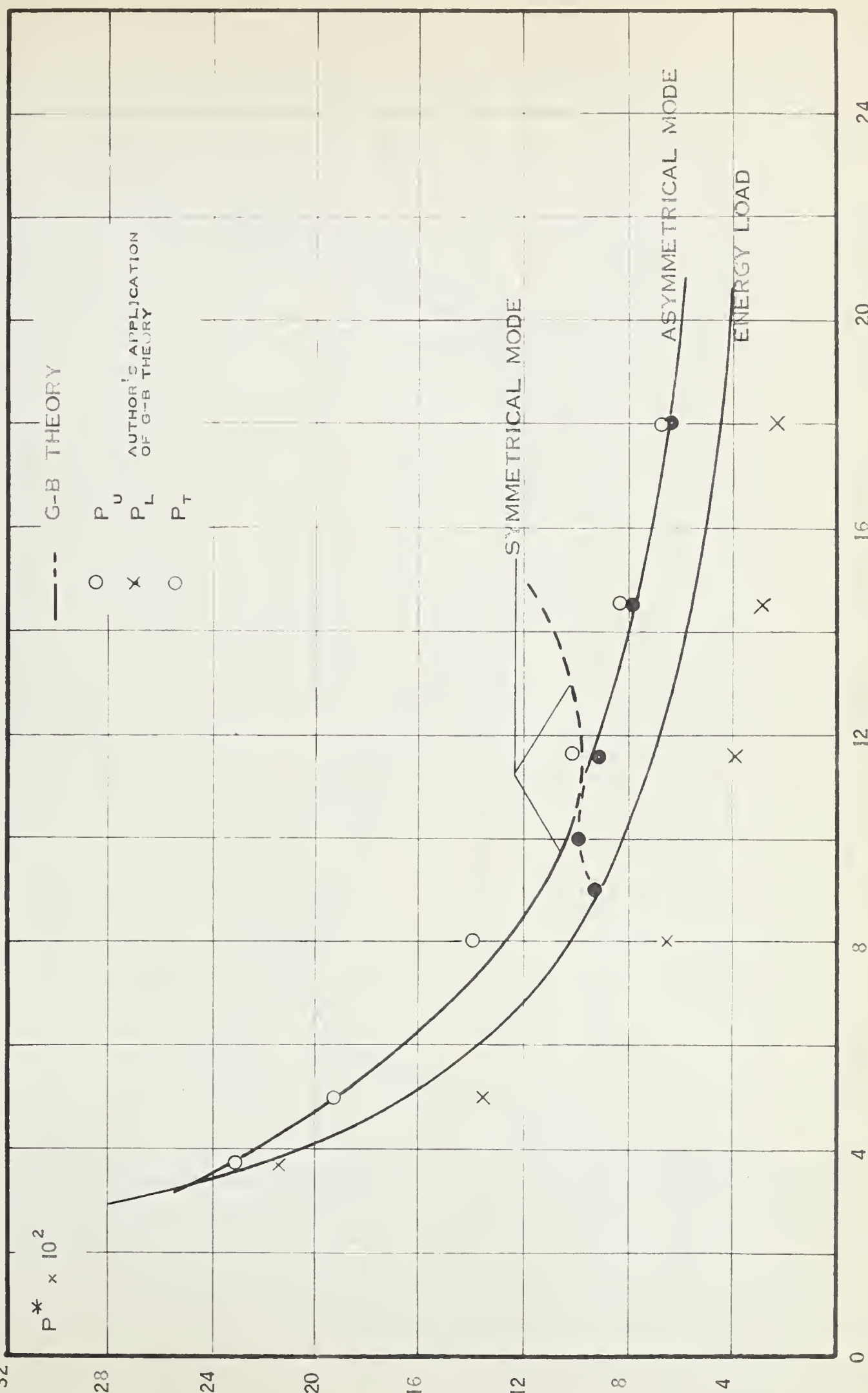


FIG. 26 COMPARISON WITH GJELSVIK AND BODNER'S THEORETICAL BUCKLING LOAD CALCULATIONS

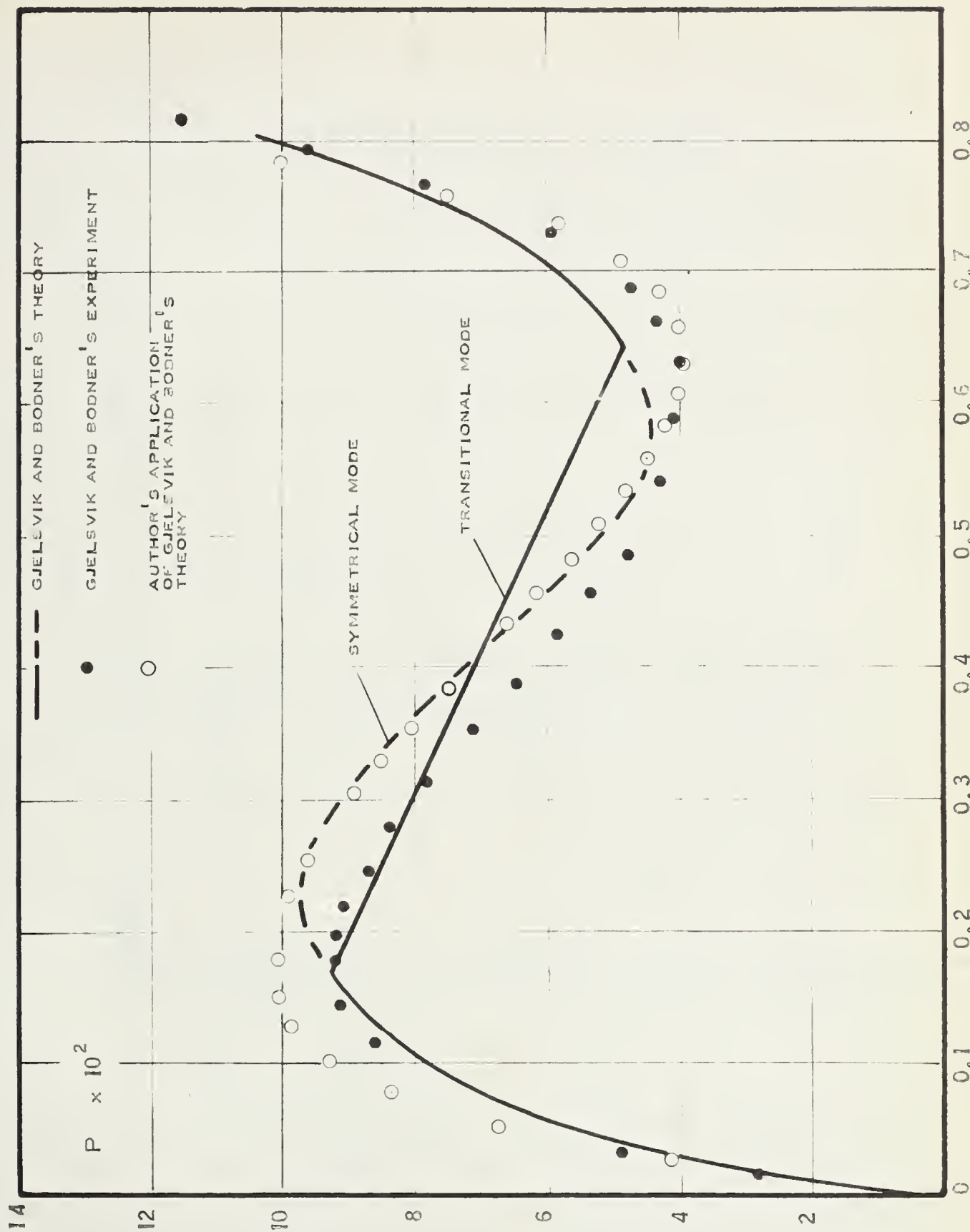


FIG. 27 COMPARISON WITH GJELVIK AND BODNER'S RESULTS,

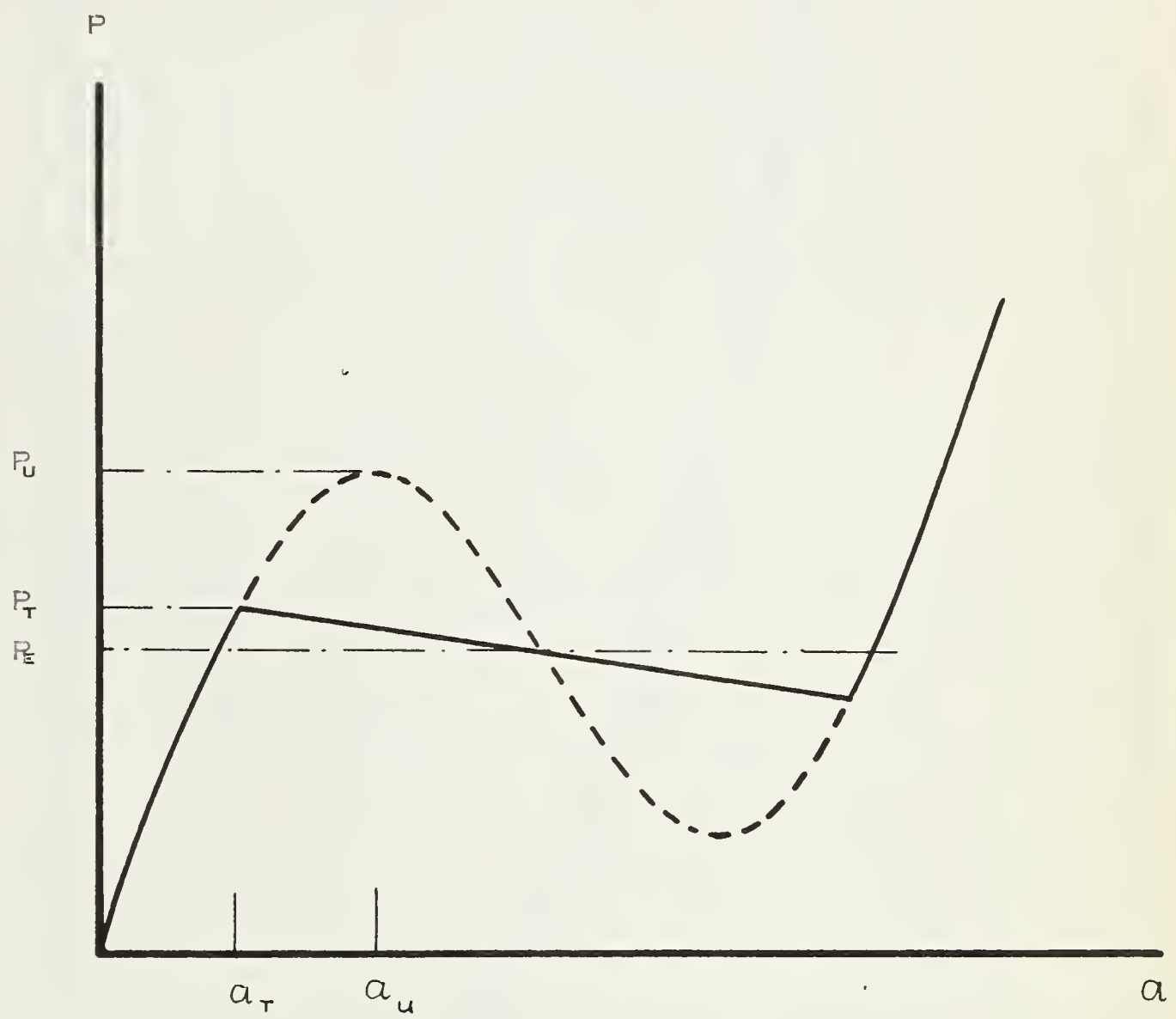


FIG. 28 LOAD DEFLECTION CURVE PREDICTED BY GJELSVIK
AND BODNER FOR LARGE X VALUES

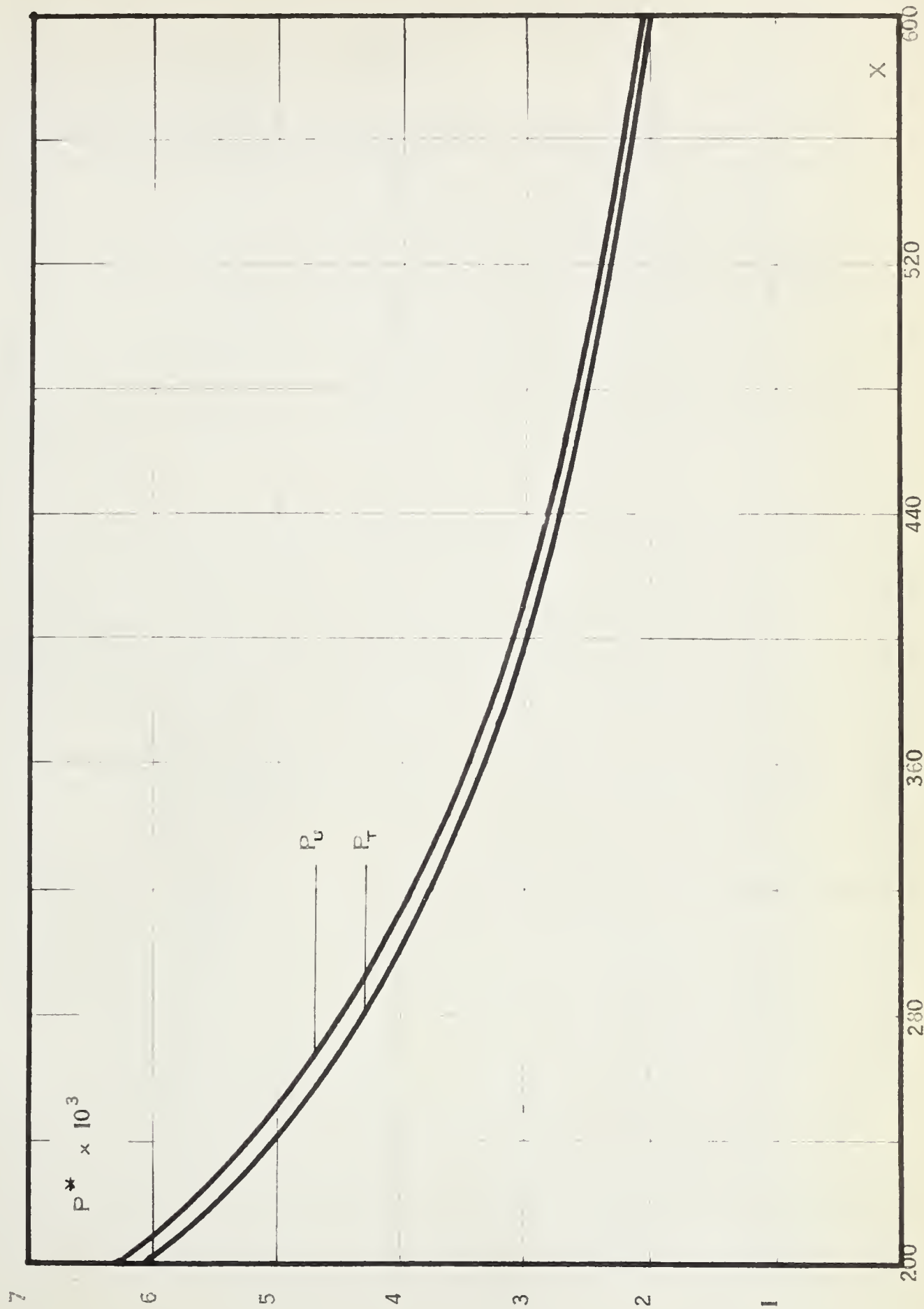


FIG. 29 THEORETICAL UPPER AND TRANSITIONAL BUCKLING LOADS

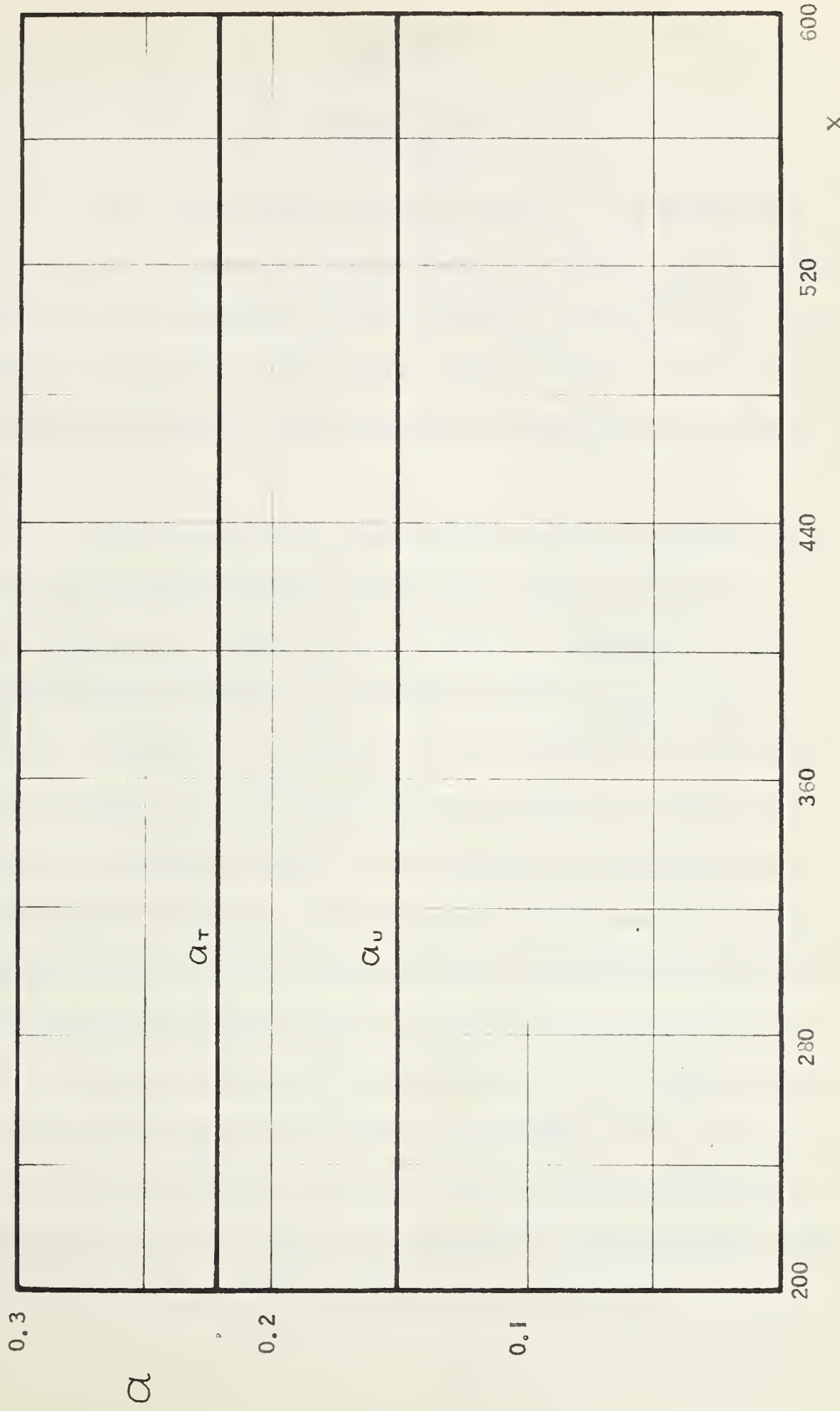


FIG. 30 THEORETICAL BUCKLING DISPLACEMENTS

CHAPTER 5

CONCLUSIONS

For the common consideration of symmetrical buckling the Gjelsvik-Bodner theory and the van Wijngaarden theory agree closely with each other, provided X is greater than 20. It would thus appear that the two term series solution is indeed most adequate to describe the buckled shape.

It is difficult to assess why the variation in dimensional elimination techniques exists and why van Wijngaarden seems to have used a stronger set of factors than Gjelsvik and Bodner, although both are correct. Duncan, in his text on the subject⁶, indicates that commonly occurring quantities, such as flexural rigidity, should be used in preference to an arbitrary selection of indices. The author's findings confirm this. Analyses which do not make any such consideration initially terminate with several choices for the various indices, as the existing boundary conditions do not supply enough equations to satisfy the indice unknowns. It appears that in the Gjelsvik-Bodner theory, the factors chosen were selected rather for their arithmetical convenience, than for their relative non-dimensional advantage.

Both theories neglect any weight consideration. It is felt that this omission is a large source of error for the arch-springs considered in this thesis, and in fact for any very light arches with a large radius of curvature. In the range Gjelsvik and Bodner investigated, a weightless consideration would be satisfactory because of the large buckling load to weight ratios. However, as it stands, their theory would indicate that it may be applied to any value of X , but since they appear to suggest that P_U^* attains large proportions after the critical value of 10.6, then it would follow, perhaps, that such a restriction would be overworked. Still, as far as can be judged, their curve for transitional buckling concurs with the author's and if so, such a weight neglection would bring in errors.

Theoretical predictions were therefore higher than results obtained by experimental investigation, although the symmetrical buckling deflections recorded were in close agreement. It would seemingly be beneficial if these theories did include terms for distributed weight, albeit that this would complicate considerably the succeeding derivation of the load deflection relationship.

The author disagrees partially with Gjelsvik and Bodner in their treatment of the nature of the asymmetrical mode. He would suggest instead, that under completely

static conditions, an arch will continue to buckle at the upper buckling load, regardless of its X ratio. Then if X is of sufficient magnitude, shortly after this happening, the arch will deform asymmetrically. With the approach of the second phase of stability the asymmetry will decrease, and symmetry will be assumed just before the lower buckling load is attained. Their postulates that transitional buckling distinguishes itself by a straight line plot on a load deflection graph, and, that this line intersects with the symmetrical curve at the intermediate load value, are in keeping with the findings of this writer. Further on the evidence of Figures 23 and 26, he supports the view that for values of X less than approximately 3.5, buckling does not occur.

As Figure 23 indicates, the van Wijngaarden theory should be applied with caution for low X values. Since this theory was derived specifically for "thin rings", then such a limitation is to be expected, but as a consequence the theory gives no indication of the initially changing nature of buckling.

BIBLIOGRAPHY

1. A. van Wijngaarden, "Large Deflections of Semi-Oval Arch Rings", Proceedings Sixth International Congress of Applied Mechanics, Paris, 1946.
2. J. S. Kennedy, "Piecewise Nearly Developable Surfaces in the Large Deformation of Very Thin Shells", Unpublished Dissertation, Stanford, 1959.
3. R. Frisch-Fay, "Flexible Bars", Butterworths, 1962, pp. 145 -151.
4. A. Gjelsvik and S. R. Bodner, "An Investigation of the Energy Criterion in Snap Buckling Problems with Application to Clamped Arches", Brown University, 1962.
5. S. P. Timoshenko and J. Gere, "Elastic Stability", McGraw-Hill, 1961, p. 53.
6. W. J. Duncan, "Physical Similarity and Dimensional Analysis", Edward Arnold, 1953, p. 58.

APPENDIX A

Young's Modulus for the banding steel used in the experimental work was determined by employing a test-piece, which was about a foot in length. Along lightly scribed centre lines, two Budd Metafilm strain gauges were affixed on opposite sides of the banding steel, and a similar strain gauge was also cemented to a dummy strip of the banding steel. Before adhesion of each gauge, the surface of the steel was rubbed with fine sandpaper and cleaned with trichloroethylene.

The test length was then placed in a tension tester, and it was wired to a strain indicator and a switching box. Load was applied on the strip several times before readings were noted and the results obtained are shown graphically in Figure 31.

Young's Modulus was then calculated as follows:
Area of specimen = $0.75 \times .0150$

$$= 0.1125 \text{ sq. inches}$$

$$E = \frac{P}{e} \frac{l}{0.1125}$$

Taking the value of $\frac{P}{e}$ from the gradient of the line in Figure 31, then

$$E = \frac{269}{800} \frac{1}{0.1125}$$

so that

$$E = 29.9 \times 10^6 \text{ p.s.i.}$$

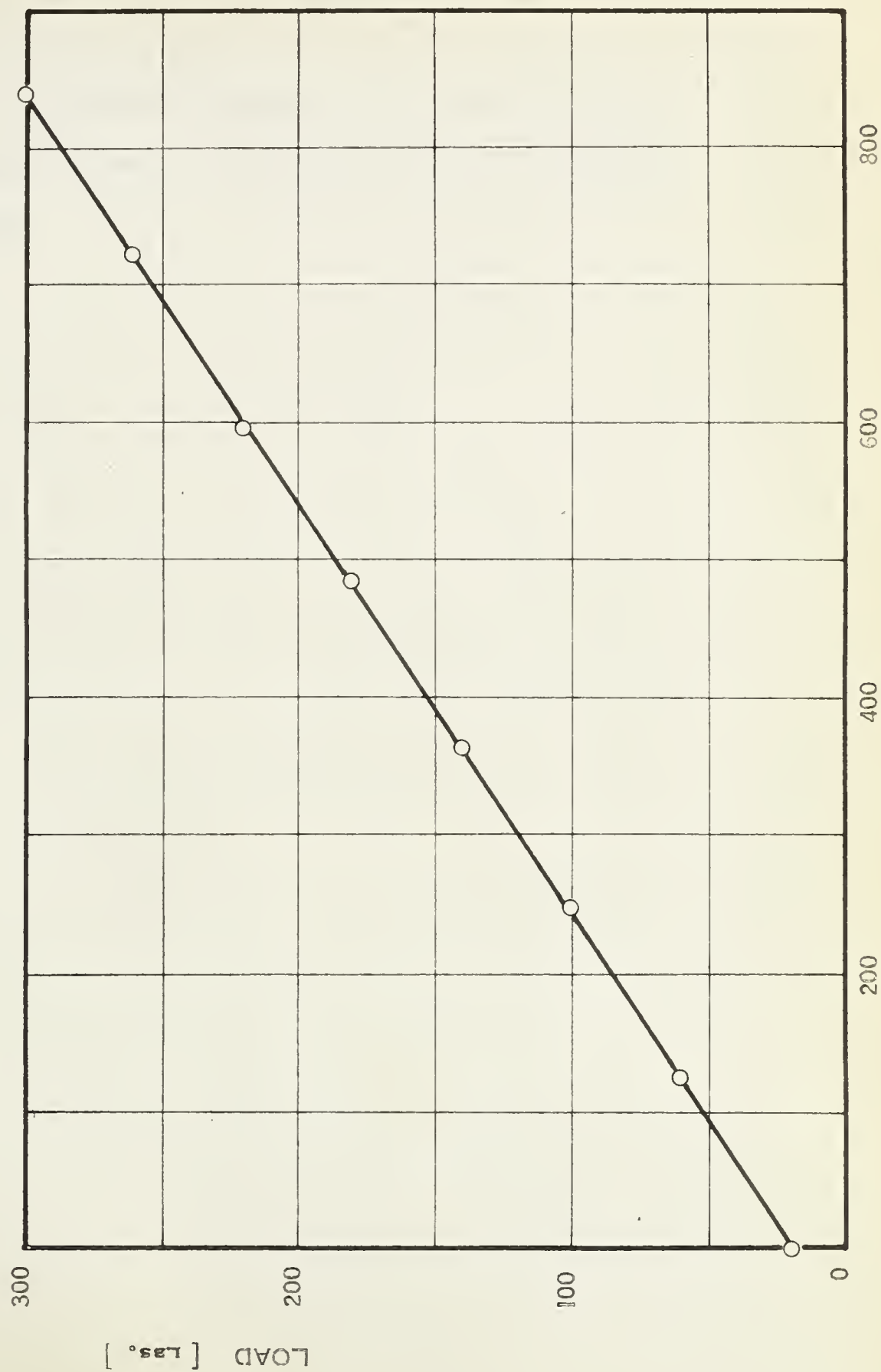


FIG. 31 LOAD STRAIN CURVE TO DETERMINE YOUNG'S MODULUS

APPENDIX B

IBM 1620 Computer programme yielding
theoretical load deflection curves for varying
X values.



-1.00
-1.25
-1.50
-1.75
-1.50
-1.25
0.25
0.50
0.75
1.00
1.25
1.50
1.75
2.00
2.25
2.50
2.75
3.00
3.25
3.50
3.75
4.00
1.00 + 0.100 = 1.10 - 4
3.60
5.00
8.00
11.62
14.50
18.00
25.00
30.00
25.00
40.00
45.00
50.00
100.00
150.00
200.00
235.00
270.50
320.00
368.00
420.00
475.00
530.60
580.00
647.60

••1 D-RETURN MEASURED DOPPLER SHIFT OF LIGHT IN KHz 00011
 ••L7AD FORTRAN EXP.UTE

82

LAMBDA= 4.6

K	A(K)	NDLOAD	AONE	ATWO
1	-4.00	• 000000	• 0000	• 0000
2	-3.75	• 048621	• 0253	-• 0043
3	-3.50	• 089915	• 0506	-• 0087
4	-3.25	• 124261	• 0754	-• 0130
5	-3.00	• 152625	• 1013	-• 0171
6	-2.75	• 175555	• 1266	-• 0211
7	-2.50	• 193671	• 1519	-• 0249
8	-2.25	• 207561	• 1773	-• 0284
9	-2.00	• 217781	• 2020	-• 0317
10	-1.75	• 224849	• 2279	-• 0346
11	-1.50	• 229247	• 2533	-• 0372
12	-1.25	• 231425	• 2786	-• 0395
13	-1.00	• 231803	• 3039	-• 0414
14	-0.75	• 230774	• 3292	-• 0428
15	-0.50	• 228711	• 3546	-• 0439
16	-0.25	• 225969	• 3793	-• 0446
17	0.25	• 214811	• 4306	-• 0444
18	0.50	• 217069	• 4559	-• 0438
19	0.75	• 215006	• 4812	-• 0428
20	1.00	• 213977	• 5066	-• 0413
21	1.25	• 214355	• 5319	-• 0395
22	1.50	• 216532	• 5572	-• 0372
23	1.75	• 220931	• 5825	-• 0346
24	2.00	• 227999	• 6079	-• 0317
25	2.25	• 238218	• 6332	-• 0284
26	2.50	• 252109	• 6585	-• 0249
27	2.75	• 270225	• 6839	-• 0211
28	3.00	• 292155	• 7092	-• 0171
29	3.25	• 321519	• 7345	-• 0130
30	3.50	• 355965	• 7599	-• 0087
31	3.75	• 397158	• 7852	-• 0043
32	4.00	• 445780	• 8105	0.0000

LAMBDA= 5.00

K	A(K)	NDLOAD	AONE	ATWO
1	-4.00	0.000000	0.0000	0.0000
2	-3.75	• 050603	• 0253	-• 0070
3	-3.50	• 091257	• 0506	-• 0141
4	-3.25	• 123225	• 0759	-• 0211
5	-3.00	• 147763	• 1013	-• 0279
6	-2.75	• 165982	• 1266	-• 0343
7	-2.50	• 178914	• 1519	-• 0404
8	-2.25	• 187446	• 1773	-• 0459
9	-2.00	• 192351	• 2026	-• 0509
10	-1.75	• 194300	• 2279	-• 0554
11	-1.50	• 193869	• 2533	-• 0592
12	-1.25	• 191550	• 2786	-• 0625
13	-1.00	• 187761	• 3039	-• 0652
14	-0.75	• 182861	• 3292	-• 0672
15	-0.50	• 177165	• 3545	-• 0687
16	-0.25	• 170955	• 3794	-• 0697
17	0.25	• 158031	• 4306	-• 0693
18	0.50	• 151820	• 4559	-• 0686
19	0.75	• 146124	• 4812	-• 0671
20	1.00	• 141224	• 5066	-• 0651
21	1.25	• 137435	• 5319	-• 0624
22	1.50	• 135116	• 5572	-• 0592
23	1.75	• 134686	• 5825	-• 0550

24	2.00	•1-00004	•0.7	-•.6
25	2.02	•141049	•6.2	-•.3452
26	2.07	•1-0071	•5587	-•.3403
27	2.15	•1-0073	•5837	-•.3443
28	3.10	•18222	•7772	-•.2770
29	3.25	•205750	•7345	-•.2111
30	3.50	•237728	•7529	-•.2141
31	3.75	•278382	•7872	-•.2070
32	4.00	•329986	•8105	-•.2000

LAMRDA= 8.01

K	A(<)	NDLOAD	AONE	ATWO
1	-4.00	•0.001000	•0000	-•.0000
2	-3.75	•048712	•0253	-•.0125
3	-3.50	•082890	•0506	-•.0245
4	-3.25	•106347	•0759	-•.0357
5	-3.00	•121988	•1013	-•.0461
6	-2.75	•131894	•1265	-•.0554
7	-2.50	•137561	•1519	-•.0636
8	-2.25	•140067	•1773	-•.0722
9	-2.00	•140197	•2026	-•.0773
10	-1.75	•138523	•2279	-•.0827
11	-1.50	•135474	•2533	-•.0873
12	-1.25	•131376	•2786	-•.0912
13	-1.00	•126486	•3039	-•.0942
14	-0.75	•121009	•3292	-•.0966
15	-0.50	•115119	•3546	-•.0983
16	-0.25	•108963	•3799	-•.0995
17	0.25	•096395	•4306	-•.0989
18	0.50	•090240	•4559	-•.0980
19	0.75	•094350	•4912	-•.0964
20	1.00	•078873	•5064	-•.0941
21	1.25	•073982	•5319	-•.0910
22	1.50	•069885	•5572	-•.0872
23	1.75	•066836	•5825	-•.0826
24	2.00	•065162	•6079	-•.0772
25	2.25	•065291	•6332	-•.0709
26	2.50	•067798	•6585	-•.0636
27	2.75	•073464	•6839	-•.0553
28	3.00	•083370	•7092	-•.0460
29	3.25	•090011	•7345	-•.0357
30	3.50	•122469	•7592	-•.0245
31	3.75	•156647	•7852	-•.0125
32	4.00	•205359	•8105	-•.0000

LAMRDA= 11.62

PTEE=	•092161	ATEE=	•2878	
K	A(<)	NDLOAD	AONE	ATWO
1	-4.00	•0.001000	•0000	-•.0000
2	-3.75	•041429	•0253	-•.0164
3	-3.50	•067187	•0506	-•.0312
4	-3.25	•083287	•0759	-•.0443
5	-3.00	•093175	•1013	-•.0558
6	-2.75	•098837	•1265	-•.0660
7	-2.50	•116877	•1519	-•.0748
8	-2.25	•102466	•1773	-•.0824
9	-2.00	•101570	•2026	-•.0890
10	-1.75	•092613	•2279	-•.0746
11	-1.50	•096783	•2533	-•.0623
12	-1.25	•097277	•2786	-•.1032
13	-1.00	•101221	•3039	-•.1063
14	-0.75	•084979	•3292	-•.1027
15	-0.50	•083382	•346	-•.103

16	-0.2	• 0.76	• 0.4	• 0.2
17	• 2	• 0.51	• 4	-0.1
18	• 7	• 0.61	• 4	-0.1
19	• 76	• 0.58	• 4	-0.1
20	• 1	• 0.58	• 1.68	-0.1
21	1.025	• 0.4780	• 1	-0.1
22	1.0	• 0.4478	• 1.2	0.4
23	1.07	• 0.4444	• 1.2	0.4
24	2.0	• 0.3378	• 5.1	0.4
25	2.022	• 0.3710	• 0.52	0.42
26	2.030	• 0.3712	• 5.7	0.44
27	2.077	• 0.416	• 0.33	-0.65
28	3.000	• 0.4838	• 7.92	-0.556
29	3.025	• 0.5827	• 7.345	0.443
30	3.050	• 0.7437	• 7.03	-0.312
31	3.075	• 1.0123	• 7.852	-0.164
32	4.0	• 14756	• 87.5	0.1

LAMBDA = 14.50

	PIFE = 0.571863	ATFE = 0.2613		
K	A(K)	NFL/LOAD	AON	ATWO
1	-4.0	• 0.5	• 0.2	0.1
2	-3.7	• 0.505	• 0.2	-0.152
3	-3.2	• 0.517	• 0.36	-0.332
4	-3.25	• 0.67598	• 0.759	-0.3476
5	-3.30	• 0.77157	• 1.13	-0.52
6	-2.75	• 0.81368	• 12.6	-0.698
7	-2.50	• 0.83285	• 15.19	-0.767
8	-2.0	• 0.852	• 1.13	-0.34
9	-2.05	• 0.8567	• 2.16	-0.37
10	-1.75	• 0.88	• 27.7	-0.57
11	-1.50	• 0.78423	• 2.13	-0.107
12	-1.25	• 0.75461	• 2.86	-0.157
13	-1.00	• 0.72118	• 3.53	0.114
14	-0.75	• 0.68496	• 5.272	-0.112
15	-0.50	• 0.64672	• 11.4	-0.111
16	0.25	• 0.602	• 2.37	-0.111
17	0.25	• 0.52714	• 4.30	-0.110
18	0.5	• 0.4767	• 4.07	-0.112
19	0.75	• 0.44947	• 4.612	-0.1126
20	1.00	• 0.41324	• 5.668	-0.113
21	1.025	• 0.37762	• 7.1	-0.112
22	1.050	• 0.3523	• 5.572	-0.1133
23	1.075	• 0.32553	• 3.32	-0.113
24	2.0	• 0.3015	• 5.0	-0.113
25	2.025	• 0.27307	• 3.32	-0.116
26	2.030	• 0.25012	• 0.32	-0.116
27	2.075	• 0.24012	• 0.553	-0.116
28	3.000	• 0.20288	• 0.12	-0.117
29	3.025	• 0.18845	• 7.545	-0.1416
30	3.050	• 0.16926	• 0.12	-0.117
31	3.075	• 0.177574	• 1.12	-0.1161
32	4.0	• 0.17447	• 0.12	-0.117

LAMBDA = 18.00

	PIFE = 0.64414	ATFE = 0.2424		
K	A(K)	NFL/LOAD	AON	ATWO
1	-4.0	• 0.5	• 0.2	0.1
2	-3.7	• 0.540	• 0.23	-0.117
3	-3.2	• 0.540	• 0.303	-0.117
4	-3.25	• 0.540	• 0.377	-0.117
5	-3.30	• 0.540	• 0.442	-0.117
6	-2.75	• 0.540	• 0.503	-0.117
7	-2.50	• 0.540	• 0.562	-0.117
8	-2.0	• 0.540	• 0.623	-0.117
9	-2.05	• 0.540	• 0.682	-0.117
10	-1.75	• 0.540	• 0.742	-0.117

1	-	•	•	-	•
2	-	2 • 11	• 2 11	-	•
3	-	2 •	• 2 2 11	• 2 2 11	-
4	-	1 • 75	• 6 5 8	• 2 2	-
5	-	1 •	• 2 5 10 2	• 2	-
6	-	1 • 2	• 2 5 10 2	• 2	-
7	-	1 • 2	• 2 5 10 2	• 2	-
8	-	1 • 2	• 2 5 10 2	• 2	-
9	-	1 • 2	• 2 5 10 2	• 2	-
10	-	1 • 2	• 2 5 10 2	• 2	-
11	-	1 • 2	• 2 5 10 2	• 2	-
12	-	1 • 2	• 2 5 10 2	• 2	-
13	-	1 • 2	• 2 5 10 2	• 2	-
14	-	1 • 2	• 2 5 10 2	• 2	-
15	-	1 • 2	• 2 5 10 2	• 2	-
16	-	1 • 2	• 2 5 10 2	• 2	-
17	-	1 • 2	• 2 5 10 2	• 2	-
18	-	1 • 2	• 2 5 10 2	• 2	-
19	-	1 • 2	• 2 5 10 2	• 2	-
20	1	0 0 0	• 2 5 10 2	• 2 5 10 2	-
21	1	0 0 2	• 2 5 10 2	• 2 5 10 2	-
22	1	0 0 2	• 2 5 10 2	• 2 5 10 2	-
23	1	0 0 2	• 2 5 10 2	• 2 5 10 2	-
24	1	0 0 2	• 2 5 10 2	• 2 5 10 2	-
25	2	0 2 5	• 2 5 10 2	• 2 5 10 2	-
26	2	0 2 5	• 2 5 10 2	• 2 5 10 2	-
27	2	0 2 5	• 2 5 10 2	• 2 5 10 2	-
28	2	0 2 5	• 2 5 10 2	• 2 5 10 2	-
29	2	0 2 5	• 2 5 10 2	• 2 5 10 2	-
30	2	0 2 5	• 2 5 10 2	• 2 5 10 2	-
31	2	0 2 5	• 2 5 10 2	• 2 5 10 2	-
32	4	0 2 5	• 2 5 10 2	• 2 5 10 2	-

LAMMIDAE = 25000

	PIFF =	• 0 4 4 0 2 A 1 E F -	• 2 0	
	A (11)	W (L, AD)	H (W)	W (W)
1	-4 • 0 2	• 0 2 0 0 0	• 2 0 0 0	• 0 0 0
2	-3 • 1 0	• 0 2 2 0 4 4	• 0 2 2 0 4 4	-• 0 2 0 0
3	-3 • 0 0	• 0 2 0 0 0 0	• 0 2 0 0 0	-• 0 2 0 0
4	-3 • 0 2 5	• 0 4 2 7 4 4	• 0 4 2 7 4 4	-• 0 2 1 0
5	-3 • 0 0 0	• 0 4 0 4 0 0	• 0 4 0 4 0 0	-• 0 0 4 0
6	-4 • 1 0	• 0 4 0 0 0 0	• 0 4 0 0 0 0	-• 0 0 4 0
7	-2 • 0 0	• 0 4 0 0 0	• 0 4 0 0 0	-• 0 0 4 0
8	-2 • 0 2 0	• 0 4 0 0 0	• 0 4 0 0 0	-• 0 0 4 0
9	-2 • 0 0 0	• 0 4 0 0 0	• 0 4 0 0 0	-• 0 0 4 0
10	-1 • 7 5	• 0 4 1 5 2 6	• 0 4 1 5 2 6	-• 0 0 4 0
11	-1 • 5 0	• 0 4 6 0 7 1	• 0 4 6 0 7 1	-• 0 0 4 0
12	-1 • 2 0	• 0 4 2 3 7	• 0 4 2 3 7	-• 0 0 4 0
13	-1 • 0 0	• 0 4 2 1 9 1	• 0 4 2 1 9 1	-• 0 0 4 0
14	-0 7 0	• 0 4 0 0 0 0	• 0 4 0 0 0 0	-• 0 0 4 0
15	-0 0 0	• 0 4 0 0 0	• 0 4 0 0 0	-• 0 0 4 0
16	-0 2 0	• 0 4 0 0 0 0	• 0 4 0 0 0 0	-• 0 0 4 0
17	0 2 0	• 0 4 0 0 0	• 0 4 0 0 0	-• 0 0 4 0
18	0 0 0	• 0 2 0 1 0 0	• 0 2 0 1 0 0	-• 0 0 4 0
19	0 0 2	• 0 2 0 1 0 0	• 0 2 0 1 0 0	-• 0 0 4 0
20	1 0 0	• 0 2 0 1 0 0	• 0 2 0 1 0 0	-• 0 0 4 0
21	1 0 2	• 0 2 0 1 0 0	• 0 2 0 1 0 0	-• 0 0 4 0
22	1 0 0	• 0 2 0 1 0 0	• 0 2 0 1 0 0	-• 0 0 4 0
23	0 0 0	• 0 1 0 1 0 0	• 0 1 0 1 0 0	-• 0 0 4 0
24	0 0 2	• 0 1 0 1 0 0	• 0 1 0 1 0 0	-• 0 0 4 0
25	0 0 0	• 0 1 0 2 0 0	• 0 1 0 2 0 0	-• 0 0 4 0
26	0 0 2	• 0 1 0 2 0 0	• 0 1 0 2 0 0	-• 0 0 4 0
27	0 0 0	• 0 1 0 2 0 0	• 0 1 0 2 0 0	-• 0 0 4 0
28	0 0 0	• 0 1 0 0 0 0	• 0 1 0 0 0 0	-• 0 0 4 0
29	0 0 2	• 0 1 0 0 0 0	• 0 1 0 0 0 0	-• 0 0 4 0
30	0 0 0	• 0 1 0 0 0 0	• 0 1 0 0 0 0	-• 0 0 4 0
31	0 0 2	• 0 4 0 0 0 0	• 0 4 0 0 0 0	-• 0 0 4 0
32	0 0 0	• 0 4 0 0 0 0	• 0 4 0 0 0 0	-• 0 0 4 0

K	A(%)	VAL	•	•	•
1	-4.0	• 1 1 1	•	•	•
2	-3.0 1	• 2 1 1 1	• 2 2	• 2 2 2 1	• 2 2 2 1
3	-3.0 2	• 2 1 1 1	• 2 2 2	• 2 2 2	• 2 2 2
4	-3.0 2	• 2 1 1 1	• 2 2 2	• 2 2 2	• 2 2 2
5	-3.0 3	• 2 1 1 1	• 2 2 2	• 2 2 2	• 2 2 2
6	-2.0 1	• 2 1 1 1	• 2 2 2	• 2 2 2	• 2 2 2
7	-2.0 2	• 2 1 1 1	• 2 2 2	• 2 2 2	• 2 2 2
8	-2.0 2	• 2 1 1 1	• 2 2 2	• 2 2 2	• 2 2 2
9	-2.0 2	• 2 1 1 1	• 2 2 2	• 2 2 2	• 2 2 2
10	-1.0 1	• 2 1 1 1	• 2 2 2	• 2 2 2	• 2 2 2
11	-1.0 2	• 2 1 1 1	• 2 2 2	• 2 2 2	• 2 2 2
12	-1.0 2	• 2 1 1 1	• 2 2 2	• 2 2 2	• 2 2 2
13	-1.0 3	• 2 1 1 1	• 2 2 2	• 2 2 2	• 2 2 2
14	-1.0 3	• 2 1 1 1	• 2 2 2	• 2 2 2	• 2 2 2
15	-1.0 3	• 2 1 1 1	• 2 2 2	• 2 2 2	• 2 2 2
16	-1.0 3	• 2 1 1 1	• 2 2 2	• 2 2 2	• 2 2 2
17	-1.0 3	• 2 1 1 1	• 2 2 2	• 2 2 2	• 2 2 2
18	-1.0 3	• 2 1 1 1	• 2 2 2	• 2 2 2	• 2 2 2
19	-1.0 3	• 2 1 1 1	• 2 2 2	• 2 2 2	• 2 2 2
20	-1.0 3	• 2 1 1 1	• 2 2 2	• 2 2 2	• 2 2 2
21	-1.0 3	• 2 1 1 1	• 2 2 2	• 2 2 2	• 2 2 2
22	-1.0 3	• 2 1 1 1	• 2 2 2	• 2 2 2	• 2 2 2
23	-1.0 3	• 2 1 1 1	• 2 2 2	• 2 2 2	• 2 2 2

LAMPRODIA = 35.00

K	A(%)	VAL	•	•	•
1	-4.0	• 0 1 4 2 0 2	• 2 2 2	• 2 2 2	• 2 2 2
2	-3.0 1	• 0 1 6 1 1	• 2 2 2	• 2 2 2	• 2 2 2
3	-3.0 1	• 0 2 1 0 4 4	• 2 2 2	• 2 2 2	• 2 2 2
4	-3.0 2	• 0 2 1 0 6 0 6	• 2 2 2	• 2 2 2	• 2 2 2
5	-3.0 3	• 0 3 0 0 2 0	• 2 2 2	• 2 2 2	• 2 2 2
6	-2.0 1	• 0 3 0 0 2 0	• 2 2 2	• 2 2 2	• 2 2 2
7	-2.0 2	• 0 3 0 0 2 0	• 2 2 2	• 2 2 2	• 2 2 2
8	-2.0 2	• 0 3 0 0 2 0	• 2 2 2	• 2 2 2	• 2 2 2
9	-2.0 2	• 0 3 0 0 2 0	• 2 2 2	• 2 2 2	• 2 2 2
10	-1.0 1	• 0 3 0 1 4 1	• 2 2 2	• 2 2 2	• 2 2 2
11	-1.0 2	• 0 3 1 0 1 0	• 2 2 2	• 2 2 2	• 2 2 2
12	-1.0 2	• 0 3 1 0 1 0	• 2 2 2	• 2 2 2	• 2 2 2
13	-1.0 3	• 0 3 1 0 2 0	• 2 2 2	• 2 2 2	• 2 2 2
14	-1.0 3	• 0 2 8 1 1 4	• 2 2 2	• 2 2 2	• 2 2 2
15	-1.0 3	• 0 2 8 1 1 0	• 2 2 2	• 2 2 2	• 2 2 2
16	-1.0 3	• 0 2 8 1 1 0	• 2 2 2	• 2 2 2	• 2 2 2
17	-1.0 3	• 0 2 8 1 1 0	• 2 2 2	• 2 2 2	• 2 2 2
18	-1.0 3	• 0 2 8 1 1 0	• 2 2 2	• 2 2 2	• 2 2 2
19	-1.0 3	• 0 2 8 1 1 0	• 2 2 2	• 2 2 2	• 2 2 2
20	-1.0 3	• 0 2 8 1 1 0	• 2 2 2	• 2 2 2	• 2 2 2
21	-1.0 3	• 0 2 8 1 1 0	• 2 2 2	• 2 2 2	• 2 2 2
22	-1.0 3	• 0 2 8 1 1 0	• 2 2 2	• 2 2 2	• 2 2 2
23	-1.0 3	• 0 2 8 1 1 0	• 2 2 2	• 2 2 2	• 2 2 2

24	1.00	• 0.00000	• 0.000	• 0.000
25	2.00	• 0.00000	• 0.000	• 0.000
26	3.00	• 0.00000	• 0.000	• 0.000
27	4.00	• 0.00000	• 0.000	• 0.000
28	5.00	• 0.00000	• 0.000	• 0.000
29	6.00	• 0.00000	• 0.000	• 0.000
30	7.00	• 0.00000	• 0.000	• 0.000
31	8.00	• 0.00000	• 0.000	• 0.000
32	9.00	• 0.00000	• 0.000	• 0.000

LAMBDA= 40.00

	PTFF=	• 30056	ATFF=	• 2251
K	A(K)	NDLOAD	AONE	ATWO
1	-4.00	• 0.00000	• 0.000	• 0.000
2	-3.75	• 014798	• 0214	• 0218
3	-3.50	• 022531	• 0506	• 0320
4	-3.25	• 026912	• 0759	• 0733
5	-3.00	• 029319	• 1013	• 0636
6	-2.75	• 030698	• 1266	• 0762
7	-2.50	• 031198	• 1519	• 0852
8	-2.25	• 031138	• 1773	• 0930
9	-2.00	• 030671	• 2026	• 0976
10	-1.75	• 029902	• 2279	• 1053
11	-1.50	• 027406	• 2533	• 1100
12	-1.25	• 027728	• 2766	• 1121
13	-1.00	• 026440	• 3039	• 1171
14	-0.75	• 025047	• 292	• 1195
15	-0.50	• 023589	• 2546	• 1212
16	-0.25	• 022085	• 2799	• 1224
17	0.25	• 019038	• 4306	• 1216
18	0.50	• 017535	• 4559	• 1208
19	0.75	• 016075	• 4812	• 1192
20	1.00	• 014682	• 5066	• 1169
21	1.25	• 013385	• 5319	• 1138
22	1.50	• 012217	• 5572	• 1099
23	1.75	• 011220	• 5825	• 1062
24	2.00	• 010451	• 6079	• 0996
25	2.25	• 009984	• 6332	• 0929
26	2.50	• 009924	• 6584	• 0852
27	2.75	• 010425	• 6830	• 0761
28	3.00	• 011723	• 7092	• 0656
29	3.25	• 014210	• 7345	• 0533
30	3.50	• 019592	• 7599	• 0389
31	3.75	• 026324	• 7852	• 0215
32	4.00	• 041123	• 8105	• 00000

LAMBDA= 45.00

	PTFF=	• 026763	ATFF=	• 2247
K	A(K)	NDLOAD	AONE	ATWO
1	-4.00	• 0.00000	• 0.000	• 0.000
2	-3.75	• 013210	• 0253	• 0216
3	-3.50	• 020083	• 0506	• 0320
4	-3.25	• 023770	• 0759	• 0535
5	-3.00	• 026173	• 1013	• 0658
6	-2.75	• 027321	• 1266	• 0764
7	-2.50	• 027760	• 1519	• 0854
8	-2.25	• 027702	• 1773	• 0932
9	-2.00	• 027283	• 2026	• 0999
10	-1.75	• 026596	• 2279	• 1055
11	-1.50	• 025707	• 2533	• 1102
12	-1.25	• 024666	• 2786	• 1141
13	-1.00	• 022511	• 3039	• 1173
14	-0.75	• 022270	• 3292	• 1197

15	-0.5	• 02 071	• 3-46	-• 1214
16	-0.2	• 01 640	• 3111	-• 1226
17	0.2	• 01 522	• 4466	-• 1118
18	0.2	• 01 542	• 5555	-• 1110
19	0.74	• 01 421	• 4 12	-• 1114
20	1.00	• 01 342	• 2065	-• 1171
21	1.25	• 01 187	• 5319	-• 1140
22	1.50	• 01 0846	• 5472	-• 1101
23	1.75	• 00957	• 5826	-• 1054
24	2.00	• 009270	• 6579	-• 0999
25	2.25	• 008851	• 6332	-• 0931
26	2.50	• 008792	• 6585	-• 0854
27	2.75	• 009232	• 6939	-• 0763
28	3.00	• 010380	• 7092	-• 0658
29	3.25	• 012583	• 7345	-• 0535
30	3.50	• 016470	• 7599	-• 0390
31	3.75	• 022343	• 7852	-• 0216
32	4.00	• 036554	• 8105	-• 0000

LAMBDA= 50.00

		PTEE= .024117 ATEE=	• 2240	
K	A(K)	NDLOAD	AONE	ATWO
1	-4.00	0.000000	• 00000	• 00000
2	-3.75	• 011925	• 0253	-• 0217
3	-3.50	• 018111	• 0506	-• 0391
4	-3.25	• 021605	• 0759	-• 0537
5	-3.00	• 023582	• 1013	-• 0660
6	-2.75	• 024610	• 1266	-• 0765
7	-2.50	• 025002	• 1519	-• 0856
8	-2.25	• 024947	• 1773	-• 0934
9	-2.00	• 024567	• 2026	-• 1000
10	-1.75	• 023947	• 2279	-• 1057
11	-1.50	• 023145	• 2533	-• 1104
12	-1.25	• 022206	• 2786	-• 1143
13	-1.00	• 021165	• 3039	-• 1174
14	-0.75	• 020047	• 3292	-• 1198
15	-0.50	• 018876	• 3546	-• 1216
16	-0.25	• 017671	• 3799	-• 1228
17	0.25	• 015227	• 4306	-• 1219
18	0.50	• 014022	• 4559	-• 1212
19	0.75	• 012850	• 4812	-• 1196
20	1.00	• 011733	• 5066	-• 1172
21	1.25	• 010691	• 5319	-• 1141
22	1.50	• 009753	• 5572	-• 1103
23	1.75	• 008951	• 5825	-• 1056
24	2.00	• 008331	• 6079	-• 0999
25	2.25	• 007951	• 6332	-• 0933
26	2.50	• 007896	• 6585	-• 0855
27	2.75	• 008287	• 6839	-• 0765
28	3.00	• 009316	• 7092	-• 0660
29	3.25	• 011293	• 7345	-• 0536
30	3.50	• 014786	• 7599	-• 0391
31	3.75	• 020972	• 7852	-• 0217
32	4.00	• 032898	• 8105	0.0000

LAMBDA= 100.00

		PTEE= .012105 ATEF=	• 2218	
K	A(K)	NDLOAD	AONE	ATWO
1	-4.00	0.000000	• 00000	• 00000
2	-3.75	• 006021	• 0253	-• 0220
3	-3.50	• 009114	• 0506	-• 0395
4	-3.25	• 010852	• 0759	-• 0541
5	-3.00	• 011833	• 1013	-• 0665

6	-2.75	.012340	.1266	-0.770
7	-2.50	.012520	.1512	-0.961
8	-2.25	.012497	.1772	-0.039
9	-2.00	.012303	.2026	-0.105
10	-1.75	.011990	.2272	-0.1061
11	-1.50	.011586	.2533	-0.1109
12	-1.25	.011114	.2786	-0.1148
13	-1.00	.010591	.3039	-0.1179
14	-0.75	.010020	.3292	-0.1203
15	-0.50	.009442	.3546	-0.1221
16	-0.25	.008827	.3790	-0.1233
17	.25	.007611	.4046	-0.1224
18	.50	.007004	.4559	-0.1216
19	.75	.006419	.4812	-0.1200
20	1.00	.005958	.5066	-0.1177
21	1.25	.005334	.5319	-0.1146
22	1.50	.004862	.5572	-0.1108
23	1.75	.004459	.5825	-0.1060
24	2.00	.004145	.6079	-0.1004
25	2.25	.003951	.6332	-0.0938
26	2.50	.003919	.6585	-0.0860
27	2.75	.004109	.6939	-0.0770
28	3.00	.004616	.7092	-0.0664
29	3.25	.005596	.7345	-0.0541
30	3.50	.007335	.7500	-0.0395
31	3.75	.010427	.7852	-0.0220
32	4.00	.016449	.8105	0.0000

LAMPDA= 150.00

PTEE=	.008076	ATEE=	.2214	
K	A(K)	NDLOAD	AONE	ATWO
1	-4.00	0.000000	0.0000	0.0000
2	-3.75	.004021	.0253	-0.0220
3	-3.50	.006083	.0506	-0.0396
4	-3.25	.007241	.0759	-0.0542
5	-3.00	.007893	.1013	-0.0665
6	-2.75	.008231	.1266	-0.0771
7	-2.50	.008357	.1519	-0.0862
8	-2.25	.008334	.1773	-0.0939
9	-2.00	.008205	.2026	-0.1006
10	-1.75	.007995	.2279	-0.1062
11	-1.50	.007725	.2533	-0.1110
12	-1.25	.007410	.2786	-0.1149
13	-1.00	.007061	.3039	-0.1180
14	-0.75	.006687	.3292	-0.1204
15	-0.50	.006295	.3546	-0.1222
16	-0.25	.005892	.3790	-0.1234
17	.25	.005074	.4046	-0.1225
18	.50	.004670	.4559	-0.1217
19	.75	.004278	.4812	-0.1201
20	1.00	.003904	.5066	-0.1179
21	1.25	.003555	.5319	-0.1147
22	1.50	.003240	.5572	-0.1108
23	1.75	.002970	.5825	-0.1061
24	2.00	.002761	.6079	-0.1005
25	2.25	.002531	.6332	-0.0939
26	2.50	.002609	.6585	-0.0861
27	2.75	.002735	.6839	-0.0771
28	3.00	.003072	.7092	-0.0665
29	3.25	.003724	.7345	-0.0542
30	3.50	.004082	.7500	-0.0395
31	3.75	.004644	.7852	-0.0220

32 4.00 .21 966 .8105 2.00 90
 LAMBDA= 200.00
 PTEE= .006158 ATEF= .2212
 K A(K) NDLOAD AONE ATWO
 1 -4.00 .003030 .000000 .000000
 2 -3.75 .003018 .0253 -0.0221
 3 -3.50 .004564 .0506 -0.0396
 4 -3.25 .005432 .0759 -0.0542
 5 -3.00 .005921 .1013 -0.0666
 6 -2.75 .006174 .1266 -0.0771
 7 -2.50 .006268 .1510 -0.0862
 8 -2.25 .006261 .1773 -0.0940
 9 -2.00 .006154 .2026 -0.1006
 10 -1.75 .005997 .2279 -0.1063
 11 -1.50 .005794 .2533 -0.1110
 12 -1.25 .005558 .2786 -0.1149
 13 -1.00 .005296 .3039 -0.1180
 14 -.75 .005015 .3292 -0.1204
 15 -.50 .004721 .3546 -0.1222
 16 -.25 .004419 .3799 -0.1234
 17 .25 .003805 .4306 -0.1225
 18 .50 .003502 .4559 -0.1218
 19 .75 .003208 .4812 -0.1202
 20 1.00 .002928 .5066 -0.1178
 21 1.25 .002666 .5319 -0.1147
 22 1.50 .002429 .5572 -0.1109
 23 1.75 .002227 .5825 -0.1062
 24 2.00 .002070 .6079 -0.1005
 25 2.25 .001972 .6332 -0.0939
 26 2.50 .001955 .6585 -0.0861
 27 2.75 .002050 .6839 -0.0771
 28 3.00 .002302 .7092 -0.0666
 29 3.25 .002792 .7345 -0.0542
 30 3.50 .003660 .7599 -0.0396
 31 3.75 .005206 .7852 -0.0220
 32 4.00 .009224 .8105 0.0000

LAMBDA= 235.00
 PTEE= .006156 ATEF= .2212
 K A(K) NDLOAD AONE ATWO
 1 -4.00 .003030 .000000 0.000000
 2 -3.75 .002569 .0253 -0.0221
 3 -3.50 .003885 .0506 -0.0396
 4 -3.25 .004623 .0759 -0.0542
 5 -3.00 .005040 .1013 -0.0666
 6 -2.75 .005255 .1266 -0.0772
 7 -2.50 .005335 .1510 -0.0862
 8 -2.25 .005321 .1773 -0.0940
 9 -2.00 .005238 .2026 -0.1006
 10 -1.75 .005104 .2279 -0.1063
 11 -1.50 .004931 .2533 -0.1110
 12 -1.25 .004730 .2786 -0.1149
 13 -1.00 .004507 .3039 -0.1180
 14 -.75 .004268 .3292 -0.1205
 15 -.50 .004018 .3546 -0.1222
 16 -.25 .003760 .3799 -0.1234
 17 .25 .003238 .4306 -0.1225
 18 .50 .002981 .4559 -0.1218
 19 .75 .002730 .4812 -0.1202
 20 1.00 .002491 .5066 -0.1178
 21 1.25 .002268 .5319 -0.1148
 22 1.50 .002067 .5572 -0.1104

23	1.75	• 011895	• 925	-• 1.052
24	2.00	• 011751	• 521	-• 1.025
25	2.01	• 011752	• 524	-• 1.025
26	2.50	• 011554	• 520	-• 1.02
27	2.75	• 011744	• 5154	-• 1.011
28	2.80	• 011950	• 1.942	-• 1.065
29	3.25	• 012215	• 245	-• 1.42
30	3.5	• 011414	• 641	-• 1.396
31	3.75	• 0104431	• 452	-• 1.221
32	4.00	• 0116999	• 81.5	-• 1.022

LAMRDAE= 270.50

K	A(K)	NDLOAD	AONE	ATWO
1	-4.00	• 0100101	• 1.1	-• 1.1
2	-3.75	• 002232	• 0253	-• 0221
3	-3.50	• 003375	• 030	-• 0371
4	-3.25	• 004017	• 0154	-• 042
5	-3.00	• 004318	• 0013	-• 0666
6	-2.75	• 004565	• 1266	-• 0712
7	-2.50	• 004615	• 1514	-• 0862
8	-2.25	• 004622	• 1773	-• 0940
9	-2.00	• 004550	• 2026	-• 1066
10	-1.75	• 004434	• 2279	-• 1063
11	-1.50	• 004284	• 2533	-• 1110
12	-1.25	• 004109	• 2786	-• 1149
13	-1.00	• 003916	• 3024	-• 1101
14	-0.75	• 003708	• 3272	-• 1202
15	-0.50	• 003491	• 3545	-• 1222
16	-0.25	• 003267	• 3749	-• 1234
17	0.25	• 002813	• 4106	-• 1226
18	0.50	• 002584	• 4154	-• 1210
19	0.75	• 002372	• 4812	-• 1202
20	1.00	• 002164	• 5066	-• 1110
21	1.25	• 001971	• 5318	-• 114
22	1.50	• 001796	• 5512	-• 110
23	1.75	• 001646	• 5825	-• 1062
24	2.00	• 001530	• 6114	-• 1036
25	2.25	• 001458	• 6452	-• 0724
26	2.50	• 001445	• 6789	-• 0602
27	2.75	• 001515	• 6838	-• 0711
28	3.00	• 001702	• 7092	-• 0666
29	3.25	• 002063	• 7345	-• 0742
30	3.50	• 002105	• 7474	-• 0710
31	3.75	• 003848	• 7852	-• 0221
32	4.00	• 006181	• 81.5	-• 1.0

LAMRDAE= 320.00

K	A(K)	NDLOAD	AONE	ATWO
1	-4.00	• 01001000	• 0003	-• 1.000
2	-3.75	• 001887	• 0223	-• 0221
3	-3.50	• 002853	• 0506	-• 0371
4	-3.25	• 003396	• 0759	-• 0542
5	-3.00	• 003711	• 1013	-• 0606
6	-2.75	• 003859	• 1266	-• 0772
7	-2.50	• 003918	• 1514	-• 0862
8	-2.25	• 003907	• 1773	-• 0940
9	-2.00	• 003846	• 2026	-• 1066
10	-1.75	• 003749	• 221	-• 1062
11	-1.50	• 003622	• 2533	-• 1110
12	-1.25	• 003474	• 2705	-• 1149
13	-1.00	• 003310	• 3034	-• 1181

14	-0.15	• 001114	• 12-6	-0.1238
15	-0.15	• 001111	• 12-6	-0.1222
16	-0.25	• 001116	• 12-7	-0.124
17	0.25	• 0011378	• 12-6	-0.125
18	0.5	• 001218	• 4-5	-0.1212
19	0.75	• 001205	• 45-7	-0.126
20	1.0	• 001220	• 5-6	-0.127
21	1.25	• 001265	• 51-7	-0.1142
22	1.5	• 001218	• 57-7	-0.1122
23	1.75	• 0011971	• 5825	-0.1152
24	2.0	• 001294	• 5-7	-0.115
25	2.25	• 001232	• 6332	-0.1093
26	2.5	• 001221	• 6285	-0.1086
27	2.75	• 001280	• 6834	-0.1171
28	3.0	• 001438	• 7092	-0.1665
29	3.25	• 001744	• 740	-0.142
30	3.5	• 002286	• 744	-0.1346
31	3.75	• 002253	• 752	-0.1221
32	4.0	• 005145	• 8135	-0.1020

LAMPDA= 358.

PTEF= • 003293 ATEF= • 1211

K	A(K)	NDLOAD	ADNF	ATWD
1	-4.0	• 001111	•	•
2	-3.75	• 001641	• 253	-0.1221
3	-3.5	• 002481	• 225	-0.1371
4	-3.25	• 002953	• 1724	-0.1242
5	-3.0	• 003219	• 1013	-0.1665
6	-2.75	• 003356	• 1255	-0.1712
7	-2.5	• 003407	• 1219	-0.1862
8	-2.25	• 003398	• 1773	-0.144
9	-2.0	• 003347	• 2026	-0.1007
10	-1.75	• 003274	• 2211	-0.1002
11	-1.5	• 003149	• 2533	-0.1112
12	-1.25	• 003021	• 2786	-0.1144
13	-1.0	• 002878	• 3034	-0.1181
14	-0.75	• 002726	• 3292	-0.1205
15	-0.5	• 002566	• 3546	-0.1222
16	-0.25	• 002401	• 3749	-0.1234
17	0.25	• 002068	• 4306	-0.1226
18	0.5	• 001905	• 4528	-0.1210
19	0.75	• 001743	• 4812	-0.1202
20	1.0	• 001591	• 5066	-0.1179
21	1.25	• 001448	• 5319	-0.1148
22	1.5	• 001320	• 5572	-0.1110
23	1.75	• 001210	• 5825	-0.1062
24	2.0	• 001174	• 5974	-0.1050
25	2.25	• 001171	• 532	-0.1044
26	2.5	• 001152	• 5785	-0.1086
27	2.75	• 001112	• 6834	-0.1111
28	3.0	• 001250	• 7072	-0.1606
29	3.25	• 001516	• 7345	-0.1542
30	3.5	• 001988	• 7549	-0.1596
31	3.75	• 002528	• 7852	-0.1221
32	4.0	• 004465	• 8135	-0.1020

LAMPDA= 42.0

PTEF= • 002885 ATEF= • 2211

K	A(K)	NDLOAD	ADNF	ATWD
1	-4.0	• 001111	•	•
2	-3.75	• 001438	• 253	-0.1221
3	-3.5	• 002174	• 225	-0.1371
4	-3.25	• 002117	• 219	-0.1242

6	-1.0	• 0118888	• 1118888	-• 1118888
5	-2.75	• 0121411	• 1121411	-• 1121411
7	-2.5	• 01215	• 11215	-• 11215
8	-2.25	• 01211	• 11211	-• 11211
9	-2.0	• 012121	• 112121	-• 112121
10	-1.75	• 012464	• 112464	-• 112464
11	-1.5	• 01255	• 11255	-• 11255
12	-1.25	• 012647	• 112647	-• 112647
13	-1.0	• 012672	• 112672	-• 112672
14	-0.75	• 0011888	• 3292	-• 1206
15	-0.5	• 02248	• 3546	-• 1222
16	-0.25	• 001104	• 3739	-• 1234
17	0.25	• 011812	• 4305	-• 1220
18	0.5	• 001058	• 4102	-• 1214
19	0.75	• 001027	• 4812	-• 1214
20	1.0	• 01134	• 5166	-• 1214
21	1.25	• 001264	• 514	-• 1148
22	1.5	• 001156	• 5572	-• 1154
23	1.75	• 001165	• 5825	-• 1162
24	2.0	• 01285	• 5117	-• 116
25	2.25	• 001929	• 6332	-• 1937
26	2.5	• 001930	• 6585	-• 1862
27	2.75	• 001975	• 6834	-• 771
28	3.0	• 001095	• 7192	-• 666
29	3.25	• 001328	• 7345	-• 5542
30	3.5	• 001142	• 7357	-• 506
31	3.75	• 002417	• 7352	-• 1221
32	4.0	• 013916	• 8135	-• 1200

LAMBDA= 475.90

K	A(K)	NDLOAD	ADNF	ADAO
1	-4.00	0.000000	0.00000	0.00000
2	-3.75	• 01269	• 253	-• 221
3	-3.5	• 001919	• 506	-• 397
4	-3.25	• 002283	• 759	-• 543
5	-3.00	• 002489	• 1013	-• 666
6	-2.75	• 002595	• 1266	-• 772
7	-2.5	• 002634	• 1519	-• 862
8	-2.25	• 002627	• 1773	-• 940
9	-2.0	• 002586	• 2026	-• 107
10	-1.75	• 002520	• 2279	-• 1063
11	-1.50	• 002435	• 2533	-• 1113
12	-1.25	• 002336	• 2786	-• 1149
13	-1.00	• 002226	• 3030	-• 1181
14	-0.75	• 002158	• 3292	-• 1215
15	-0.50	• 001984	• 3546	-• 1222
16	-0.25	• 001857	• 3739	-• 1234
17	0.25	• 001599	• 4305	-• 1226
18	0.50	• 001472	• 4559	-• 1218
19	0.75	• 001348	• 4812	-• 1202
20	1.00	• 001230	• 5066	-• 1179
21	1.25	• 001120	• 5319	-• 1148
22	1.50	• 001020	• 5572	-• 1129
23	1.75	• 000935	• 5825	-• 1062
24	2.00	• 000869	• 5117	-• 1006
25	2.25	• 000828	• 6332	-• 939
26	2.5	• 000821	• 6585	-• 862
27	2.75	• 000861	• 6929	-• 771
28	3.0	• 000867	• 7092	-• 666
29	3.25	• 001172	• 7345	-• 542
30	3.5	• 001137	• 7524	-• 526

31
32
LAMBDA= 52.6
PTEE= .2284 ATEE= .2211

K	A(K)	NDLOAD	AONF	ATWO
1	-4.00	.000000	.000000	.000000
2	-3.75	.001041	.0253	-.0221
3	-3.50	.001574	.0506	-.0397
4	-3.25	.001873	.0759	-.0543
5	-3.00	.002042	.1013	-.0666
6	-2.75	.002129	.1266	-.0772
7	-2.50	.002162	.1519	-.0862
8	-2.25	.002156	.1773	-.0940
9	-2.00	.002122	.2026	-.1007
10	-1.75	.001998	.2279	-.1063
11	-1.50	.001996	.2533	-.1110
12	-1.25	.002095	.2786	-.1149
13	-1.00	.001996	.3039	-.1181
14	-.75	.001890	.3292	-.1205
15	-.50	.001779	.3546	-.1222
16	-.25	.001665	.3799	-.1234
17	.25	.001434	.4306	-.1226
18	.50	.001320	.4559	-.1218
19	.75	.001209	.4812	-.1202
20	1.00	.001103	.5066	-.1179
21	1.25	.001004	.5319	-.1148
22	1.50	.000915	.5572	-.1109
23	1.75	.000839	.5825	-.1062
24	2.00	.000780	.6079	-.1006
25	2.25	.000743	.6332	-.0939
26	2.50	.000736	.6585	-.0862
27	2.75	.000772	.6839	-.0771
28	3.00	.000867	.7092	-.0666
29	3.25	.001051	.7345	-.0542
30	3.50	.001378	.7599	-.0397
31	3.75	.001961	.7852	-.0221
32	4.00	.003100	.8105	0.0000

LAMBDA= 580.00
PTEE= .002089 ATEE= .2211
K A(K) NDLOAD AONF ATWO

K	A(K)	NDLOAD	AONF	ATWO
1	-4.00	.000000	.000000	.000000
2	-3.75	.001041	.0253	-.0221
3	-3.50	.001574	.0506	-.0397
4	-3.25	.001873	.0759	-.0543
5	-3.00	.002042	.1013	-.0666
6	-2.75	.002129	.1266	-.0772
7	-2.50	.002162	.1519	-.0862
8	-2.25	.002156	.1773	-.0940
9	-2.00	.002122	.2026	-.1007
10	-1.75	.002068	.2279	-.1063
11	-1.50	.001998	.2533	-.1110
12	-1.25	.001916	.2786	-.1149
13	-1.00	.001826	.3039	-.1181
14	-.75	.001729	.3292	-.1205
15	-.50	.001628	.3546	-.1222
16	-.25	.001523	.3799	-.1234
17	.25	.001312	.4306	-.1226
18	.50	.001207	.4559	-.1218
19	.75	.001106	.4812	-.1202
20	1.00	.001009	.5066	-.1179
21	1.25	.000910	.5319	-.1148

22	1.0	• 001300	• 000000	• 000000
23	1.00	• 001160	• 000000	• 000000
24	1.0	• 001120	• 000000	• 000000
25	1.025	• 001140	• 6332	• 000000
26	1.05	• 001164	• 6585	• 000000
27	1.075	• 001166	• 6839	• 000000
28	1.050	• 0011793	• 7142	• 000000
29	1.025	• 0011962	• 7345	• 000000
30	1.050	• 001261	• 7599	• 000000
31	1.075	• 001794	• 7852	• 000000
32	1.000	• 002836	• 8105	• 000000

LAMBDA= 647.60

PTFE= 0.001871 ATEE=

K	A(K)	NDLOAD
1	-4.00	0.000000
2	-3.75	• 000932
3	-3.50	• 001410
4	-3.25	• 001678
5	-3.00	• 001829
6	-2.75	• 001907
7	-2.50	• 001936
8	-2.25	• 001931
9	-2.00	• 001900
10	-1.75	• 001852
11	-1.50	• 001789
12	-1.25	• 001716
13	-1.00	• 001635
14	-0.75	• 001540
15	-0.50	• 001458
16	-0.25	• 001364
17	0.25	• 001175
18	0.50	• 001081
19	0.75	• 000990
20	1.00	• 000904
21	1.25	• 000823
22	1.50	• 000750
23	1.75	• 000687
24	2.00	• 000639
25	2.25	• 000608
26	2.50	• 000603
27	2.75	• 000632
28	3.00	• 000710
29	3.25	• 000861
30	3.50	• 001129
31	3.75	• 001607
32	4.00	• 002540

• 2211

AONE

• 000000	ATWO
• 0253	-• 0221
• 2506	-• 1397
• 2759	-• 0543
• 3013	-• 0666
• 3266	-• 0772
• 3519	-• 0862
• 3773	-• 0940
• 2026	-• 1007
• 2279	-• 1063
• 2533	-• 1110
• 2786	-• 1149
• 3039	-• 1181
• 3292	-• 1205
• 3546	-• 1222
• 3799	-• 1234
• 4306	-• 1226
• 4559	-• 1218
• 4812	-• 1202
• 5066	-• 1179
• 5319	-• 1148
• 5572	-• 1109
• 5825	-• 1062
• 6079	-• 1006
• 6332	-• 0939
• 6585	-• 0862
• 6839	-• 0771
• 7092	-• 0666
• 7345	-• 0542
• 7599	-• 0397
• 7852	-• 0221
• 8105	0.0000





B29815